Editorial

Catherine Beswick

This thematic edition of CLIVAR Exchanges is devoted to CLIVAR's ocean basin panels; the Pacific Ocean panel, the Atlantic implementation panel, the Southern Ocean panel, and the Indian Ocean panel. The issue has provided an opportunity for these panels to communicate recent projects related to panel activities. Pulling in the paleo perspective, we also have a contribution from members (and co-authors) of the CLIVAR/PAGES working group, highlighting the Ocean2k initiative.

At the end of January the International CLIVAR Project Office (ICPO) bid farewell to Bob Molinari, as he embarked on his retirement. I am sure I am not alone in thanking Bob for all of the hard work dedicated to the ICPO and the wider CLIVAR community. We wish him and his wife Pat all the very best during their final weeks in the UK and on their journey back to the US.

In the hunt to find a suitable replacement for Bob, I have stepped into the role of acting director, and will endeavour to serve the ICPO and CLIVAR well during this temporary term. Otherwise the project office continues with its activities, including the launch of a new CLIVAR bulletin earlier this month to keep our community more informed of activities of CLIVAR, WCRP, and other related programmes (to sign up to the monthly bulletin, see the CLIVAR website www.clivar.org).

We also had a presence at the recent 2012 Ocean Sciences Meeting, 21 February, Salt Lake City USA. Martin Visbeck, CLIVAR SSG co-chair, kicked off the evening event with a brief overview of CLIVAR objectives and organisation. He emphasised that international CLIVAR focused on problems that require international coordination or cooperation and outlined how CLIVAR fits into the bigger scheme of WCRP and the other international Global Change programmes. He then invited comments from the audience on what a future WCRP programme that focuses on the ocean-atmosphere component of the climate system should encompass. Suggestions from the floor can be viewed here on the CLIVAR website (http://www.clivar.org/resources/news/clivar-town-hall-meeting).

Front Cover Image: Courtesy of Weldong Yu

South Atlantic Meridional Overturning Circulation (SAMOC) - Fourth Workshop

Silvia Garzoli[1], Povl Abrahamsen[2], Isabelle Ansorge[3], Arne Biastoch[4], Edmo Campos[5], Mauricio Mata[6], Chris Meinen[1], Jose Pelegri[7], Renellys Perez[8,1], Alberto Piola[9], Chris Reason[3], Mike Roberts[10], Sabrina Speich[11], Janet Sprintall[12], Randy Watts[13], and all of the SAMOC IV participants.

1 NOAA/AOML (USA)
2 British Antarctic Survey (UK)
3 University of Cape Town (South Africa)
4 Kiel (Germany)
5 Univeriity of Sao Paulo (Brazil)
6 Fundação Universidade do Rio Grande (Brazil)
7 BU (Spain)
8 Univeristy of Miami (USA)
9 SHN (Argentina)
10 Oceans and Coasts (South Africa)
11 LPO (France)
12 SIO (USA)
13 URI (USA)

Corresponding author: Silvia.Garzoli@noaa.gov

The fourth workshop of the South Atlantic Meridional Overturning Circulation (SAMOC 4) took place in Simons Town, South Africa, on 27-29 September 2011. The main objectives of the workshop were to: highlight recent modeling results related to the importance of observing the South Atlantic components of the Atlantic Meridional Overturning Circulation (AMOC); provide an overview of results from ongoing pilot arrays and related observational programs; discuss the status of proposals submitted for observations and modeling; and coordinate new proposals aimed at SAMOC goals. Discussions on ship time availability to support the proposed fieldwork in the region, and on developing new agreements for sharing these resources, also took place.

In the morning of the first day several scientists made short presentations on science relevant to the SAMOC goals. These presentations focused on role of Agulhas eddies in the South Atlantic and highlighted the significance of recent changes in surface temperature, wind stress and wind stress curl associated with southward displacement of zonal winds. Brief presentations were made on new modeling results and

observations, followed by plenary discussions on current and future plans. A review of recent results from ongoing modeling experiments demonstrated that 30-35°S was the best latitude to monitor the MOC variability, confirming previous results derived from the analysis of numerical and theoretical modeling studies conducted in the United States, the United Kingdom, Brazil and the Netherlands. Firstly, higher latitudes provide stronger density gradients and a larger Coriolis parameter, leading to improved signal-to-noise characteristics for geostrophic velocity calculations. Secondly, the strongest signals are more tightly confined to the boundaries at higher latitudes, particularly at the eastern boundary, indicating that a more limited portion of the trans-basin array would require more intense horizontal resolution. Thirdly, estimation of the stability of the MOC – a crucial factor in attribution of observed signals – is more favorable at higher latitudes. Finally, ocean model studies indicate that at higher latitudes it is possible to utilize less expensive mooring technologies (i.e. pressure-equipped inverted echo sounders – PIES), reducing the cost of the overall system and its maintenance.

The status of and future plans for existing observing programs were discussed. Details of funded, submitted and to be submitted projects are given in the attached Table 1.

One crucial component of the overall SAMOC observing system, the proposed trans-basin array at 34.5°S, was thoroughly discussed; the comments from the US-NSF proposal were also reviewed. The consensus of the workshop attendees was that the proposal should be resubmitted with modifications. The array will be proposed with approximately 20 ocean moorings, a combination of tall 'dynamic height' moorings and PIES, coupled with several shorter direct velocity moorings on the shelf on either side of the basin.

Measurements at the boundaries were considered crucial to close the budgets. A group of North and South American countries operating through the Inter-American Institute for Global Change Research (IAI) has a large shelf-monitoring program funded for the western boundary that would fit well with the western end of the recommended trans-basin array. In addition, a Brazilian proposal to augment the shallow array close to the current US-funded PIES deployed at 34.5°S was funded. At the eastern boundary, South African scientists at the Centre for Operational Oceanography were funded to deploy an array of 5 ADCP moorings from the coast out to the French array of CPIES.

The group was in agreement that attribution of the observed signals at 30-35°S will require both the continuation and augmentation of the existing concurrent interocean exchange observing systems: the GoodHope array and the Drake Passage programs. Observations along the GoodHope transect will, in conjunction with the German array of PIES/CPIES and altimetry, help quantify the Agulhas rings shed at the retroflection, while the Drake Passage observations will aid in determining flow via the cold-water route. The group also agreed it was important to analyze the products of different ocean general circulation models to study the different branches of the Deep Western Boundary Current in the South Atlantic.

Crucial to the success of the program will be the availability of an impressive research fleet. South Africa is building a new global class ship that will become operational in 2012. The University of Sao Paulo (Brazil) has purchased a regional class ship that will also be available in 2012. Brazilian scientists have also obtained funds to buy new oceanographic equipment and refurbish the Brazilian Navy vessel Cruzeiro do Sul. In Argentina, in addition to the currently available R/V Puerto Deseado, a 40 foot catamaran will be available for near shore mooring services.

One action item from the workshop is the preparation of a SAMOC implementation plan to be submitted to International CLIVAR for endorsement. The SAMOC V workshop will take place in Miami, US. The local organizers are Renellys Perez and Chris Meinen.

The SAMOC IV workshop was hosted by Isabelle Ansorge and Chris Reason (University of Cape Town). It was chaired by Silvia L. Garzoli (AOML, USA), Sabrina Speich (LPO, France), and Alberto Piola (SHN, Argentina). The workshop was attended by 43 scientists and students from eight countries (Argentina, Brazil, France, Germany, Spain, South Africa, the United Kingdom, and the United States). Support for the workshop came from the South African National Antarctic Programme (SANAP) Development Grant and the Johann Lutjeharms NRF rated researchers award. The meeting was dedicated to the memory of Johann Lutjerhams, UCT's Professor, one of Southern Africa's leading marine scientists and the foremost authority on the Agulhas Current, who died on 8 June 2011.

Component	Funding Agency	Principal Investigators	Country	Status
Western boundary pilot measurements (4 PIES, 1 spare)	NOAA	C. Meinen, S. Garzoli, M. Baringer, G. Goni	USA	Funded
Quarterly AX18 XBT transect + Argo floats	NOAA	G. Goni, M. Baringer, S. Garzoli	USA	Funded
Twice a year transect AX25 + Argo floats	NOAA/UCT	Garzoli, Goni, Ansorge	US/South Africa	Funded
Eastern boundary pilot measurements (4 CPIES)	IFREMER/CPER	S. Speich	France	Funded
Eastern boundary ADCPs (5)	South Africa, IFREMER	M. Roberts,		
S. Speich	South Africa, France	Funded		
GoodHope PIES (7), CPIES (7)	Germany	A. Macrander, O. Boebel	Germany	Funded
Western boundary ADCP (1), BPR (1), western boundary hydrographic, turn-around, recovery cruises	CNPq/INCT	E. Campos, F. Niencheski	Brazil	Funded
The CALSA Project (Numerical Modeling)	FAPESP	E. Campos	Brazil	Funded
The ATLAS-B, the NAP-MC and FAPESP-MC Projects (Atlas mooring, currentmetry and cruises in the Santos Bight, ~23-28S)	FAPESP, CNPq-INCT &USP	E.Campos	Brazil	Funded
The South Atlantic Climate Change Consortium (SACC):.Shelf/slope observations and models	IAI	A. Piola, E.Campos/R. Matano/K.Brink/M. Barreiro	Argentina/ Brazil/US/ Uruguay	Funded
Drake Passage, XBT and CTD SADCP lines	NOAA, Shirshov , NOCS	J. Sprintal, S. Glady-shev, B. King	US, Russia, UK	Funded
CTD section in the South Atlantic 40°S (can be moved north)	Univ. of Barcelona	J.L. Pelegri	Spain	Funded
Western boundary CPIES (3), western boundary hydrographic, turn-around, recovery cruises	FAPESP/FACEPE	E. Campos, A. Fetter	Brazil	Funded
(1) Eastern boundary CPIES (6), (2) Goodhope PIES (7), (3) Marisonde buoys (5)	ANR	S. Speich	France	Funded
Western boundary PIES (4), interior PIES-DP (4)	NOAA	R. Perez, S. Dong, C. Meinen, G. Goni, S. Garzoli, M. Baringer	USA	Proposed
Shelf circulation along altimeter line near 40S	France Argentina MOU	A. Piola, C. Provost	Argentina/ France	Proposed
(1) Dynamic height moorings (8) (2) Deployment and trans-basin hydrographic cruise	NSF	S. Dong, R. Perez, J. Sprintall, R. Fine, G. Flierl, S. Baker-Yeboah	USA	To be pro-posed
24ffiS western boundary moorings, trans-basin hydrographic cruise	NERC	E. McDonagh	UK	To be pro-posed
Western boundary instrumentation, western boundary hydrographic, turn-around, recovery cruises	Argentina	A. Piola, A. Triosi	Argentina	To be pro-posed
Western boundary (possibly trans-basin) hydrographic cruise	Spain	J. Pelegri	Spain	To be pro-posed
Eastern boundary hydrographic, turn-around, recovery cruises	SANAP	I. Ansorge, C. Reason	South Africa	To be pro-posed
Goodhope hydrographic, deployment, recovery cruises	Russian Acad. Sci.	S. Gladyshev, A. Sokov	Russia	To be pro-posed

SAMOC RELATED PROGRAMS

Component	Funding Agency	Principal Investigators	Country	Status
The INCT-Mar-CARBOM and INCT-Mar-COI Projects			Brazil	Funded
OOI	NSF	WHOI/SIO	USA	Funded

Table 1: List of funded, proposed, and to-be-proposed projects related to the goals of SAMOC. Projects highlighted in gray are funded.

Observations of Brazil Current baroclinic transport near 22°S: variability from the AX97 XBT transect

Mauricio M. Mata[1], Mauro Cirano[2, 4], Mathias R. van Caspel[1], Caio S. Fonteles[1], Gustavo Goñi[3] and Molly Baringer[3]

1. Institute of Oceanography - Federal University of Rio Grande-FURG, Brazil
2. Department of Environmental Physics – Federal University of Bahia-UFBA, Brazil
3. Physical Oceanography Division – NOAA/AOML, USA
4. Aquatic Sciences, South Australia Research and Development Institute, Australia

Contact: mauricio.mata@furg.br

1. Introduction

The Brazil Current (BC) is the Western Boundary Current (WBC) associated to the wind-driven circulation of the South Atlantic. This current can be identified furthest north where the southern branch of the westward flowing South Equatorial Current (SEC) bifurcates close to the South American coast near 15°S [e.g. Stramma and Schott, 1999]. As much as 15 to 22 Sv of the volume transport of the SEC flows northward as part of the inter-hemispheric flow of the North Brazil Current/Undercurrent [Silveira et al., 1994], leaving a relatively weak BC to close the subtropical wind-driven circulation in the western boundary at these latitudes. As the BC flows southwards to higher latitudes its depth and associated transport are increased, reaching 7.7 Sv in the upper 750 m to the south of the Vitoria-Trindade Ridge (Figure 1) [e.g. Campos et al., 1995]. Further south, the BC intensifies with the volume transport reaching values as high as 22 Sv near the Brazil-Malvinas Confluence at about 38°S [e.g. Peterson and Stramma, 1991]. Nevertheless, the BC is still classified as relatively weak when compared to its northern hemisphere counterparts, such as the Gulf Stream and the Kuroshio Current. Despite the recognized importance of the WBCs to the oceanic and climate systems from regional to basin-wide scales, the BC remains one of the least studied and understood of all WBCs, especially in terms of its variability or its relationship to the larger-scale subtropical gyre variations.

Recent progress in understanding the BC mean flow and associated features has been achieved [e.g. Stramma and England, 1999; Oliveira et al., 2009], however several aspects of BC low-latitude variability remain unexplained mostly due to the lack of observations. For example, south of 18°S, the BC poleward flow is normally thought to be largely composed of eddies, which leads to an ill-defined mean current with strong temporal and spatial fluctuations [e.g. Campos et al., 1995; Campos, 2006]. In order to increase the number of observations of the BC in this area, Brazilian institutions and NOAA have partnered to implement a long-term high-density XBT (eXpendable-BathyThermograph) transect in the southwestern Atlantic. This project has been named MOVAR (Monitoring the upper ocean transport variability in the western South Atlantic) and the XBT transect has been designated as AX97 running between Rio de Janeiro and Trindade Island (30°W, 20°S). One of the main objectives of this transect is to build a long-term time series of the BC baroclinic transports (and associated features) in order to improve understanding of the mean and temporal variations of the BC in this infrequently-sampled area of the South Atlantic Ocean. In addition, these observations contribute to the South Atlantic Meridional Overturning Circulation (SAMOC) initiative. Therefore, using a combination of the XBT data and satellite altimetry observations, this study analyzes the BC observed variability near 20°S and examines its possible causes.

2. Data Sources and Methods

The MOVAR project collects XBT data from Brazilian Navy supply ships, which sail from Rio de Janeiro to Trindade Island up to five times per year. A total of 29 complete realizations of the AX97 transect have been carried out between August 2004 to December 2011. The typical XBT deployment spacing is ~27 km along the transect and ~18 km near the boundaries. Most of the XBT probes were used to measure temperature up to 760 m (Sippican Deep Blue®), but several deep probes were also used (Sippican T-5® up to 1830m). Following the approach by Hansen and Thacker [1999], the salinity is estimated for each XBT profile based on an empirical relationship between historical salinity and temperature data collected in the region (Figure 1) from CTD (conductivity-temperature-depth) profiles, which are available in both US and Brazilian National Oceanographic Data Centers [van Caspel et al., 2010]. The dynamic method was then used to compute the baroclinic component of the geostrophic flow for each pair of stations along AX97 referenced to 400 dbar, level accepted as the typical interface between the southward flowing BC and the northward flow of its associated undercurrent in the region [Silveira et al., 2008]. To allow for direct comparisons between the repeat realizations, the velocity field was objectively mapped onto a regular longitude vs. depth grid of 0.25° by 10m and the transports were estimated by vertically integrating the gridded fields.

To gain further insight on the large-scale nature of the variability observed along AX97, we use the regional surface geostrophic circulation fields derived from the Maps of Absolute Dynamic Topography (MADT) dataset, which were objectively derived and distributed by AVISO Project. The MADT dataset uses data from all available satellite altimeters

(up to four) added to a mean sea level [Rio and Hernandez, 2004; AVISO, 2011]. These maps are provided with a resolution of 1/3° x 1/3° every seven days.

3. Baroclinic current field and transports from XBT data

The mean AX97 baroclinic velocity field, as derived from XBT observations, indicates the presence of the main BC clearly confined to the west of 39°W with its mean core position located at about 200 km from the coast, at a local water depth of about 2200 m (Figure 2, upper panel). The maximum mean baroclinic velocity exhibits values of up to 0.2 m s^{-1} in the core of the BC. The standard deviation of the BC is of comparable magnitude to the mean (0.2 m s^{-1}) in the BC core (Figure 2, middle panel), highlighting the importance of the spatial and temporal variability in the BC regime at 20°S. In addition, relatively large coherent mesoscale structures along the entire AX97 transect are evident in the mean and in the standard deviation sections, which suggests that a longer time series than what is used here may be needed to determine the mean dynamic structure in the region.

The zonally integrated transports across all AX97 realizations reveal that the variability observed in the velocity sections is translated into net baroclinic transport estimates, which are only weakly different from zero (Figure 2, bottom panel). The transport increases until reaching its maximum value of about 2.3 Sv near 39°W, a value that is roughly kept constant until the end of the section. The high variability in the transports across this section can be identified as three different 'typical' situations found during our AX97 cruises (Figure 3). The first case shows the baroclinic velocity field from the April 2007 realization (Figure 3, upper panel), which reveals a very strong BC with speeds up to 0.7 m s^{-1} and a net southward transport of up to 6 Sv. The current main core was positioned to the west of 40°W, close to the shelf break. The zonally integrated transport increases up to 8 Sv near 37°W. In the second case, exemplified by the February 2006 realization (Figure 3, middle panel), the flow right next to the coast is moving towards the equator. This suggests a change of configuration of the BC main axis (or even a current reversal near the shelf break). Indeed, the baroclinic velocity field shows that the BC jet is now positioned further offshore (to the east of 40°W), with surface velocities reaching up to 0.6 m s^{-1} and an associated transport of 5 Sv. Inshore of the southward moving BC (west of 40°W), the northward flowing current contains surface speeds reaching up to 0.2 m s^{-1} and associated transports of ~1.5 Sv. In a third configuration, here exemplified in the August 2004 realization (Figure 3, bottom panel), there seems to be no evidence of a strong BC baroclinic jet anywhere along the AX97 transect. During this time, the zonally integrated transports have no clear direction, fluctuating around zero.

These three different regimes of the BC jet examined here also help to explain the high levels of baroclinic velocity variability west of 38°W (Figure 2). These results support the hypothesis that the observed variability is associated with the spatial fluctuations of the BC core, which can exceed 150 km in the region. Furthermore, when the BC jet moves offshore to the east of 40°W, the onset of a northward circulation inshore of the main jet next to the continental slope is observed. Finally, the third case (Figure 3, bottom) suggests that the BC is not always present as a poleward jet across AX97, which helps to explain why the variability levels are greater than the mean in this region.

4. Regional circulation and variability

The altimetry from the MADT dataset confirms the dominance of the three regimes (dates) examined in the previous section. During April 2007, the MADT pattern and corresponding circulation (Figure 4, upper panel) suggests the presence of a strong southward flowing BC that is broadly fed by flow to the west of 37°W. In particular, the high-sea level is centred along the AX97 line near 37.5°W and 22°S. This high-sea level "cell" is part of a double-cell structure at the western end of the South Atlantic subtropical gyre, first proposed by Tsuchiya [1985]. The centre of the second cell is located near 32°S just off the western boundary (not shown). In a more recent study, Mattos [2006] uses in situ data from the Brazilian Navy database to confirm the presence of the northernmost cell and uses a quasi-geostrophic model to conclude that the high-sea level cell is a ubiquitous large-scale feature of the southwestern Atlantic. This feature is also well depicted and consistent in the mean surface circulation as obtained from the GRACE satellite gravimetry mission [Vianna et al., 2007] and from multi-mission satellite altimetry [Vianna and Menezes, 2011]. In addition, the field from April 2007 reveals a very strong state of the northern high-sea level cell with its "crest" clearly crossing the AX97 transects. In the corresponding velocity fields, the BC appears as a swift jet next to the western boundary confined mostly to the west of 40°W. During this time, the BC jet is also well observed to the north of AX97. Furthermore, the corresponding mean surface geostrophic circulation shows a complex pattern, where the BC jet is fed by two main inflows, at ~22°S and further north at ~18°S.

The regional surface circulation field during the February 2006 realization is different from the April 2007 case. During this time the northern high cell seems somewhat less defined and the BC jet is meandering offshore just south of 22°S to cross the AX97 section to the east of 40°W (Figure 4, middle panel). The high-sea level cell is closer to the coast almost reaching the continental boundary near 24°S. Further to the north from AX97, the BC jet seems to be present right next to the slope but not as clearly as in the April 2007 time frame. Between 22°S and 23°S, the MADT field contains a low-sea level feature suggesting the presence of cyclonic circulation right next to the coast. The presence of this cyclonic cell is consistent with the recurrent unstable quasi-stationary BC frontal meander named the Cape São Tomé eddy [Silveira et al., 2008; Calado et al., 2010]. This cyclonic cell produces northward flow inshore from the BC main jet observed during some of the AX97 realizations (Figure 3, middle panel).

The regional circulation during August 2004 (Figure 4, bottom panel), which corresponds to the third regime, indicates that the crest of the northern high cell was even further to the south, almost not crossing AX97 at all. The main finding here is that that the BC is weaker and most of

the velocity vectors appear parallel to the section, hence explaining the absence of the BC main jet from the in situ observations (Figure 3, bottom panel). In this case, the BC seems to intensify further to the south of the AX97 transect.

5. Summary

The variability of the baroclinic velocity associated with the BC along the AX97 XBT transect is related to both the migration of the South Atlantic gyre northern high-sea level cell and, closer to the continental boundary, to the development of a cyclonic vortex off Cape São Tomé. As the BC mean flow is relatively weak, these features can impose strong spatial and temporal variability to the associated transports leading to weak mean baroclinic transports. Ongoing research using AX97 observations will be able to document this observed variability and link the BC transport changes to other sources of variability in the area, such as the rough topography of the Vitoria-Trindade submarine ridge, a major topographic feature just to the north of this XBT transect.

References

AVISO, 2011: Ssalto/Duacs User handbook: (M)SLA and (M)ADT Near-Real Time and Delayed Time Product. Ref: CLS-DOS-NT-06-034, 57pp.

Calado, L., I. C. A. Silveira, A. Gangopadhyay, and B. M. Castro, 2010: Eddy-induced upwelling off Cape São Tomé (22°S, Brazil). Cont. Shelf Res., 30, 1181-1188.

Campos, E. J. D., 2006: Equatorward translation of the Vitoria Eddy in a numerical simulation, Geophys. Res. Lett., 33(22), L22607, doi:10.1029/2006GL026997.

Campos, E. J. D., J. E. Gonçalves, and Y. Ikeda, 1995: Water mass characteristics and geostrophic circulation in the South Brazil Bight - summer of 1991. J. Geophys. Res., 100(C9), 18537-18550.

Hansen, D. V., and W. C. Thacker, 1999: Estimation of salinity profiles in the upper ocean. J. Geophys. Res., 104(C4), 7921-7933.

Mattos, R., 2006: Feições de meso e grande escalas da Corrente do Brasil ao largo do sudeste brasileiro. MSc Thesis, University of Sao Paulo, 126 pp.

Oliveira, L. R., A. R. Piola, M. M. Mata, and I. D. Soares, 2009: Brazil Current surface circulation and energetics observed from drifting buoys, J Geophys Res, 114, C10006, doi:10.1029/2008JC004900.

Peterson, R. G., and L. Stramma, 1991: Upper-level circulation in the South Atlantic Ocean. Prog. Oceanogr., 26, 1–73.

Rio, M. H., and F. Hernandez, 2004: A mean dynamic topography computed over the world ocean from altimetry, in situ measurements, and a geoid model. J. Geophys. Res., 109, C12032, doi:10.1029/2003JC002226.

Silveira, I. C. A., L. B. de Miranda, and W. S. Brown, 1994: On the origins of the North Brazil Current. J. Geophys. Res., 99(C11), 22501-22512.

Silveira, I. C. A., L. Calado, B. M. Castro, M. Cirano, J. A. M. Lima, and A. D. S. Mascarenhas, 2004: On the baroclinic structure of the Brazil Current-Intermediate Western Boundary Current system at 22°-23°S, Geophys. Res. Lett., 31(14), L14308, doi:10.1029/2004GL020036.

Silveira, I. C. A., J. A. M. Lima, A. C. K. Schmidt, W. Ceccopieri, A. Sartori, C. P. F. Franscisco, and R. F. C. Fontes, 2008: Is the meander growth in the Brazil Current system off Southeast Brazil due to baroclinic instability? Dynam. Atmos. Oceans., 45(3-4), 187-207.

Stramma, L., and M. England, 1999: On the water masses and mean circulation of the South Atlantic Ocean. J. Geophys. Res., 104(C9), 20863-20883.

Stramma, L., and F. Schott, 1999: The mean flow field of the tropical Atlantic Ocean, Deep-Sea Res. Pt II, 46(1-2), 279-303.

Tsuchiya, M., 1985: Evidence of a double-cell subtropical gyre in the South Atlantic Ocean. J. Mar. Res., 43, 57–65.

van Caspel, M. R., M., Mauricio, and M. Cirano, 2010: On the TS relationship in the central region of the Southwest Atlantic: a contribution for the study of ocean variability in the vicinity of the Vitória-Trindade chain, Atlântica, 32(1), 95-110.

Vianna, M. L., V. V. Menezes, and D. P. Chambers, 2007: A high resolution satellite_only GRACE_based mean dynamic topography of the South Atlantic Ocean, Geophys. Res. Lett., 34, L24604, doi:10.1029/2007GL031912.

Vianna, M. L., and Menezes, V. V., 2011: Double-celled Subtropical Gyre in the South Atlantic Ocean: Means, Trends and Interannual Changes. J. Geophys. Res., 116, C03024, doi:10.1029/2010JC006574.
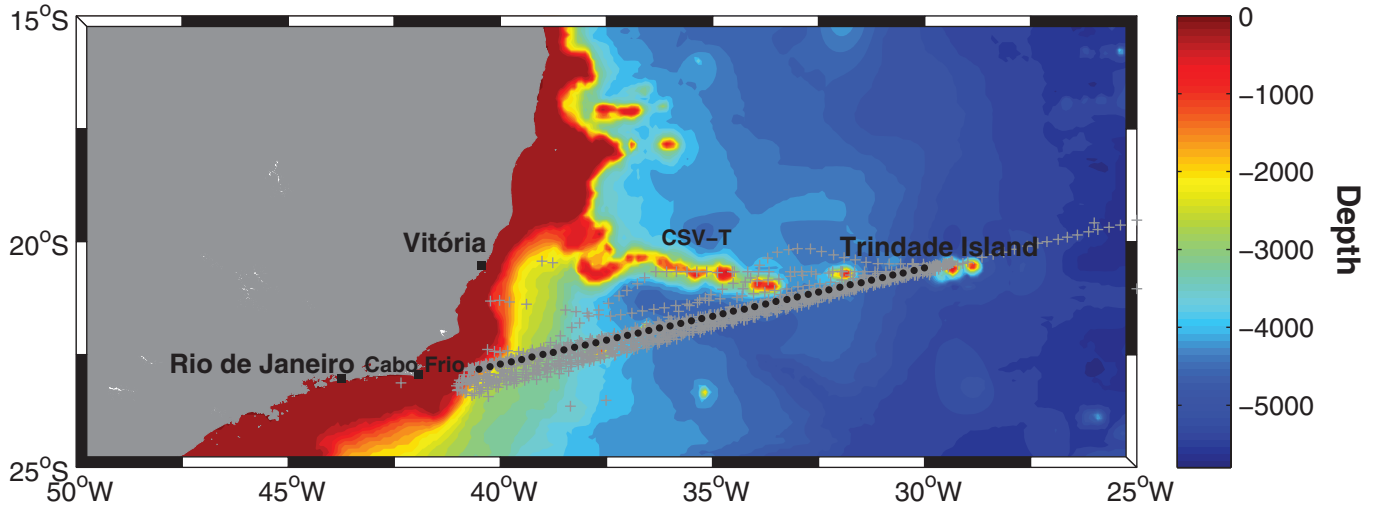
Fig 1: The AX97 transect with deployment positions (grey) and the reference transect (black dots). The main ship route goes from Cabo Frio City to Trindade Island. The regional bathymetry is shown in the background (units in metres). The position of the Vitoria-Trindade Submarine Ridge is indicated (CSV-T).
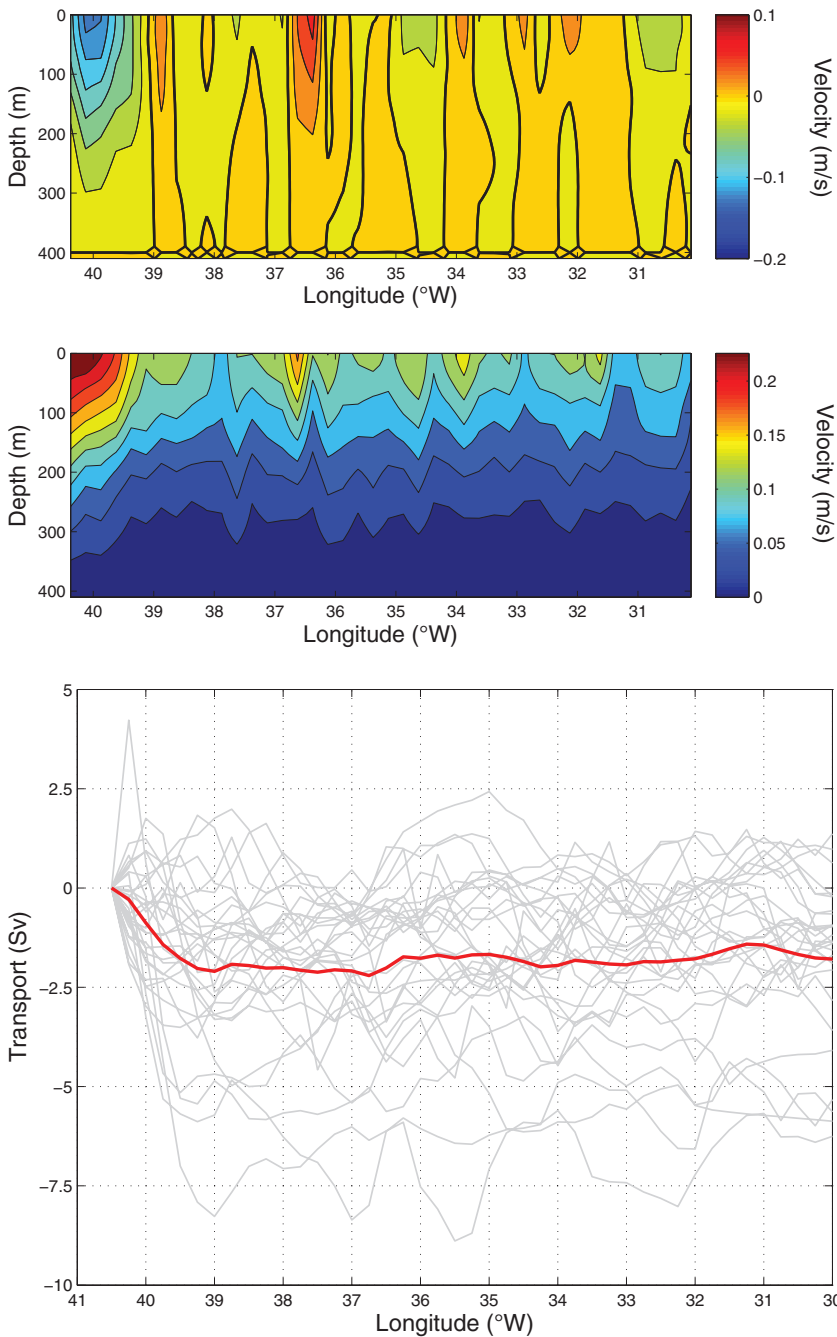

Fig 2: (top) The average baroclinic velocity field along the AX97 transect (referenced to 400 dbar) and (middle) the corresponding standard deviation. Negative values indicate southward flows and the zero velocity line is marked in bold. (bottom) Zonally integrated baroclinic transports (in Sv, referenced to 400 dbar) for the 29 available AX97 realizations (grey) and the corresponding average (red).
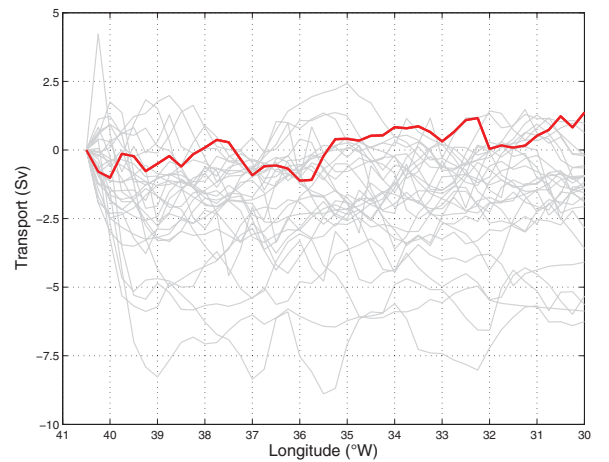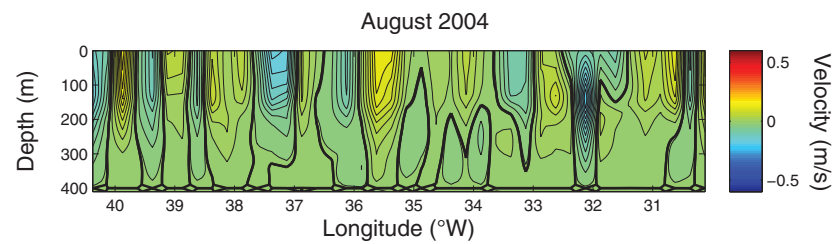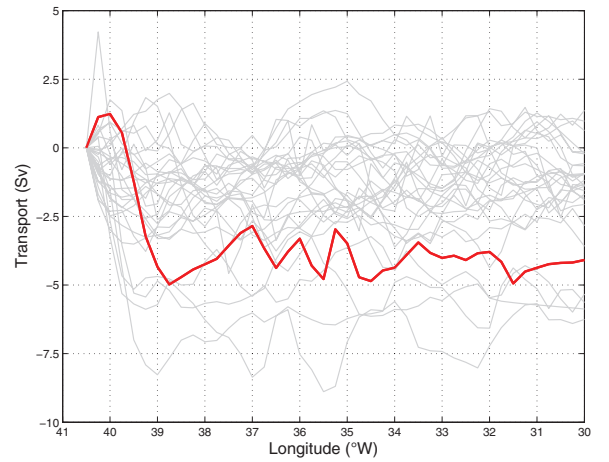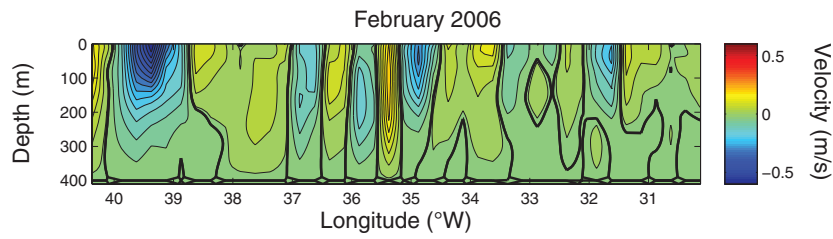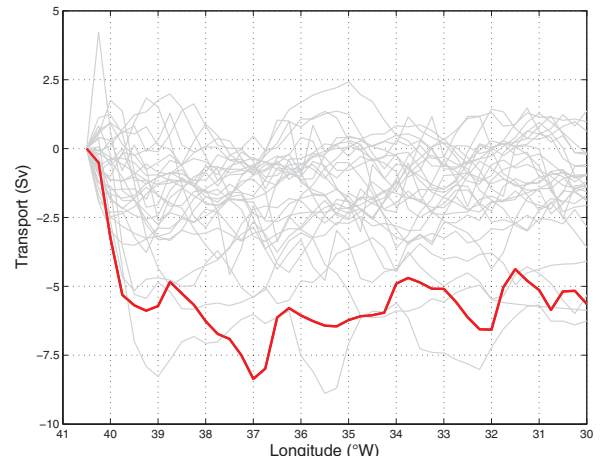
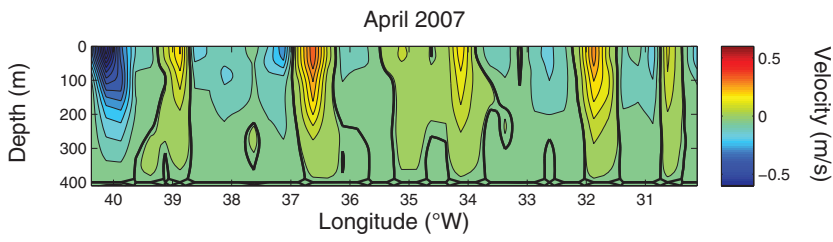Fig 3: The baroclinic velocity field along the AX97 transect referenced to 400 dbar (left) and the corresponding zonally integrated transports (right) for the following cruises: (top) April 2007, (middle) February 2006 and (bottom) August 2004. The units are m.s-1 and Sv for the velocity field and transports, respectively. Negative values indicate southward flow and the zero velocity line is marked in bold.
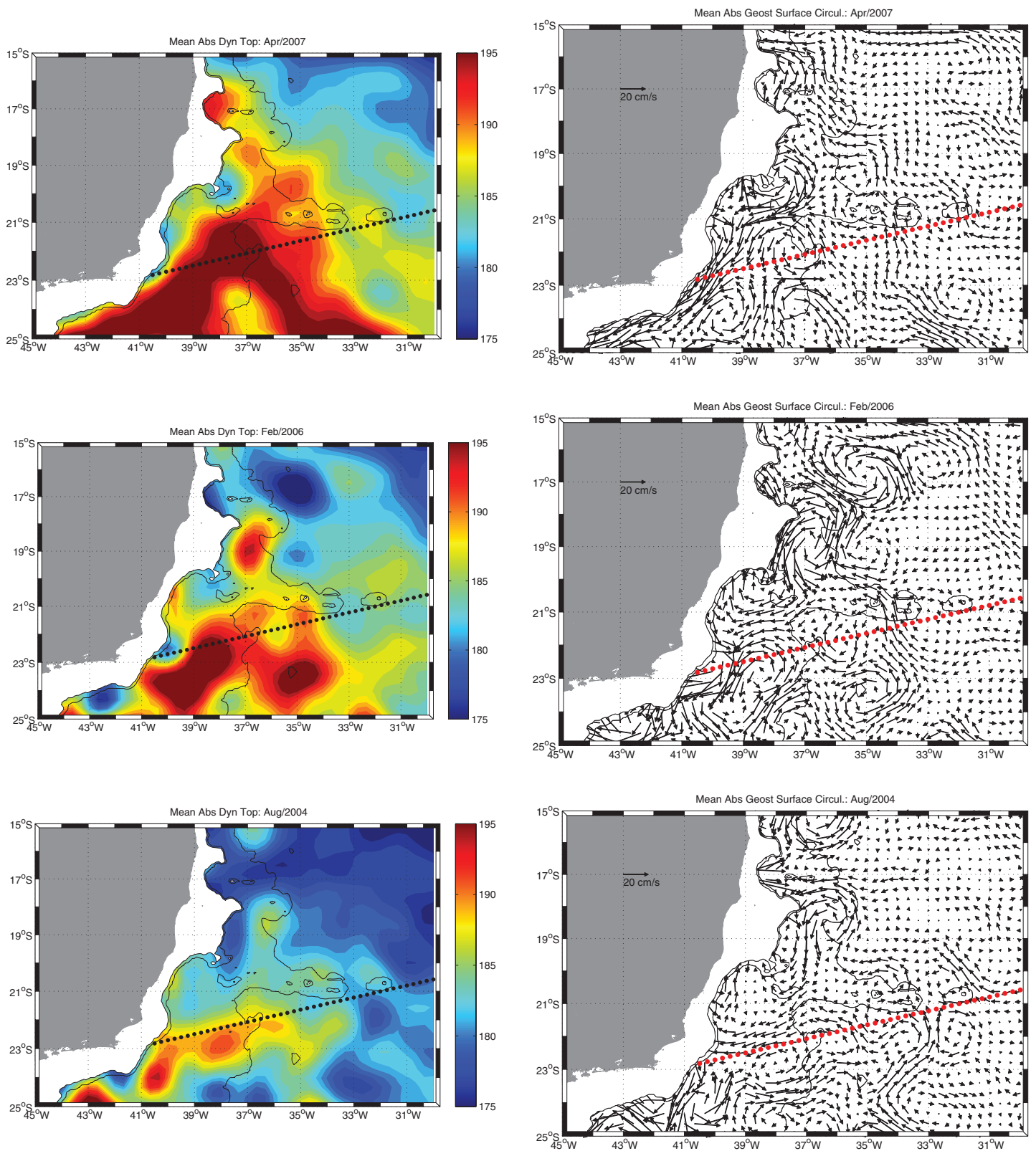
Fig 4: The regional Absolute Dynamical Topography field (left) and the corresponding surface geostrophic circulation (right) for the following cruises: (top) April 2007, (middle) February 2006 and (bottom) August 2004. The units are dyn.cm and cm.s-1 for the dynamical topography and surface geostrophic currents, respectively. The dots indicate the AX97 reference line.

SFB 754: Climate-Biogeochemistry Interactions in the Tropical Ocean

A. Oschlies[1,2], P. Brandt[1,2], C.K. Schelten[2], L. Stramma[2] and the SFB 754 consortium[1,2,3]

1   Christian-Albrechts University of Kiel, Germany
2   Helmholtz Centre for Ocean Research Kiel (GEOMAR), Germany
3   Max Planck Institute for Marine Microbiology, Bremen, Germany

Project summary

The Collaborative Research Centre (Sonderforschungsbereich, SFB) 754 has been funded by the German Research Foundation (Deutsche Forschungsgemeinschaft, DFG) since January 2008. After passing a thorough evaluation by an international review board, the second research period started in January 2012. The SFB 754 addresses climate induced ocean deoxygenation, with a focus on tropical oxygen minimum zones (OMZ) in the Atlantic and Pacific, and implications for the global marine biogeochemical system.

The overall scientific goal of the SFB 754 is to understand the coupling of tropical climate variability and circulation with the ocean's oxygen and nutrient budgets, to quantitatively evaluate the functioning of oxygen-sensitive microbial processes and their impact on biogeochemical cycles, and to assess potential consequences for the ocean's future. The overall goal can be broken down into three main scientific questions:

1   How does subsurface dissolved oxygen in the tropical ocean respond to variability in ocean circulation and ventilation?

2   What are the sensitivities and feedbacks linking low or variable oxygen levels, organic matter dynamics, and key nutrient source and sink mechanisms? In the benthos? In the water column?

3   What are the magnitudes and time scales of past, present and likely future variations in oceanic oxygen and nutrient levels? On the regional scale? On the global scale?

In addressing these basic science issues, the SFB 754 will be able to answer questions of key relevance for assessing impacts of climate change on the future ocean and its ecosystem; e.g., what is the likelihood that future climate change will lead to significant shifts in the ventilation, oxygen balance and hence nutrient cycling of tropical oceans, and ultimately, the entire ocean? More specifically: will the present-day oxygen minimum zones grow further in intensity and extent? How sensitive are oceanic nutrient inventories to changes in oxygen minimum zones? Could the tropical Atlantic low oxygen zone develop to become like today's very low oxygen zones in the Indian and Pacific Oceans with their significantly different biogeochemistry and ecosystems? Could positive feedbacks in a future warmer and high CO_2 world eventually result in interior ocean anoxia as has happened in the past?

The project consists of more than 80 researchers from the Christian-Albrechts University of Kiel, the Helmholtz Centre for Ocean Research Kiel (GEOMAR) and the Max-Planck Institute for Marine Microbiology (Bremen), working closely together in eight projects in the thematic area "Circulation and Oxygen" and eight projects in the thematic area "Redox-dependent Biogeochemistry" with tightly integrated modelling and field-work activities. In this article we will focus on the CLIVAR related work in subprojects of the thematic area "Circulation and Oxygen" in the tropical Atlantic (see Fig. 1).

Background

Oxygen-poor waters, called oxygen minimum zones (OMZs), occupy large volumes of the intermediate-depth eastern tropical oceans in the depth range between 100 and 900 m. They are a consequence of the combined effect of weak ocean ventilation, which supplies oxygen, and strong respiration, which consumes oxygen. Accordingly, the geographic location of OMZs in the open ocean is to a first order determined by the proximity to upwelling areas with associated high biological productivity and restricted to regions of generally sluggish horizontal transport, namely the "shadow zones of the ventilated thermocline" (Luyten et al., 1983) along the eastern boundaries.

The Northern Tropical Atlantic hosts two oxygen minima at about 70 m and 400 m depth, respectively. The shallow minimum is most pronounced near the coast between Senegal and the Cape Verde Islands and linked to subsurface remineralisation associated with high biological productivity and a shallow mixed layer (Karstensen et al., 2008). Offshore the deeper oxygen minimum exhibited record low minimum concentrations slightly less than 40 µmol l^{-1} during recent SFB 754 cruises (Stramma et al., 2009). In contrast to the Pacific the Northern Tropical Atlantic regime displays a nitrite maximum near the base of the euphotic zone, but lacks the second maximum within the OMZ. This is indicative that neither N_2O is consumed, nor denitrification is happening, consistent with measurements of the isotopic signature of nitrate in this region.

Project results of the first phase (2008-2011)

At the start of SFB 754, a detailed analysis of dissolved oxygen records from a few selected areas with sufficient data coverage in the tropical ocean revealed negative trends for the last 50 years in all ocean basins (Stramma et al., 2008), indicating a measurable expansion of the oxygen minimum zone in the Atlantic both horizontally and vertically. The strongest linear trend for the 300 to 700 m depth layer was found for an area in the eastern tropical North Atlantic (Fig. 2) with a loss of 0.34 +/- 0.13 µmol kg^{-1} per year since 1960. A more spatially expansive analysis conducted by comparing data between 1960 and 1974 with those from 1990 to 2008 supports the local analysis in that it identified oxygen decreases in most tropical

regions with an average rate of 2-3 μmol kg⁻¹ per decade (Stramma et al., 2010). Furthermore, at 200 dbar, the area with oxygen < 70 μmol kg⁻¹, where some large macro-organisms are unable to abide, has increased by 4.5 million km² between these two time periods. For the North Atlantic OMZ, data collected on the SFB cruises in the Atlantic revealed the lowest North Atlantic oxygen concentrations ever measured (Stramma et al., 2009), as well as a decrease in the scatter in the local oxygen-salinity relation, suggesting reduced ventilation by mesoscale eddies and zonal jets (Brandt et al., 2010). However, several open ocean regions also have experienced an increase in dissolved oxygen in the thermocline.

Although numerical models used and developed further during Phase I of the SFB have been able to reproduce many features of the marine oxygen distribution with some degree of realism (Oschlies et al., 2008), the simulated oxygen change over the last decades still shows little resemblance with the change inferred from observations. Likely reasons for these discrepancies are deficiencies in both the simulated circulation patterns and the biogeochemical processes. A common notion has been that high levels of numerically induced diapycnal mixing may explain the general failure of coarse-resolution models to adequately reproduce the OMZs (Keeling et al., 2010). However, Duteil and Oschlies (2011) showed that even coarse-resolution models could be run with realistic levels of diapycnal mixing and that this had relatively little impact on the still limited ability of the models to reproduce observed oxygen changes.

The contribution of physical and/or biogeochemical processes responsible for the observed oxygen decline remains largely unknown. Possible explanations for how changes in ocean physics may cause a decrease in the oceanic oxygen content include (i) changes in solubility, which has been found to explain about a quarter of the observed and simulated oxygen decline (Matear and Hirst, 2003), and (ii) changes in ocean circulation and ventilation (Bopp et al., 2002). Using an advection-diffusion tracer model, Brandt et al. (2010) showed that observed changes in the strength of the latitudinally altering zonal jets from 1972-85 to the more recent period 1999–2008 could contribute to the on-going deoxygenation of the eastern tropical North Atlantic OMZ. Results of the high-resolution modelling studies of the SFB 754 indicate that changes in tropical wind regime and the interhemispheric Atlantic meridional overturning circulation may affect the relative contribution of northern and southern source waters to the ventilation of the tropical North Atlantic OMZ. Since the history and oxygen content of northern and southern source waters differ considerably, this may have immediate impacts on the extent of the OMZ.

Possible biological and biogeochemical mechanisms that may cause a decrease in oceanic oxygen content were also investigated by the SFB. Extrapolating the findings of mesocosm studies of changes in carbon-to-nitrogen drawdown in response to changes in atmospheric pCO_2 (Riebesell et al., 2007), a global model study postulated a substantial increase in heterotrophic respiration due to excess organic carbon formed at elevated CO_2 levels (Oschlies et al., 2008). For a business-as-usual CO_2 emission scenario, the model predicted

a 50% increase in the volume of suboxic waters by the end of the 21st century, whereas standard Redfield models suggest essentially unchanged suboxic water volumes at realistic levels of diapycnal mixing (Duteil and Oschlies, 2011).

In order to better constrain the oxygen supply by diapycnal mixing, a tracer release experiment was conducted in the northeast Atlantic OMZ. The experiment was designed to estimate the diapycnal mixing rate at the upper boundary of the deeper part of the OMZ. In April 2008, 92 kg of SF_5CF_3 was injected at 8°N, 23°W in the Guinea Dome area on the density surface σ_θ=26.88 kg m⁻³ at a depth of about 350 m. The tracer distribution was mapped out during three subsequent SFB cruises; 7, 20 and 30 months after the tracer release. Combining the best estimate diffusivity of $(1.2 \pm 0.1) \times 10^{-5}$ m²s⁻¹ (Banyte et al., 2012, under revision) with the observed vertical oxygen profiles, it has been shown that oxygen supply into the OMZ via diapycnal diffusion can explain 25-50% of the total oxygen consumption (Fischer, 2011; Karstensen et al., 2008). Thus, the majority of the oxygen consumed in the North Atlantic OMZ must be supplied by lateral transport mechanisms.

The mean circulation in the central tropical Atlantic – as observed by a large number of recent research cruises including those of the first phase of the SFB 754 as well as of the CLIVAR TACE (Tropical Atlantic Climate Experiment) program – is characterized by narrow east- and westward current bands. Because of a large-scale mean east-west gradient in the dissolved oxygen concentration in the central and intermediate water layers, eastward currents are generally associated with higher oxygen concentrations than westward currents. At the core depth of the tropical eastern North Atlantic OMZ at about 400 m, strongest eastward flow is found within the Northern Intermediate Countercurrent (NICC) at about 2°N. Above 400 m and below the surface mixed layer, the main supply pathways for oxygen-rich waters towards the eastern North Atlantic are the Equatorial Undercurrent (EUC) at the equator between the surface and 200 m, and the weaker eastward flow of the North Equatorial Undercurrent at about 5°N and the northern branch of the North Equatorial Countercurrent that is located at about 9°N.

Along the equator, a broad equatorial oxygen maximum is present in the observational dataset that is largely underestimated by or even absent in state-of-the-art GCMs. In conjunction with lateral eddy mixing it represents an important ventilation pathway toward the eastern tropical North Atlantic OMZ. This equatorial oxygen maximum cannot be explained alone by the mean circulation consisting of a westward flow, i.e., the Equatorial Intermediate Current (EIC) between the eastward NICC and Southern Intermediate Countercurrent (SICC) that are part of the latitudinally alternating zonal jet system. However, narrow oxygen tongues were identified to be superimposed to the mean EIC and could be traced from the western to eastern equatorial Atlantic (Brandt et al. 2008). These oxygen tongues are found to be associated with the presence of equatorial deep jets (EDJ) and are thought to be a ventilation pathway missing even in relatively high-resolution numerical models. The dynamics and periodicity of EDJ were studied using moored, float and satellite observations. These observations revealed a quasi-periodic behaviour of EDJ with period of about 4.5

years and amplitude of 10 to 20 cm/s (Brandt et al. 2011). The interannual variability of EDJ should be linked to a similar variability of the equatorial oxygen distribution, which is indeed suggested by meridional ship sections.

Project plans of the second phase (2012-2015)

The second phase of SFB 754 moves forward from the more exploratory first phase, which provided a very concise overview over the physics and biogeochemistry of OMZs, into targeted process studies that are required to obtain a complete and coherent picture of the relevant transport pathways, microbial processes, and ecological controls on the maintenance and the climate sensitivity of OMZs and their role in global nutrient cycles. The observational program of the second phase of SFB 754 in Thematic Area A "Circulation and Ocean" includes a tracer release experiment, an extension of moored time series stations and repeated ship sections as well as studies focussing on submesocale processes and on the fluxes of solutes released from or up taken by the sediments (Fig. 1).

An "Oxygen Supply Tracer Release Experiment (OSTRE)" will be performed in the centre of the OMZ at the density level of lowest dissolved oxygen concentration to estimate the lateral and vertical oxygen transfer. A simultaneous glider swarm study will be carried out and will focus on the fine scale structures of submesoscale features. Besides the moored and shipboard observations along 23°W, a new aspect will be process modelling that aims to better understand the dynamics of latitudinally altering zonal jets and EDJ, and a quantification of their contribution to the ventilation of the eastern tropical North Atlantic OMZ. Results of the process models are expected to lead to improved parameterizations that will allow a better understanding of the effects of advective ventilation pathways in ocean general circulation models. Relevant processes at the Mauritanian and Peruvian continental slopes and shelves will be studied, using measurements of solutes and microstructure profiling, by a mooring/lander program for measuring benthic fluxes and by glider campaigns aimed at identifying meso- and submesoscale physical processes relevant to the formation and retention of OMZs.

The focus of the high-resolution coupled ecosystem-circulation models will be on physical and biogeochemical processes in the evolution of the OMZs. A detailed analysis of the mechanisms by which different atmospheric forcing mechanisms can impact on oxygen supply to the tropical OMZs will be performed with very high-resolution models. A recently funded EUR-OCEANS Flagship project, closely linked to SFB 754, will explore to what extent vertical grid architecture (sigma vs z coordinates) can affect simulated oxygen dynamics close to the shelf. A direct confrontation with observed recent changes in physical and biogeochemical property distributions will provide information as to what extent forced circulation changes can explain observed changes. Biological and biogeochemical mechanisms that have been hypothesised to generate changes in oxygen concentrations (Taucher and Oschlies, 2011) will also be investigated.

Finally, SFB 754 will exploit coupled climate models to extrapolate impacts of climate change on simulated oxygen fields over the next 100 years. Possible effects of CO_2-induced climate change in the farther future will be investigated with coarser resolution Earth system models. The SFB 754 will also exploit paleo information on large changes in oxygen during the Holocene and during the onset of the Cretaceous anoxic events. The large signals suggested by sedimentary records may give valuable information on the underlying mechanisms despite the still considerable uncertainties about the state of the past ocean.

During the second phase of SFB 754, work on the thematic area "Circulation and Oxygen" described above will be carried out in close collaboration with projects of the thematic area "Redox-dependent Biogeochemistry". Thereby, we expect that we can develop a consistent picture of the interplay of the relevant physical, chemical, and biological processes associated with OMZs. The expected outcome will be a mechanistic understanding of controls on, and the impacts of, changing OMZs, and the provision of modelling tools adequate to predict the fate of tropical OMZs and their role in the climate system for various scenarios of environmental change.

References
Banyte, D., T. Tanhua, M. Visbeck, D.W.R. Wallace, J. Karstensen, G. Krahmann, B. Schneider, and L. Stramma, 2012: Diapycnal diffusivity at the upper boundary of the tropical North Atlantic oxygen minimum zone. J. Geophys. Res., (under revision).

Bopp, L., C. Le Quere, M. Heimann, A. C. Manning, and P. Monfray, 2002: Climate-induced oceanic oxygen fluxes: Implications for the contemporary carbon budget. Global Biogeochem Cycles, 16, 1022, doi:10.1029/2001GB001445.

Brandt, P., V. Hormann, B. Bourlès, J. Fischer, F. A. Schott, L. Stramma, and M. Dengler, 2008: Oxygen tongues and zonal currents in the equatorial Atlantic. J. Geophys. Res., 113, C04012, doi:10.1029/2007JC004435.

Brandt, P., V. Hormann, A. Körtzinger, M. Visbeck, G. Krahmann, L. Stramma, R. Lumpkin and C. Schmid, 2010: Changes in the ventilation of the oxygen minimum zone of the tropical North Atlantic. J. Phys. Oceanogr., 40, 1784–1801, doi: 10.1175/2010JPO4301.

Brandt, P., A. Funk, V. Hormann, M. Dengler, R.J. Greatbatch, J.M. Toole, 2011: Interannual atmospheric variability forced by the deep equatorial Atlantic Ocean. Nature, 473, 497-500, doi: 10.1038/nature10013.

Duteil, O., and A. Oschlies, 2011: Sensitivity of simulated extent and future evolution of marine suboxia to mixing intensity. Geophys. Res. Lett., 38, L06607, doi:10.1029/2011GL046877.

Fischer, T., 2011: Diapycnal diffusivity and transport of matter in the ocean estimated from underway acoustic profiling and microstructure profiling. PhD thesis, CAU Kiel, 106pp.

Karstensen, J., L. Stramma, and M. Visbeck, 2008: Oxygen minimum zones in the eastern tropical Atlantic and Pacific oceans. Prog. Oceanogr., 77, 331-350.

Keeling, R.F., A. Körtzinger, and N. Gruber, 2010: Ocean deoxygenation in a warming world, Ann. Rev. Mar. Sci, 2, 199-229.

Luyten, J.R., J. Pedlosky, and H. Stommel, 1983: The ventilated thermocline. J. Phys. Oceanogr., 13, 292-309.

Matear, R.J. and A.C. Hirst, 2003: Long term changes in dissolved oxygen concentrations in the ocean caused by protracted global warming. Global Biogeochem. Cycles, 17(4), 1125, doi: 10.1029/2002GB001997.

Oschlies, A., K.G. Schulz, U. Riebesell, and A. Schmittner, 2008: Simulated 21st century's increase in oceanic suboxia by CO_2-enhanced biological carbon export. Global Biogeochem. Cycles, 22, GB4008, doi:10.1029/2007GB003147.

Riebesell, U., K.G. Schulz, R.G.J. Bellerby, P. Fritsche, M. Meyerhöfer, C. Neill, G. Nondal, A. Oschlies, J. Wohlers, and E. Zöllner, 2007: Enhanced biological carbon consumption in a high CO_2 ocean. Nature, 450, 545-548.

Stramma, L., G.C. Johnson, J. Sprintall, and V. Mohrholz, 2008: Expanding oxygen-minimum zones in the tropical oceans, Science, 320, 655-658.

Stramma, L., M. Visbeck, P. Brandt, T. Tanhua, and D. Wallace, 2009: Deoxygenation in the oxygen minimum zone of the eastern tropical Atlantic, Geophys. Res. Lett., 36, L20607, doi:10.1029/2009GL039593.

Stramma, L., S. Schmidtko, L.A. Levin, and G.C. Johnson, 2010: Ocean oxygen minima expansions and their biological impacts. Deep-Sea Res. I, 57, 587-595.

Taucher, J., and A. Oschlies, 2011: Can we predict the direction of marine primary production change under global warming? Geophys. Res. Lett., 38, L02603, doi:10.1029/2010GL04534.
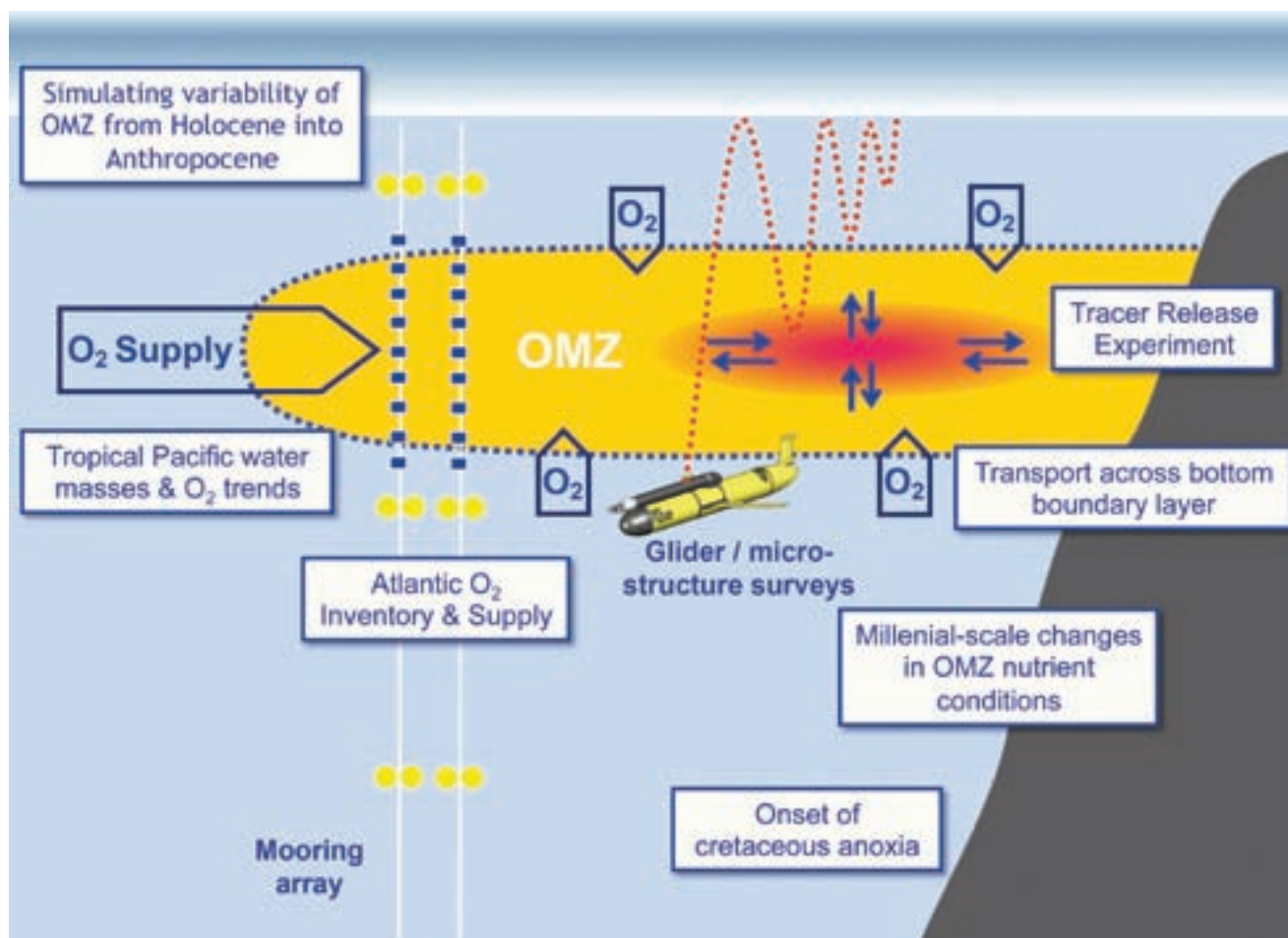
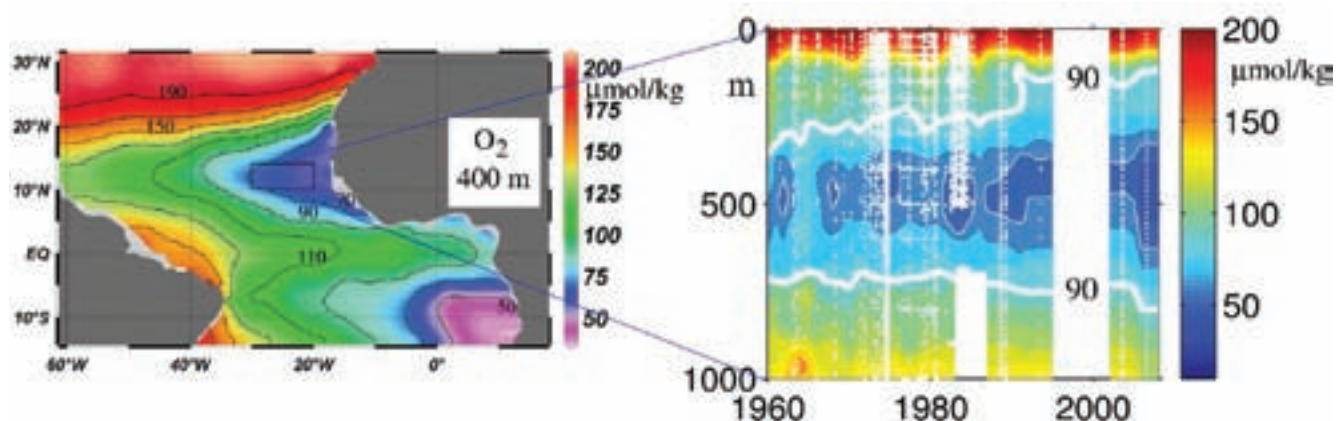Fig. 1: Research topics of projects in thematic area "Circulation and Oxygen".

Fig. 2: Climatological mean dissolved oxygen concentration (µmol kg^{-1}) in the tropical Atlantic at 400 m depth (left) and oxygen concentration changes versus time (1960-2008) and depth in the eastern tropical North Atlantic 10° to 14°N, 20° to 30°W (right) (after Stramma et al. 2008).

OCEAN2K

Placing historical marine conditions into the context of the past 2,000 years

A Progress report on the PAGES (Past Global Changes)/ Ocean2k Project

Ocean2k Project Members[1]

Following a suggestion from the CLIVAR Scientific Steering Group (SSG) and a meeting of the PAGES 2k[1] network leadership in Bern, July 2011, the PAGES Scientific Steering Committee (SSC) endorsed the formation of a ninth group focusing on the global oceans during the last 2,000 years (2K): Ocean2K. Motivating this project is an interest in placing observed historical marine conditions into the context of climatic variation over the past 2,000 years (Box 1). A description of project goals was described in PAGES News, 20(1), 2012[1]; this report is a brief progress update since. Two outputs are planned: a metadatabase of Ocean2k-relevant paleodata and paleomodeling simulations; and a preliminary synthesis of the principal common features in the underlying data and model output, both to be developed in time for consideration in the IPCC's Working Group I Fifth Assessment Report, and ultimately contributing to the PAGES2K synthesis planned for 2014/2015.

> ### Box 1: Motivating questions
> • What are the principal patterns of variation in ocean properties observed in both paleodata and paleomodeling simulations forced with realistic external forcings?
> • What are the most likely underlying mechanisms?

Phase I: Paleodata metadatabase construction.

Our first goal is a metadatabase[1] (Box 2) of Ocean2k-relevant paleoproxy records and model output from publicly-accessible and citable sources. As development of the CMIP5/PMIP3 modeling databases is not yet complete, we decided early on to first develop the paleodata metadatabase, create robust data syntheses therefrom, and then extract suitable comparison diagnostics from available paleoclimate model output. As of January 31, 2012, over 100 volunteers have evaluated or shortly will evaluate 984 candidate proxy records from different marine carbonate archives. Of these records, almost 290 meet criteria for relevance to Ocean2k goals (Box 2). About 300 potential records remain to be screened. This is an impressive volunteer community effort! Secondary screening and analysis of the paleodata (Figure 1) is just beginning, but we hope that we can detect in the data and simulations the ocean imprint of large-scale variations in processes such as the Atlantic Meridional Overturning Circulation, annular mode activity, monsoon circulations, and El Nino-Southern Oscillation (ENSO).

> ### Box 2: Ocean 2K metadatabase components and criteria
> • Paleoproxy metadatabase of marine origin: from the public NOAA/WDC-A (http://www.ncdc.noaa.gov/paleo/) and PANGAEA (http://pangaea.de/) data portals
>   - Variable: local interpretation of the measured proxy data
>   - Time interval: any portion of the past 2000 years
>   - Minimum chronological resolution: 1 date per 200 years, as applicable
>   - Uncertainty: internal and/or external reproducibility; interpretation, or bulk uncertainty
>   - Reference: a citation in the peer-reviewed literature is available
>   - Data link: A URL to the data source in a publicly accessible data repository
> • Climate model output metadatabase: from the public CMIP5 (http://cmip-pcmdi.llnl.gov/cmip5/data_portal.html) and PMIP3 (http://pmip3.lsce.ipsl.fr/) data portals
>   - Variable, time interval, uncertainty, reference
>   - Metadata to be determined by results of paleodata metadatabase development
>   - Data link: A URL to the model output in a publicly-accessible data repository

Phase II: Preliminary Paleodata/Model Synthesis

The second goal is a synthesis paper, and our initial focus will be to examine whether surface temperature or proxy data compilations are consistent with existing paleoclimate reconstructions primarily derived from terrestrial datasets (the primary focus of the other PAGES 2K working groups). As a simple illustration and practical target, we will study whether the conventional wisdom of a generally warm Medieval Climate Anomaly (MCA; roughly 950-1300 AD) and cold Little Ice Age (LIA; roughly 1450-1850 AD), is valid for the oceans. We will review the principal interpretable features in the data and paleosimulations, discuss likely underlying mechanisms, identify leading uncertainties in the data, model output, and results of our analysis, and highlight areas for future research. Given the short timeline of this phase of the project, our plan is to proceed as follows (Box 3). About 36 project members have volunteered for the synthesis phase of the project.

Box 3: Planned Preliminary synthesis

- Finish reviewing candidate data for inclusion into the Ocean2k paleodata metadatabase.
- Perform secondary screening of the candidate data.
- Organize synthesis group into small teams by expertise.
- Perform simple, reproducible, traceable data analyses on selected subsections of the paleoproxy data, concentrating initially on large-scale surface temperature estimates and widely available proxy measurements, such as oxygen isotopic composition of marine carbonates.
- Evaluate whether the Ocean2k synthesis is consistent with existing and terrestrial-based proxy evidence for climate variability and change over the past 2000 years.
- Identify for future work if variations in processes such as the thermohaline circulation, El Nino-Southern Oscillation (ENSO), and the Atlantic Multidecadal Oscillation (AMO) are detectable in the paleodata and paleomodeling simulations.
- Develop, revise and submit a preliminary Ocean2k synthesis paper by July 2012.

Ocean2k is currently not planning project meetings. Instead, we are working independently, using weekly-to-biweekly internet-based teleconferencing for regular discussions. Further information on project goals is regularly updated at the Ocean2k webpages: http://www.igbp-pages.org/workinggroups/ocean2k/

We look forward to your comments on this project. Would you like to participate in the Ocean2k project? Please contact Mike Evans (mnevans@geol.umd.edu).

Fig 1: Map of the location of proxy records meeting Ocean2k criteria, first screening (December 2011-January 2012). Red and blue markers indicate "high" (>1 measurement/decade) and "low" (>1 measurement/200 years) resolution paleoproxy data, respectively; map current as of February 1, 2012. Secondary screening of the metadata entries for adherence to Ocean2k inclusion criteria (Box 2), and data synthesis, is underway. Purple shaded areas indicate approximate synthesis regions for the other indicated PAGES 2K projects.

SIBER and IOP: Joint activities and science results

Raleigh Hood[1], Weidong Yu[2], Yukio Masumoto[3], Jerry Wiggert[4], Wajih Naqvi[5], Jay McCreary[6], Zuojun Yu[6], and Lynnath Beckley[7]

1   Horn Point Laboratory, University of Maryland Center for Environmental Science, 2020 Horns Point Road, Cambridge, MD, 21613 USA
2   Center for Ocean and Climate Research, First Institute of Oceanography, SOA, Qingdao 266061, China
3   Research Institute for Global Change, Japan Agency for Marine-Earth Science and Technology, 3173-25 Showa-machi, Kanazawa-ku, Yokohama, Kanagawa 236-0001, Japan
4   Department of Marine Science, University of Southern Mississippi, 1020 Balch Blvd., Stennis Space Center, MS, 39529-9904 USA
5   National Institute of Oceanography, Dona Paula - 403 004, Goa, India
6   International Pacific Research Center, 1680 East-West Road, University of Hawaii, Honolulu, Hawaii, 96822 USA
7   School of Environmental Science, Murdoch University, South Street, Murdoch, 6150, Western Australia

1. Introduction to SIBER

The Sustained Indian Ocean Biogeochemistry and Ecosystem Research (SIBER) program is an emerging basin-wide, international research initiative sponsored jointly by the Integrated Marine Biogeochemistry and Ecosystem Research (IMBER) project and the Indian Ocean Global Ocean Observing System (IOGOOS) (Hood et al., 2011). The long-term goal of SIBER is to understand the role of the Indian Ocean in global biogeochemical cycles and the interaction between these cycles and marine ecosystem dynamics.

SIBER has been motivated by the deployment of coastal and open-ocean observing systems in the Indian Ocean that have created new opportunities for carrying out biogeochemical and ecological research. As described in Yu et al. (2012), the Indian Ocean Panel (IOP) is coordinating the deployment of a basin-wide observing system in the Indian Ocean (the Indian Ocean Observing System, IndOOS, which includes the Research Moored Array for African-Asian-Australian Monsoon Analysis and Prediction, RAMA). These deployments, which are already well underway, are accompanied by efforts to maintain the Argo float network and a variety of physical oceanographic survey and mooring support cruises. In addition, several nations in the Indian Ocean are deploying coastal observing systems. These observatories, which are focused primarily on physical measurements, provide foundational infrastructure that can support a wide variety of biogeochemical and ecological studies in both coastal waters and the open ocean. SIBER is a decade-long (Figure 1), multidisciplinary international effort that is designed to leverage these observing systems and other international programs in order to advance our understanding of biogeochemical cycles and ecosystem dynamics of the Indian Ocean in the context of climate and human-driven changes.

2. The emergence of SIBER and its linkage to the IOP

CLIVAR formed IOP in 2004 as an international committee charged with the duty of guiding sustainable ocean observing and climate research in the Indian Ocean: the IOP activities focus primarily on physical processes, e.g., atmosphere and ocean circulation and air-sea exchange at intraseasonal, interannual and multi-decadal time scales. The overarching goal of the IOP is to improve our understanding of the physical dynamics of the Indian Ocean and its teleconnections with the other ocean basins, with a view toward improving models and prediction. The IOP leadership recognized from its start the importance of establishing meaningful interdisciplinary ties and collaborations aimed at understanding how physical processes impact biogeochemical cycles and particularly air-sea CO_2 exchange and carbon export. Toward this end, they established a tradition of inviting chemists, biologists and ecologists to attend their annual panel meetings. The lead author of this article was invited to attend the 2006 IOP meeting in Hawaii. At that time the IOP was planning IndOOS/RAMA. However, in 2006 there was no equivalent panel or committee to act as a compliment to the IOP for guiding biogeochemical and ecological research in the Indian Ocean. The identification of this gap was the motivation for developing the SIBER program, i.e., to address the need for an international committee/program that can guide biogeochemical and ecological research in the Indian Ocean and capitalize on this opportunity to "piggy back" this research on emerging physical oceanographic studies and infrastructure buildup in the basin.

After several years of meetings, planning and negotiation the SIBER program emerged under IMBER and IOGOOS with close ties to the IOP. The connection to the IOP is maintained in two ways. First, cross membership between the IOP and SIBER Scientific Steering Committee (SSC) is arranged to promote continuous communication and exchange between the two groups. Second, the SIBER SSC and the IOP convene back-to-back meetings every year, which include a joint session to explicitly discuss ongoing and potential new interdisciplinary collaborations. Typically, several members of the SIBER SSC (composed mostly of biological, chemical and fisheries oceanographers) attend the entire IOP (composed mostly of physical oceanographers and atmospheric scientists) meeting and vice versa. This co-convening of annual meetings provides an important forum for a group of scientists to learn about ongoing and planned research in the Indian Ocean in disciplines outside their own. Though, perhaps, the most important function of these meetings is to provide an opportunity to get to know one another, which helps to foster long-term interdisciplinary collaborations.

3. Research themes, implementation strategy and timeline

The SIBER Science Plan and Implementation Strategy (Hood et al., 2011) ultimately emerged from concepts that were formulated and discussed at the first SIBER Conference convened in Goa, India in October 2006 (Hood et al., 2007, Hood et al., 2008) involving more than 200 participants, and significantly refined during a second SIBER Workshop convened in Goa, India in November 2007 (Hood et al., 2008) involving 30 participants. Both meetings were interdisciplinary and included scientists from Indian Ocean rim nations, Europe and North America. The information and ideas from these meetings have been condensed into six major research themes, each of which identify key issues and priority questions that need to be addressed in order to improve our understanding of the biogeochemical and ecological dynamics of the Indian Ocean and develop a capability to predict future changes. These themes can be broadly separated into three that are regionally focused and three that address broad scientific questions.

Regional Scientific Themes:

Theme 1: Boundary current dynamics, interactions and impacts *(How are marine biogeochemical cycles and ecosystem processes in the Indian Ocean influenced by boundary current dynamics?)*

Theme 2: Variability of the equatorial zone, southern tropics and Indonesian Throughflow and their impacts on ecological processes and biogeochemical cycling *(How do unique physical dynamics of the equatorial zone of the Indian Ocean impact ecological processes and biogeochemical cycling?)*

Theme 3: Physical, biogeochemical and ecological contrasts between the Arabian Sea and the Bay of Bengal *(How do differences in natural and anthropogenic forcing impact the biogeochemical cycles and ecosystem dynamics of the Arabian Sea and the Bay of Bengal?)*

General Scientific Themes:

Theme 4: Controls and fates of phytoplankton and benthic production in the Indian Ocean *(What are the relative roles of light, nutrient and grazing limitation in controlling phytoplankton production in the Indian Ocean and how do these vary in space and time? What is the fate of this production after it sinks out of the euphotic zone?)*

Theme 5: Climate and anthropogenic impacts on the Indian Ocean and its marginal seas *(How will human-induced changes in climate and nutrient loading impact the marine ecosystem and biogeochemical cycles?)*

Theme 6: The role of higher trophic levels in ecological processes and biogeochemical cycles *(To what extent do higher trophic level species influence lower trophic levels and biogeochemical cycles in the Indian Ocean and how might this be influenced by human impacts, e.g., commercial fishing?)*

The implementation plan for SIBER is divided into three major areas of science activity: 1) remote sensing studies, 2) modeling studies, and 3) in situ observations that all have the potential for leveraging existing physical observational infrastructure (See the SIBER Science Plan and Implementation Strategy for details at http://www.incois.gov.in/Incois/siber/siber.jsp or http://www.imber.info/index.php/Science/Regional-Programmes/SIBER). The timeline for SIBER meetings and symposia that have been convened to date and that are planned for the future are detailed in Figure 1.
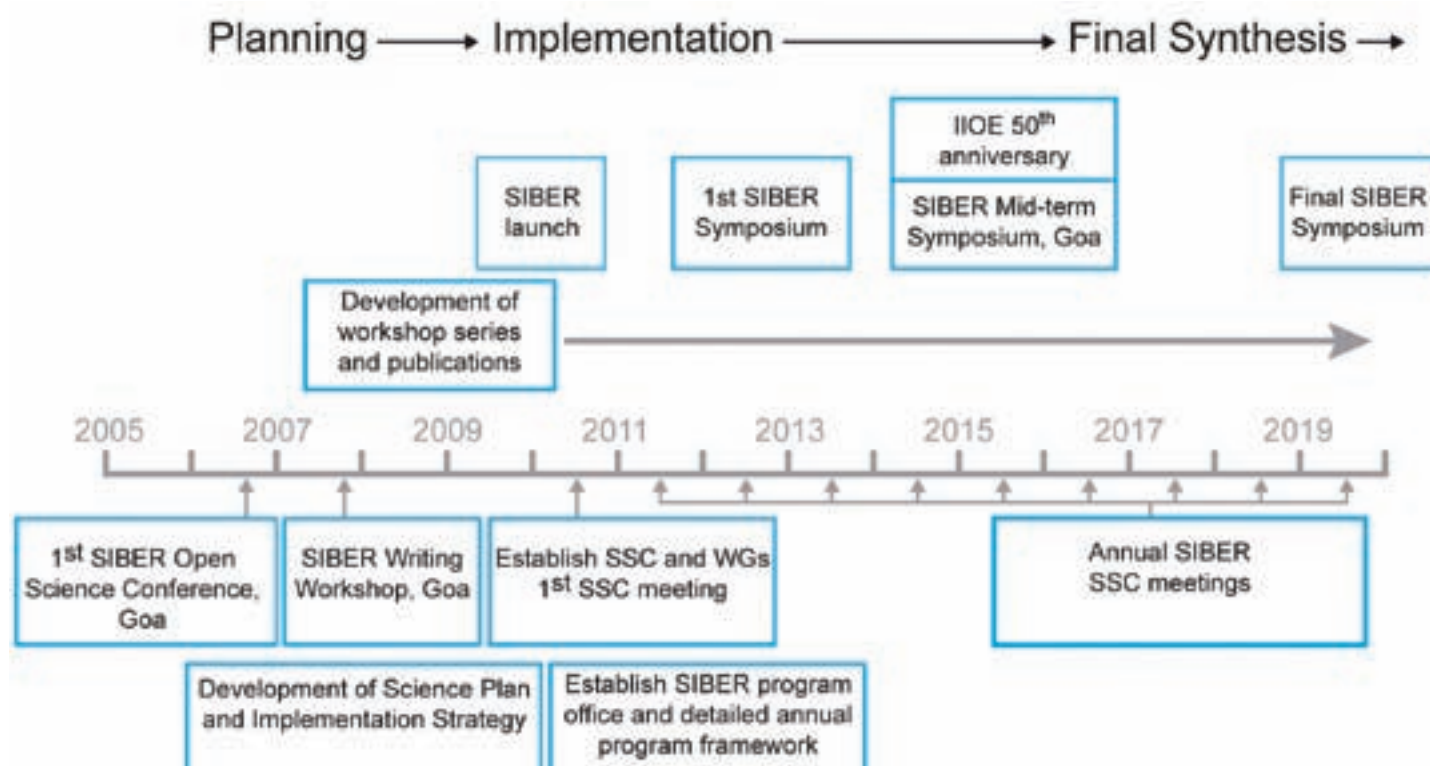

Fig 1: SIBER Program timeline from Hood et al. (2011)

4. Some emerging science activities and results

Several on-going interdisciplinary research activities have been instigated by SIBER and the IOP or have benefited from the programmatic framework that this linkage provides. For example, the 2006 SIBER conference motivated an interdisciplinary modeling study of the physical and biological factors that determine the spatial distribution of the oxygen minimum zone in the Arabian Sea (for a preview of this study see McCreary et al., 2011). The Arabian Sea Oxygen Minimum Zone (OMZ) is one of the most intense open-ocean OMZs in the world, with near-total depletion of oxygen at depths from 200 to 1000 m (e.g., Morrison et al., 1998). Yet, the physical and biological factors that determine the location and intensity of this feature have not been quantified and few, if any, models have successfully reproduced it. Of particular interest is the "eastward shift" of the upper OMZ into the central and eastern basin of the Arabian Sea. This shift is surprising because biological production is the largest in the western basin due to upwelling off Somalia and Oman. McCreary et al. (2011) have succeeded in simulating the major features of the observed oxygen field in the Indian Ocean, including the eastward shift (Figure 2).
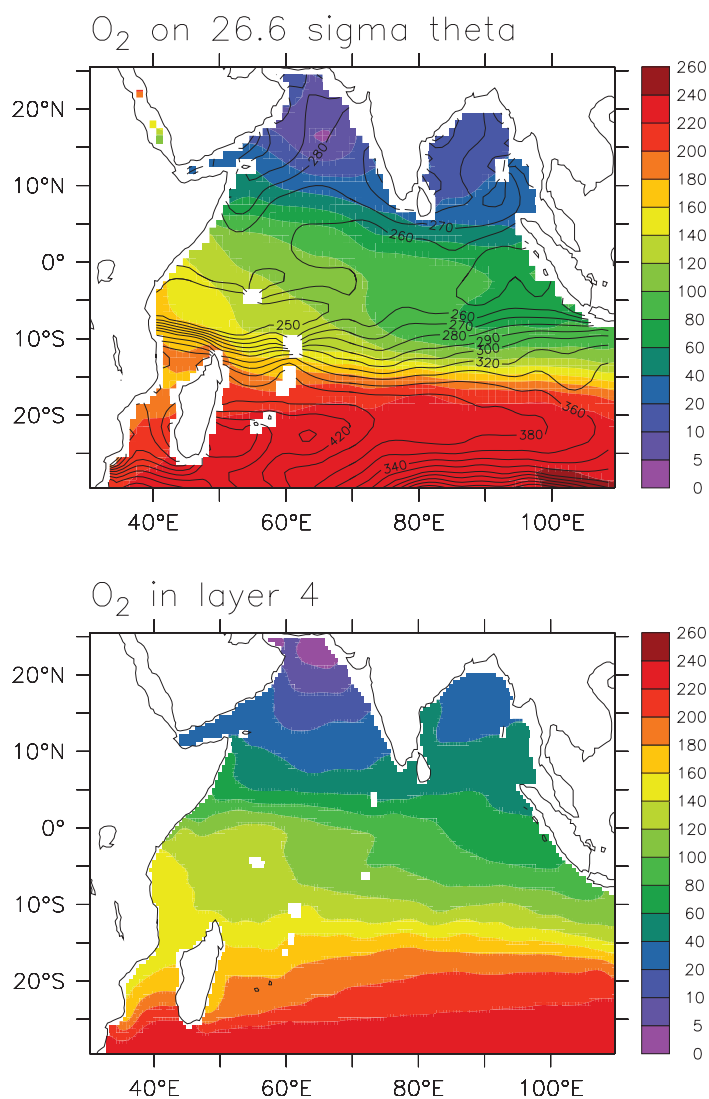

Fig 2: Maps of annual-mean oxygen concentrations from WOA05 on the 26.6-σ_θ surface (top) and from layer 4 (upper OMZ) of the physical model (bottom). Figure and caption modified from McCreary et al. (2011).

Among other things, they concluded that the eastward shift of the upper Arabian Sea OMZ results from two causes: 1) primarily northward advection of oxygenated waters along the western boundary of the basin; and 2) eddy-enhanced horizontal mixing, which is more vigorous along the west coast. In addition, they stressed that the remineralization and sinking rates of detritus must be sufficiently low for these two processes to impact the oxygen budget.

Similarly, exchanges between physical and biological oceanographers at joint SIBER/IOP meetings have led to new interdisciplinary collaborations focusing on the biogeochemical impacts of the Indian Ocean Dipole (IOD) (e.g., Wiggert et al., 2009). There has been a considerable amount of research over the last decade characterizing how the IOD modifies basin-wide physical variability. Along with this physical response, a clear biological impact has been revealed in ocean color data acquired by remote sensing platforms such as SeaWiFS. The signature feature illustrating IOD alteration of chlorophyll variability is the phytoplankton bloom that first appears in September along the eastern boundary of the Indian Ocean in tropical waters that are normally highly oligotrophic (Figure 3). Positive chlorophyll anomalies are also apparent (albeit less consistently) in the southeastern Bay of Bengal, while negative anomalies are observed over much of the Arabian Sea (Figure 3). Despite the clear basinwide influence of IOD events on biological variability, the accompanying influence on biogeochemical cycling that must occur has received little attention. Using a combination of satellite-derived physical and biological measurements (SST, SSH, surface winds, ocean color and primary production) Wiggert et al. (2009) show that there is a profound redistribution of where primary production and carbon uptake occurs in response to IOD events, with the eastern Indian Ocean deriving a significant enhancement at the expense of the western tropical Indian Ocean and to a lesser degree the Arabian Sea.

Several interdisciplinary studies are ongoing that are focused on the southern hemisphere boundary currents in both the western and eastern Indian Ocean and many of these projects fit both into SIBER Theme 1 and are also of considerable interest to the IOP (for an overview of these projects see Beckley, 2011). For example, studies of the transport by the east Madagascar Current, shelf-edge upwelling in northern Mozambique as well as zooplankton and seabirds associated with Mozambique Channel eddies. In the eastern Indian Ocean, much research relating to IOP interest in the physical dynamics of boundary currents and SIBER Theme 1 is ongoing off the west and northwest coast of Australia. Most of this research is multi-disciplinary and has benefitted from considerable governmental investment in Australia's Integrated Marine Observing System (IMOS) through installation of oceanographic moorings, reference stations, coastal radar, acoustic monitoring and deployment of gliders and Argo floats in the region that are being used to provide the physical observational context for biogeochemical and higher trophic level studies. At IMOS reference stations regular biological measurements are being made and the gliders are collecting fluorescence data.

At present, SIBER and IOP efforts are focused on finding the resources needed to deploy biogeochemical sensors on IndOOS/RAMA moorings (see SIBER SPIS, Appendix IV, available at http://www.imber.info/siber.html). The overarching objectives of this effort are to provide data for: 1) Defining biogeochemical variability in key regions of the Indian Ocean and for understanding the physical, biological and chemical processes that govern it; 2) Developing and validating models of ocean-atmosphere-biosphere interactions; and 3) Assessing the impacts of climate change on oceanic primary productivity and air-sea CO_2 exchange. Some preliminary attempts to deploy biogeochemical sensors on RAMA buoys have been carried out. NOAA instrumented a fluorometer at 25 m depth on one of its buoys deployed on 22 May 2010 at location 80.5°E, °N to measure the chlorophyll concentrations. FIO (First Institute of Oceanography, SOA, China) recently deployed its Bailong Buoy equipped with a pCO_2 system to measure the air-sea CO_2 flux at location 10°E, 8S on 28 Feb. 2011 (see Yu et al., 2012). Further plans and funding are now in place to deploy multiple biogeochemical sensor packages on RAMA and Indian moorings in the Bay of Bengal with the generous support from the Bay of Bengal Large Marine Ecosystem project (BOBLME, www.boblme.org).

5. Conclusions and legacy

Collaboration between SIBER and IOP offers a unique opportunity to mobilize the multidisciplinary, international research effort that will be required to develop a new level of understanding of the physical, biogeochemical and ecological dynamics of the Indian Ocean in the context of the global ocean and the Earth System. This understanding will be required to predict the impacts of climate change. It also provides an important new model for carrying out basin-scale interdisciplinary research that can lead to the long-term collaborations needed to achieve this goal. The collaboration between SIBER and the IOP has already fostered several new interdisciplinary studies in the Indian Ocean. This model can and should be applied in the other ocean basins.

References:
Beckley L (2011) SIBER Theme 1: Boundary current dynamics, interactions and impacts. IMBER Newsletter: No. 19

Hood R, Naqvi W, Wiggert J, Goes J, Coles V, McCreary J, Bates N, Karuppasamy PK, Mahowald N, Seitzinger S, Meyers G (2008) Research opportunities and challenges in the Indian Ocean. EOS, Transactions, American Geophysical Union 89:125-126

Hood RR, Naqvi SWA, Wiggert JD, Landry MR, Rixen T, Beckley LE, Goyet C, Cowie GL (2011) SIBER Science Plan and Implementation Strategy, IMBER Report No. 4, IOGOOS: pr: 07: SIBER/01, SIBER Report No. 1

Hood RR, Naqvi SWA, Wiggert JD, Subramaniam A (2007) Biogeochemical and ecological research in the Indian Ocean. EOS, Transactions, American Geophysical Union 88:144

McCreary J, Hood R, Yu Z (2011) Modelling the Arabian Sea oxygen minimum zone (ASOMZ). IMBER Newsletter: No. 19

Morrison JM, Codispoti LA, Gaurin S, Jones B, Manghnani V, Zheng Z (1998) Seasonal variation of hydrographic and nutrient fields during the US JGOFS Arabian Sea Process Study. Deep-Sea Research, Part II 45:2053-2101

Wiggert JD, Vialard J, Behrenfeld M (2009) Basinwide modification of dynamical and biogeochemical processes by the positive phase of the Indian Ocean Dipole during the SeaWiFS era. In: Wiggert JD, Hood RR, Naqvi SWA, Smith SL, Brink KH (eds) Indian Ocean Biogeochemical Processes and Ecological Variability. American Geophysical Union, Washington, D. C., p 385-407

Yu W, McPhaden MJ, Ning C, Wang H, Liu Y, Feitag HP (2012) Bailong Buoy: A new Chines contribution to RAMA. CLIVAR Exchanges, this issue
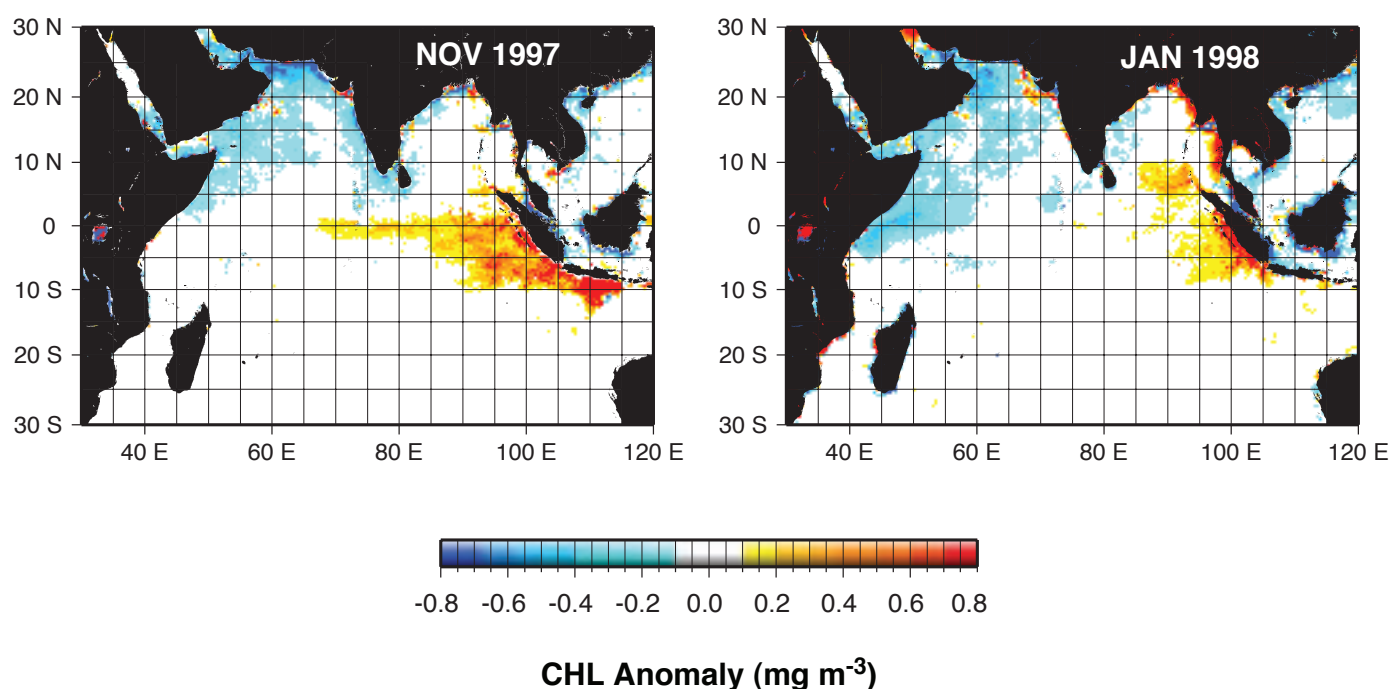
Fig 3: Distribution of chlorophyll anomaly observed by SeaWiFS during the 1997/98 IOD. Values in the range of ±0.1 mg m^{-3} have been masked in order to highlight the features of interest. Figure and caption modified from Wiggert et al. (2009).

Evaluation of Air-sea heat and momentum fluxes for the tropical oceans and introduction of TropFlux

B. Praveen Kumar[1], J. Vialard[2],
M. Lengaigne [1,2], V.S.N. Murty[3],
M.J. McPhaden[4], M.F. Cronin[4]
and K. Gopala Reddy[5]

1   National Institute of Oceanography, Council of Scientific and Industrial Research, Dona Paula, Goa, India
2   Laboratoire d'Océanographie: Expérimentation et Approches Numériques, CNRS, UPMC, IRD, Paris, France
3   National Institute of Oceanography, Regional Centre, Vishakhapatnam, India
4   NOAA/Pacific Marine Environmental Laboratory, Seattle, WA, USA
5   Centre for Bay of Bengal Studies, Department of Meteorology and Oceanography, Andhra University, Vishakhapatnam, India

Corresponding author: Jérôme Vialard, jerome.vialard@locean-ipsl.upmc.fr

Air-sea fluxes in the tropics

The tropics play an important role in the earth's climate and energy cycle. The tropical oceans gain heat from downward shortwave radiation, allowing for very high surface temperature (above 28 °C) in the Indo-Pacific and Atlantic warm pools. This high sea surface temperature can cause the atmospheric boundary layer to destabilize through upward latent and sensible fluxes and by providing moisture through evaporation, leading to the development of deep atmospheric convection. These air-sea interactions are crucial in setting up the Walker circulation, an essential component of the earth's climate. These interactions are also active through a continuum of time scales, from diurnal to interannual, and are involved in many tropical climate modes. At the intraseasonal timescale, for example, air-sea heat fluxes play a central role in theories of the Madden and Julian Oscillation, and in the monsoon active and break phases (Sobel et al., 2008). At the interannual timescale, air-sea momentum fluxes play a key role in the Bjerknes feedback, a positive feedback between the surface wind signal related to deep atmospheric convection and its dynamical oceanic response, which is critical to phenomena like El Niño (e.g. McPhaden et al., 2006) and the Indian Ocean Dipole (Webster et al., 1999; Saji et al., 1999). Those examples illustrate how an accurate knowledge of air-sea heat and momentum fluxes is required to understand the main modes of tropical climate variability.

There are a number of data sources for heat and momentum fluxes in the Tropics, and we are not aiming at an exhaustive description here. Historically, air-sea flux atlases were based on in-situ observational databases like those from the ICOADS project (http://icoads.noaa.gov/). While fluxes based on those products form an indispensable ground truth, the scarcity of in-situ data over the oceans allows monthly estimates at best. Since we aim at resolving intraseasonal variability, we will focus on products that offer a daily (or better) resolution. Satellite products have offered a considerable improvement for flux estimates, in particular in terms of spatial coverage of the surface wind estimates. We will focus here on the following widely used re-analyses: NCEP (1948-present, Kalnay et al., 1996), NCEP/DOE also known as NCEP2 (1979-present, Kanamitsu et al., 2002), ERA-Interim (1979-present, Dee et al., 2011). We will also consider two additional widely-used products: the OAFlux turbulent fluxes (Yu and Weller, 2007) combined with the International Satellite Cloud Climatology (ISCCP) Project radiative fluxes (Zhang et al., 2004) for heat fluxes and the QuikSCAT-derived gridded wind stresses estimated by CERSAT (Bentamy et al., 2002). We will also introduce our own heat and momentum flux estimates, which are largely derived from ERA-Interim and ISCCP data (Praveen Kumar et al., 2011, 2012).

Most of the flux estimates above are difficult to validate, for two reasons. The first difficulty is that there are no direct turbulent fluxes measurements, and one must rely on estimates of those fluxes (generally obtained from bulk algorithms, or, more rarely, through surface layer turbulence measurements). The second is that most available surface meteorological data are used in existing re-analyses, and therefore comparisons with those data is more an "evaluation" or "consistency test" rather than a true independent validation. In this paper, we take advantage of surface heat and momentum fluxes from the global tropical moored buoy array (McPhaden et al., 2010), which provides long-term surface meteorological time-series in the three tropical oceans (McPhaden et al., 1998; Bourlès et al., 2008; McPhaden et al., 2009). We will hereafter refer to this database as "TPR", for TAO/TRITON, PIRATA & RAMA arrays. Surface fluxes are estimated at TPR sites using the COARE v3.0 bulk algorithm (Fairall et al., 2003), through the methodology described in Cronin et al. (2006). This very large high quality data set from the TPR array can be used to check how well various products fit observed estimates at TPR sites, which is at least a guarantee of the quality of the re-analyses at those sites. The analyses shown below are however supported by extra comparisons with fully independent data (Praveen Kumar et al., 2011, 2012).

The TropFlux heat and momentum fluxes

The TropFlux project aims at producing timely and accurate heat and momentum fluxes over the tropical oceans. The TropFlux project is the result of a succesful collaboration between the National Institute of Oceanography (NIO/CSIR, India) and the Laboratoire d'Océanographie: Experimentation et Approches Numériques (LOCEAN/IPSL, France), sponsored by Institut de Recherche pour le Développement (IRD, France). A much more detailed description and evaluation of TropFlux heat and momentum fluxes can be found in Praveen Kumar et al. (2011, 2012). We only summarize the salient features of these papers below.

The following input variables are necessary to estimate heat and momentum fluxes from the COARE bulk algorithm: winds at 10 m, air temperature and specific humidity at 2 m, downward shortwave and longwave fluxes and sea surface temperature. The TropFlux strategy is to select the best source data for basic meteorological variables and apply appropriate ad-hoc corrections for possible caveats in bias and amplitude of variability. The corrections were applied on the basis of comparisons with TPR data. The corrected variables are then used with COARE v3.0 algorithm (Fairall et al., 2003) to develop TropFlux turbulent fluxes.

Extensive evaluation of the basic meteorological variables (Praveen Kumar et al., 2011), suggest that the ERA-Interim re-analysis 10 m winds and 2 m air temperature and specific humidity agree best with TPR data, despite some biases and underestimated variability amplitude. Sea surface temperature products display less contrast, and generally have the same level of performance. Finally, shortwave fluxes from re-analysis are generally much inferior to the ISCCP product. TropFlux is hence based on corrected ERA-I wind, air temperature and humidity and longwave radiations, and corrected ISCCP shortwave fluxes. Since TropFlux is computed from daily average quantities, a gustiness correction was applied to the wind to account for unresolved meso-scale variability, following a strategy close to the one in Cronin et al. (2006). Since ISCCP shortwave radiation is not routinely updated (available until 2009 at the time of writing), we also propose a strategy to provide a lower-quality but more timely estimate. This simple estimate uses the ISCCP shortwave mean seasonal cycle, but evaluates shortwave non-seasonal anomalies linearly from outgoing longwave radiations (OLR) non-seasonal anomalies. This strategy works very well in deep convection regions, but its performance is inferior to the ISCCP product (but superior to re-analyses) in other regions.

Evaluations of heat and momentum fluxed in the tropical region

In this section, we provide an evaluation of NCEP, NCEP2, ERA-Interim, TropFlux and OAFlux / QuikSCAT net heat and momentum fluxes against high quality estimates from the TPR array. Figure 1 shows correlation and rms-differences of the net heat flux and wind stress products to daily estimates from the TPR array over a 10-year period (2000-2009).

Wind stress products generally display higher correlations (between 0.8 and 0.95) than net heat fluxes (between 0.55 and 0.85), and are of more consistent quality. This is confirmed by quantitative analyses (Praveen Kumar et al., 2012), which indicate that there is generally more spread amongst net heat flux products than amongst wind stress products. This is probably due to three factors. First, surface winds appear to be of better quality than other surface meteorological parameters (air temperature and humidity), probably because they are more constrained by data (scatterometers, ship and buoy data, pressure measurements, etc.). Second, as mentioned earlier, most re-analyses seem to have difficulty in producing as good quality surface radiative fluxes as products like ISCCP, claiming for stronger constraints on those products in re-analyses. Third, the bulk algorithm used in the re-analyses to compute the heat fluxes can cause significant biases (Jiang et al., 2005).

NCEP re-analyses display the poorest agreement with TPR heat fluxes (r < 0.6 and rmsd > 50 Wm^{-2}). ERA-Interim has rather high quality heat fluxes (r~0.8 and rmsd~40 Wm^{-2}), but displays systematic biases (Praveen Kumar et al., 2011). OAFlux and TropFlux display the weakest systematic biases (not shown), and provide the best agreement to TPR net heat fluxes (r > 0.85 and rmsd < 30 Wm^{-2}).

The two NCEP re-analyses display poorer agreement to TPR wind stresses (r~0.8 and rmsd > 0.015 Nm^{-2}) than ERA-Interim (r~0.9 and rmsd~0.012 Nm^{-2}). ERA-I however suffers from an underestimated wind stress variability, which is largely corrected by TropFlux (Praveen Kumar et al., 2012) that displays the best agreement to TPR wind stresses (r=0.95 and rmsd<0.01 Nm^{-2}).

QuikSCAT wind stresses, which are generally considered as very high quality and used in many studies of the tropical ocean dynamical response, are in fact not better than NCEP wind stresses, and tend to overestimate mean wind stresses and their variability relative to the TPR estimates. Praveen Kumar et al. (2012) show from comparisons with TPR data that the QuikSCAT wind stress difference with TPR data clearly increases with rainfall, a very clear indication of contamination of scatterometer data by intense rainfall. In comparison, the dependency of the error on surface currents is weaker (the influence of surface currents on wind stress has also been mentioned as another possible source of difference between QuikSCAT wind stresses and other products).

The evaluations above suggest that TropFlux provides one of the best wind stress and heat flux daily product for an extended period (1979-2010 is now available) in the Tropics. The simple evaluations presented here are supported by more in-depth evaluations in Praveen Kumar et al. (2011, 2012), including validation to independent data. These evaluations also show that TropFlux agrees best with TPR data at most sites (and not only on average), and at various timescales (intraseasonal, seasonal, interannual).

Figure 2 allows one to get a feeling of the consistency and differences amongst various flux products, for a climatically relevant phenomenon. Figure 2 shows time-series of outgoing longwave radiation (OLR, a proxy of deep atmospheric convection), rainfall and surface heat and momentum fluxes at the RAMA 15°N, 90°E site, during the 2009 summer monsoon. The summer monsoon is associated with intraseasonal variations of the convection, at a quasi bi-weekly and at a 30-50 day timescale (e.g. Goswami 2005), which modulate rainfall over India. Those intraseasonal oscillations have a clear surface temperature response in the Bay of Bengal (e.g. Vialard et al., 2012), which may feedback on the atmospheric convection (e.g. Sobel et al., 2008). The grey stripes on Figure 2 are associated with "active" periods of intense convection (local minima in OLR values, Figure 2a). During these periods, there are strong winds in the Bay of Bengal that result both in strong wind stresses (Figure 2b), and intense latent heat fluxes. These intense latent heat fluxes combine with decreased surface shortwave radiation (due to clouds), and result in decreased net heat fluxes (Figure 2c).

While all products display qualitatively increased wind stresses and decreased heat fluxes for active convection phases, there are non-negligible differences between products. Not all products have the same quality, and the statistics for this site (see the rmsd indicated on Figures 2bc) generally confirm the overall statistics of Figure 1. QuikSCAT generally agrees with the other products, except during intense rainfall spells recorded by the mooring, when it strongly overestimates wind stress (Figure 2a and 2b). If QuikSCAT is excluded, there is generally a better agreement amongst wind stress products (Figure 2b) than amongst net heat flux products (Figure 2c). Indeed, while the rms-error of all wind stress products (< .04 Nm^{-2}) is generally weak compared to the active/break phase amplitude (up to 0.2 Nm^{-2}), this is not the case for heat fluxes (up to 101 Wm^{-2} compared to ~150 Wm^{-2}). Finally, on an event-to-event basis, there can be quite large differences between various products, in particularly in terms of fluxes. For example, Figure 2c shows a large spread amongst all flux products during the July 2009 active convection phase, and they all differ from TPR data.

Concluding Remarks

We have constructed a new air-sea heat and momentum flux product for the tropical oceans, named TropFlux. TropFlux displays among the best agreement with TPR data at most locations, and at all timescales. We hence think that this is a valuable product for studies of air-sea interactions in the tropical regions. TropFlux includes surface meteorological parameters (sea surface and air temperature, surface specific humidity and wind speed), heat flux components (latent, sensible fluxes, shortwave and longwave heat fluxes), wind stresses and its components. They are available on a 1°x1° grid between 30°S and 30°N, at daily and monthly resolutions from 1979 to 2010. We have plans to regularly update the product up to 3-4 months behind present. TropFlux products are freely available for scientific use and can be downloaded from http://www.locean-ipsl.upmc.fr/tropflux/ or from http://www.nio.org.

Another important outcome of this work is the evaluation of several widely used air-sea flux products in the Tropical regions. The main messages that come out of this evaluation are the following. 1) Wind stress products agree better amongst themselves than net heat flux products. 2) Most re-analyses suffer from systematic biases, and generally have deficient surface shortwave radiations. 3) The best available options are ERA-I / TropFlux for wind stresses and OAFlux / TropFlux for net heat fluxes.

We would have mainly two recommendations to formulate on the basis of this work. First, from the tropical air-sea interactions community perspective, it seems to be important to try to reduce systematic bias in re-analysed 2 m air temperature and specific humidity, and to try to constrain better surface shortwave radiations in re-analyses. Second, data sources like scatterometers and the TAO-Triton, PIRATA and RAMA moored networks are of utmost importance, both to constrain and evaluate re-analyses.

References

Bentamy. A., K.B. Katsaros, A. Mestas-Nuñez, W. Drennan, E. Forde, and H. Roquest, 2003: Satellite estimates of wind speed and latent heat flux over the global oceans, J. Climate, 16, 637-656.

Bourlès, B., R. Lumpkin, M. J. McPhaden, F. Hernandez, P. Nobre, E. Campos, L. Yu, S. Planton, A. J. Busalacchi, A. D. Moura, J. Servaom, and J. Trotte, 2008: The PIRATA Program : History, Accomplishments and Future Directions, Bull. Am. Meteorol. Soc., 89, 1111-1125.

Cronin, M. F., C. Fairall, and M. J. McPhaden, 2006: An assessment of buoy-derived and numerical weather prediction surface heat fluxes in the tropical Pacific. J. Geophys, Res, 111, C06038, doi:10.1029/2005JC003324.

Dee et al, 2011: The ERA-Interim reanalysis: configuration and performance of the data assimilation system. Quarterly Journal of the Royal Meteorological Society, 137, 553 597.

Fairall, C. W., E. f. Bradley, J. E. Hare, A. A. Grachev, and J. B. Edson, 2003: Bulk parameterization on air-sea fluxes : Updates and verification for the COARE algorithm. J. Climate, 16, 571-591.

Goswami, B.N., 2005, South Asian Monsoon. In Intraseasonal Variability in the Atmosphere-Ocean Climate System, W.K.M. Lau and D.E. Waliser (eds.), Praxis Springer, Berlin, 19-55.

Jiang, C., M.F. Cronin, K.A. Kelly, and L. Thompson, 2005: Evaluation of a hybrid satellite- and NWP-based turbulent heat flux product using Tropical Atmosphere-Ocean (TAO) buoys. J. Geophys. Res., 110, doi:10.1029/2004JC002824.

Kalnay et al., 1996: The NCEP/NCAR 40-year reanalysis project, Bull. Amer. Meteor. Soc, 77, 437-470.

Kanamitsu, M., W. Ebisuzaki, J. Woolen, J. Potter and M. Fiorino, 2002: NCEP/DOE AMIP-II Reanalysis (R-2). Bull. Amer. Met. Soc. 83, 1631-1643.

McPhaden, M. J., S. E. Zebiak, Sand, M.H. Glantz, 2006: ENSO as an integrating concept in Earth science. Science, 314, 1740-1745.

McPhaden, M.J., K. Ando, B. Bourlès, H.P. Freitag, R. Lumpkin, Y. Masumoto, V.S.N. Murty, P. Nobre, M. Ravichandran, J. Vialard, D. Vousden, and W. Yu, 2010: The global tropical moored buoy array. In Proceedings of the «OceanObs'09: Sustained Ocean Observations and Information for Society» Conference (Vol. 2), Venice, Italy, 21–25 September 2009, Hall, J., D.E. Harrison, and D. Stammer, Eds., ESA Publication WPP-306.

McPhaden, M. J., A. J. Busalacchi, R. Cheney, J. R. Donguy, K. S. Gage, D. Halpern, M. Ji, P. Julian, G. Mayers,, G. T. Mitchum, P. P. Niiler, J. Picaut, R. W. Reynolds, N. Smith, K. Takeuchi, 1998: The Tropical Ocean-Global Atmosphere (TOGA) observing system: A decade of progress. J. Geophys. Res., 103, 14,169-14,240.

McPhaden, M. J., G. Meyers, K. Ando, Y. Masumoto, V. S. N. Murty, M. Ravichandran, F. Syamsudin, J. Vialard, W. Yu, L. Wu, 2009: RAMA: Research Moored Array for African-Asian-Australian Monsoon Analysis and Prediction. Bull. Am. Met. Soc., 90, 459-480.

Praveen Kumar, B., J. Vialard, M. Lengaigne, V.S.N. Murty and M.J. McPhaden, 2011: TropFlux: Air-Sea Fluxes for the Global Tropical Oceans – Description and evaluation. Clim. Dynamics, online, doi: 10.1007/s00382-011-1115-0.

Praveen Kumar, B., J. Vialard, M. Lengaigne, V.S.N. Murty, M.J. McPhaden, M.F. Cronin and K. Gopala Reddy, 2012: TropFlux wind stresses over the tropical oceans: evaluation and comparison with other products. Clim. Dynamics, submitted.

Saji NH, Goswami BN, Vinayachandran PN, Yamagata T, 1999: A dipole mode in the tropical Indian Ocean. Nature, 401, 360−363

Sobel, A.H., E.D. Maloney, G. Bellon and D.M. Frierson, 2008: The role of surface fluxes in tropical intraseasonal oscillations. Nat. Geoscience, 1, 653-657.

Vialard. J., A. Jayakumar, C. Gnanaseelan, M. Lengaigne, D. Sengupta, 2012: Processes of intraseasonal sea surface temperature variability in the Northern Indian Ocean during boreal summer. Clim. Dynamics, online, DOI: 10.1007/s00382-011-1015-3.

Webster, P. J., Moore, A. M, Loschnigg, J. P, and Leben, R. R, 1999: Coupled oceanic-atmospheric dynamics in the Indian Ocean during 1997-98, Nature, 401, 356-360.

Yu, L., and R. A. Weller, 2007: Objectively Analyzed air-sea heat Fluxes (OAFlux) for the global oceans. Bull. Ameri. Meteor. Soc., 88, 527-539.

Zhang, Y. C., W. B. Rossow, A. A. Lacis, V. Oinas, and M. I. Mishchenko, 2004: Calculation of radiative fluxes from the surface to top of atmosphere based on ISCCP and other global data sets: Refinements of the radiative transfer model and the input data. J. Geophys. Res., 109, D19105, doi:10.1029/2003JD004457.
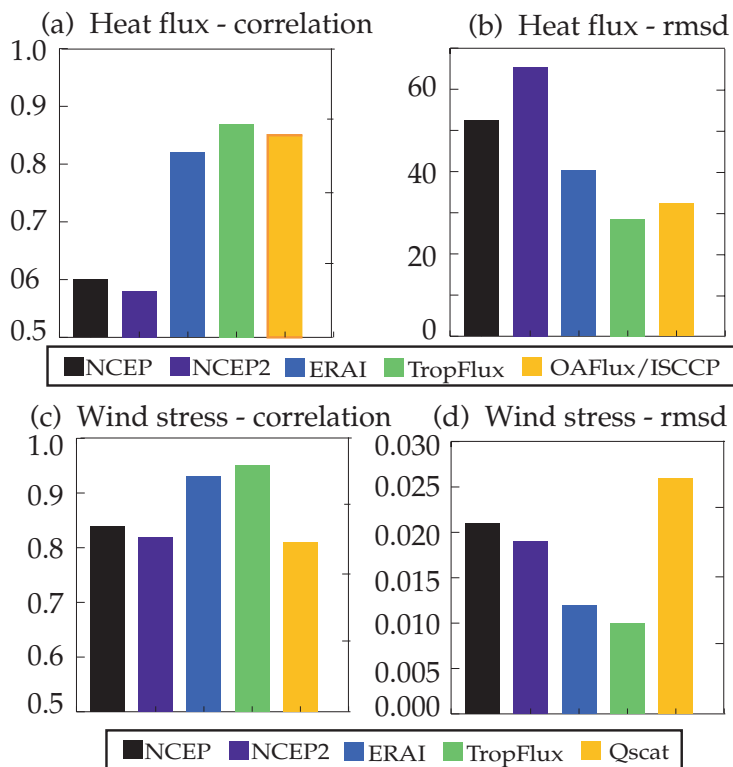
Fig 1: Bar diagrams showing correlations (a and c) and root mean square differences (b and d) of various net heat flux (a and b) and wind stress module (c and d) products to TPR array daily estimates. Statistics are computed over the 2000-2009 period at each site, and average statistics for all sites with more than two years of data are shown here. Root mean square differences are in W m^{-2} for net heat flux and N m^{-2} for wind stress module.

Fig 2: Time series of seven-day low-passed a) Outgoing longwave radiation (a proxy of deep atmospheric convection, Wm^{-2}), b) wind stress (Nm^{-2}) and c) net air-sea flux (positive downward, Wm^{-2}) at the 15°N, 90°E RAMA mooring during the 2009 monsoon. Low values in the first panel indicate deep atmospheric convection (monsoon active phases, roughly outlined from the grey stripes). The rain rate measured by the mooring is shown in red on panel a (mm hr^{-1}). Panels b and c show the RAMA mooring-derived air-sea fluxes estimates (thick, red curve) and estimates from the other products in various colors. The root-mean square difference of each product with TPR is indicated on panel b (in Nm^{-2} and c (in Wm^{-2}).
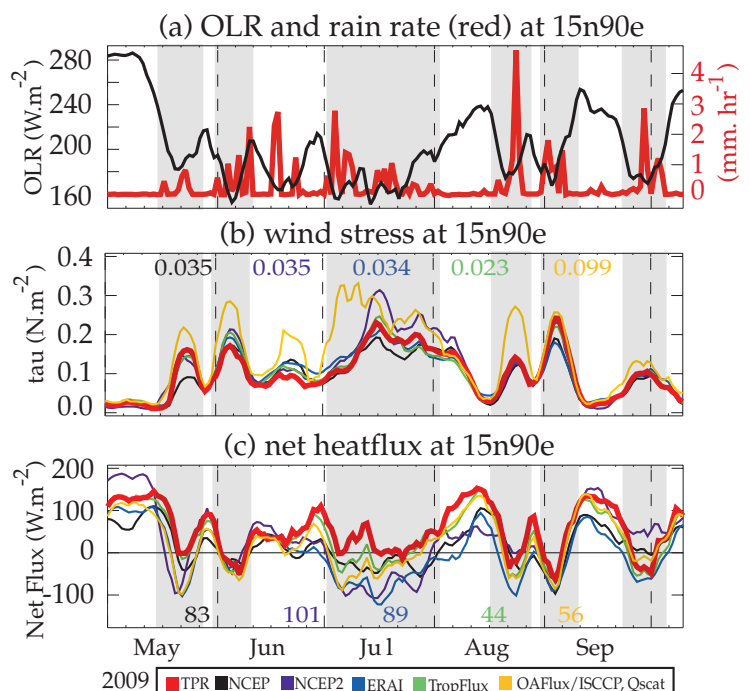
Bailong Buoy: A new Chinese contribution to RAMA

Yu W.[1], M. J. McPhaden[2], C. Ning[1],
H. Wang[1], Y. Liu[1], H. P. Freitag[2]

1   Center for Ocean and Climate Research, First Institute of
    Oceanography, SOA, China
2   Pacific Marine Environmental Laboratory, NOAA, USA

1. Introduction

The unique ocean-land configuration around the Indian Ocean brings forth the most significant monsoon climate system on earth, the African-Asian-Australian monsoon, through complex ocean-atmosphere-land interactions in response to seasonal variations in solar radiation. This monsoon climate influences billions of people through its seasonally alternating atmospheric circulation and rainfall. Whereas the monsoon reversals of wind and rain recur each year, they do so with sufficient variability to create floods and drought over vast parts of Southern and Eastern Asia, while tele-connections carry the climate anomalies to remote regions of the global scale. In response to this recognized role of the Indian Ocean in regional and global climate, the Indian Ocean Observing System (IndOOS) was planned (International CLIVAR Project Office, 2006) and implemented (Masumoto et al., 2010) under the guidance of the CLIVAR-GOOS Indian Ocean Panel (IOP). Among the various components of IndOOS, a key element is the Research Moored Array for African-Asian-Australian Monsoon Analysis and Prediction (RAMA) (McPhaden et al., 2009), which is the counterpart of TAO/TRITON in tropical Pacific and PIRATA in tropical Atlantic (McPhaden et al., 2010). The RAMA array is being implemented through international collaboration with mooring systems contributed by NOAA's Pacific Marine Environmental Laboratory (PMEL), the Japan Agency for Marine-Earth Science and Technology (JAMSTEC), the National Institute of Oceanography (NIO) of India and the First Institute of Oceanography (FIO) of China.

FIO is a new emerging player with its first Bailong buoy deployment at 8°S, 100°E in the tropical Southeastern Indian Ocean on 25 February 2010. The real time data stream has been publically released on the RAMA Webpage at http://www.pmel.noaa.gov/tao/rama/ and has been available since 29 May 2010. The Bailong buoy provides a third complementary mooring system (after PMEL's ATLAS and JAMSTEC's TRITON systems) to better understand the broad spectrum of air-sea interactions over the Equatorial Eastern Indian Ocean (EEIO), where variability associated with the Indian Ocean Dipole (IOD) is especially pronounced.

The present paper describes Bailong's technical configuration (section 2), demonstrates its scientific value in understanding the IOD (section 3) and highlights its utility for studies of air-sea CO_2 flux measurements (section 4). Finally we review overall progress in implementing RAMA array in section 5.

2. Technical configuration of the Bailong buoy

The Bailong buoy is designed as a flux-enhanced taut-line deep ocean mooring and is modeled after PMEL's ATLAS system used in TAO, PIRATA and RAMA. Its sensor configuration is similar to ATLAS (McPhaden et al., 2009) with some notable differences. For meteorological measurements, the ultrasonic wind sensor (WindSonic from Gill Instruments) is used to measure the wind. One of its advantages is no moving parts in comparison to the conventional cup and vane or propeller wind sensors. For oceanographic measurements, temperature and salinity measurements are made by seven SBE-37 CT sensors (at nominal depths of 1 m, 10 m, 20 m, 40 m, 60 m, 80 m and 100 m) and six SBE-39 T sensors (at nominal depths of 120 m, 140 m, 200 m, 300 m, 500 m and 700 m). Additionally, four Teledyne RDI Doppler Volume Sampler (DVS) current meters are mounted at 10 m, 20 m, 40 m and 100 m depths to measure the current in the mixed layer and in the thermocline. The Bailong mooring also integrates a CO_2 system (Pro-Oceanus Systems Inc.) into the measurement suite, to measure surface and subsurface pCO_2 alternatively at three-hour intervals.

The surface and subsurface data are collected by the DT-80 data logger through cable and inductive coupling transmission. The original 10-minute interval and variously averaged data are transmitted to FIO through Iridium satellite at 3-hour intervals. Iridium transmission provides immediate real time, large data volume and two-way communication, which efficiently improves the real time data return rate.

3. Identifying the barrier layer effect in the 2010 negative IOD event

The tropical Indian Ocean hosts a wide spectrum of variations, among which the Indian Ocean Dipole is considered as one prominent air-sea coupled mode with impacts not only in the region but also further far field through atmospheric teleconnections (Saji et al., 1999; Schott et al., 2009; Webster et al., 1999). In this regard, RAMA data will help improve our understanding of the dynamics and thermodynamics of the IOD, which further sets the guidelines of climate model assessment and improvement (Liu et al., 2011). It is noteworthy that 2010 witnessed a strong negative IOD event, which was the only negative IOD since 1992, in dramatic contrast to the recent highly active period of positive IOD events. Its uniqueness lies in at least two aspects. Firstly, there is an amplitude asymmetry with strong negative events being quite rare (Hong et al., 2008a, 2008b). Secondly, there is a recent unprecedented skew towards the positive IOD events, which is possibly the consequence of climate change (Cai et al. 2009a, 2009b). Therefore, it is scientifically interesting to examine the details of the negative IOD.

Data from the Bailong buoy provides a wonderful chance to look into one important process among others, i.e. oceanic barrier layer variations. It is understood that the barrier layer exits in the Eastern Equatorial Indian Ocean (EEIO) (Sprintall and Tomczak, 1992) with some seasonal variations (Qu and Meyers, 2005). However little is known about its

interannual variations, especially its potential contribution to IOD development. The first operational cycle (Mar. 2010 - Feb. 2011) of the Bailong buoy captured the formation of the thick barrier layer in response to heavy rainfall associated with the negative IOD. The temperature and salinity profile measured by the Bailong buoy is shown in Fig.1, where the isothermal layer depth (defined by the temperature criteria of 0.5ºC degree colder than SST) and mixed layer depth (defined by density criteria of 0.2 Kg m^{-3} greater than the surface density) are also shown. It is clear that the barrier layer separated the bottom of mixed layer from the upper thermocline. From March to July, the barrier layer thickness remained almost stable at around 10-20 m. A dramatic increase of barrier layer thickness (up to ~40 m) occurred in August, although there were some intraseasonal variations. This increase was caused by the shoaling of the mixed layer and deepening of the isothermal layer. In November, the barrier layer thickness reached almost 60 m when the mixed layer depth became less than 10 m and the isothermal layer deepened to more than 60 m. From the salinity structure, we can understand that the significant shoaling of the mixed layer after July was controlled by salinity-caused stratification. Based on TRMM data analysis (figure not shown), the southeastern tropical Indian Ocean received anomalously heavy rainfall, favoring strong stratification in the upper ocean. With the existence of a thick barrier layer, the cooling from the upwelling was heavily suppressed, hence favoring positive SST anomaly development. The positive SST anomalies could then potentially lead to enhanced rainfall. In this sense, there may have been a positive feedback between rainfall and SST, which favored the surprisingly strong negative IOD in 2010. The resultant excessive rainfall has profound social impacts, which in fact induced wet conditions during the usual Indonesian (especially in Java) dry season (June-September) and transition season (October-November).

4. Measuring air-sea CO_2 flux

The CLIVAR Indian Ocean Panel not only promotes the implementation of IndOOS, but also works closely with the Sustained Indian Ocean Biogeochemistry and Ecological Research (SIBER) program to initiate multidisciplinary research by taking full advantage of the RAMA array. Both programs include air-sea CO_2 flux measurement among their action list of high priorities and mutual interests. In situ CO_2 measurements are rare in the Indian Ocean, making it difficult to estimate the contribution of the highly variable Indian monsoons to global oceanic CO_2 fluxes (Takahashi et al., 2009).

FIO made the first buoy-based CO_2 flux measurement in the tropical Indian Ocean by deploying its CO_2-enhanced Bailong buoy in 28 February 2011. Forty-five days of CO_2 partial pressure in the air and surface water were obtained before the CO_2 sensor was damaged for undetermined reasons. Fig.2 shows that pCO_2 in the air was rather stable around 370 μatm, while the pCO_2 in the surface water showed more profound diurnal variations around 350 μatm. This buoy-observed pCO_2 is very consistent with 24 hours of pCO_2 measurements from the nearby ship. Further analysis (figure not shown) confirms that the variations of pCO_2 level in the surface water were mainly controlled by the SST diurnal cycle and that the influence from biological processes was rather weak during this period. These data clearly show that the tropical Southeastern Indian Ocean behaves as a CO_2 sink during the monsoon transition period. Longer time series data are necessary to assess the annual cycle of air-sea CO2 flux, especially during the boreal summer monsoon season.

5. Status of RAMA Implementation

The design of RAMA was based on a detailed scientific rationale (International CLIVAR Project Office, 2006). Initial RAMA implementation and early scientific progress up to 2008 were reviewed by McPhaden et al. (2009). By early 2012, the array is 65% complete, with 30 of the proposed 46 total mooring sites occupied (Fig. 3). This progress is the result of many fruitful bilateral and multi-lateral collaborations among nations both within and outside the Indian Ocean region. Instrumentation, equipment, ship time, personnel, and logistical support have been contributed by the United States, India, Japan, Indonesia, China, France, South Africa, the nine east and southern African nations that comprise the Aguhlas and Somali Current Large Marine Ecosystem (ASCLME) program and (as of September 2012) Australia. The existing 30 moorings cover the southern and eastern tropical Indian Ocean, leaving the northwestern tropical Indian Ocean yet to be completed.

RAMA benefits include scientific advances in our understanding of Indian Ocean variability and its impact on climate, as evident in a growing bibliography of refereed journal articles using RAMA data (http://www.pmel.noaa.gov/tao/rama/ramapubs.html). Because they are available on the GTS in real time, RAMA data are also utilized at operational weather, climate, and ocean forecasting centers around the world. Capacity building and technology transfer are also systematically being pursued as part of RAMA, with technical exchanges and training workshops held regularly each year.

Piracy in the northwest Indian Ocean is a major challenge to implementation and requires the development of security measures for cruises. Vandalism by fishermen, a common problem in TAO/TRITON and PIRATA, is likewise an issue in RAMA. Other challenges included provision of sufficient ship time and coordination of available ship time by various nations. These ongoing challenges will require solutions at intergovernmental levels. The IndOOS Resource Forum (IRF), which was established in 2010, helps to address these challenges in addition to coordinating national research commitments on behalf of the IOP. The IOGOOS office and the International CLIVAR Project Office provide logistic and financial support for IOP and the IOGOOS Office serves at the Secretariat for the IRF.

Reference

Cai, W., T. Cowan, and A. Sullivan, 2009a. Recent unprecedented skewness towards positive Indian Ocean Dipole occurrences and its impact on Australian rainfall, Geophys. Res. Lett., 36, L11705, doi:10.1029/2009GL037604.

Cai, W., A. Sullivan, and T. Cowan, 2009b. Climate change contributes to more frequent consecutive positive Indian Ocean Dipole events, Geophys. Res. Lett., 36, L23704, doi:10.1029/2009GL040163.

Hong, C.-C., T. Li, LinHo, J.-S. Kug, 2008a. Asymmetry of the Indian Ocean Dipole. Part I: Observational Analysis. J. Climate, 21:18, 4834-4848.

Hong, C.-C., T. Li, and J.-J. Luo, 2008b. Asymmetry of the Indian Ocean dipole. Part II: Model diagnosis. J. Climate, 21, 4849–4858.

International CLIVAR Project Office, 2006. Understanding The Role Of The Indian Ocean In The Climate System — Implementation Plan For Sustained Observations. January. International CLIVAR Project Office, CLIVAR Publication Series No.100.

Lin L., W. Yu and T. Li, 2011. Dynamic and Thermodynamic Air-Sea Coupling Associated with the Indian Ocean Dipole diagnosed from 23 WCRP CMIP3 Models, J. Climate. Doi: 10.1175/2011JCLI4041.1.

Masumoto, Y., W. Yu, G. Meyers, N. D'Adamo, L. Beal, W.P.M. de Ruijter, M. Dyoulgerov, J. Hermes, T. Lee, J.R.E. Lutjeharms, J.P. McCreary, Jr., M.J. McPhaden, V.S.N. Murty, D. Obura, C.B. Pattiaratchi, M. Ravichandran, C. Reason, F. Syamsudin, G. Vecchi, J. Vialard, and L. Yu, 2010. Observing systems in the Indian Ocean. In Proceedings of the "OceanObs'09: Sustained Ocean Observations and Information for Society" Conference (Vol. 2), Venice, Italy, 21–25 September 2009, Hall, J., D.E. Harrison, and D. Stammer, Eds., ESA Publication WPP-306.

McPhaden, M.J., G. Meyers, K. Ando, Y. Masumoto, V.S.N. Murty, M. Ravichandran, F. Syamsudin, J. Vialard, L. Yu, and W. Yu, 2009. RAMA: The Research Moored Array for African–Asian–Australian Monsoon Analysis and Prediction. Bull. Amer. Meteor. Soc., 90, 459–480. doi:10.1175/2008BAMS2608.1.

McPhaden, M.J., K. Ando, B. Bourlès, H.P. Freitag, R. Lumpkin, Y. Masumoto, V.S.N. Murty, P. Nobre, M. Ravichandran, J. Vialard, D. Vousden, and W. Yu, 2010. The global tropical moored buoy array. In Proceedings of the "OceanObs'09: Sustained Ocean Observations and Information for Society" Conference (Vol. 2), Venice, Italy, 21–25 September 2009, Hall, J., D.E. Harrison, and D. Stammer, Eds., ESA Publication WPP-306.

Qu, T. and G. Meyers, 2005. Seasonal variation of barrier layer in the southeastern tropical Indian Ocean, J. Geophys. Res., 110, C11003, doi:10.1029/2004JC002816.

Saji, N. H., B. N. Goswami, P. N. Vinayachandran, and T. Yamagata, 1999. A dipole mode in the tropical Indian Ocean, Nature, 401, 360– 363.

Schott, F. A, S.-P. Xie, and J. P. McCreary Jr., 2009. Indian Ocean circulation and climate variability. Rev. Geophys., 47, RG1002, doi:10.1029/2007RG000245.

Sprintall, J. and M. Tomczak, 1992. Evidence of the barrier layer in the surface layer of the tropics, J. Geophys. Res., 97, 7305–7316.

Takahashi, T., S. C. Sutherland, R. Wanninkhof, C. Sweeney, R. A. Feely, D. W. Chipman, B. Hales, G. Friederich, F. Chavez, A. Watson, D. C. E. Bakker, U. Schuster, N. Metzl, H. Yoshikawa-Inoue, M. Ishii, T. Midorikawa, Y. Nojiri, C. Sabine, J. Olafsson, Th. S. Arnarson, B. Tilbrook, T. Johannessen, A. Olsen, Richard Bellerby, A. Körtzinger, T. Steinhoff, M. Hoppema, H. J. W. de Baar, C. S. Wong, Bruno Delille and N. R. Bates, 2009. Climatological mean and decadal changes in surface ocean pCO2, and net sea-air CO2 flux over the global oceans. Deep-Sea Res. II, 56, 554-577.

Webster, P. J., A. Moore, J. Loschnigg and M. Leban, 1999. Coupled ocean-atmosphere dynamics in the Indian Ocean during 1997-98. Nature, 401, 356-360.
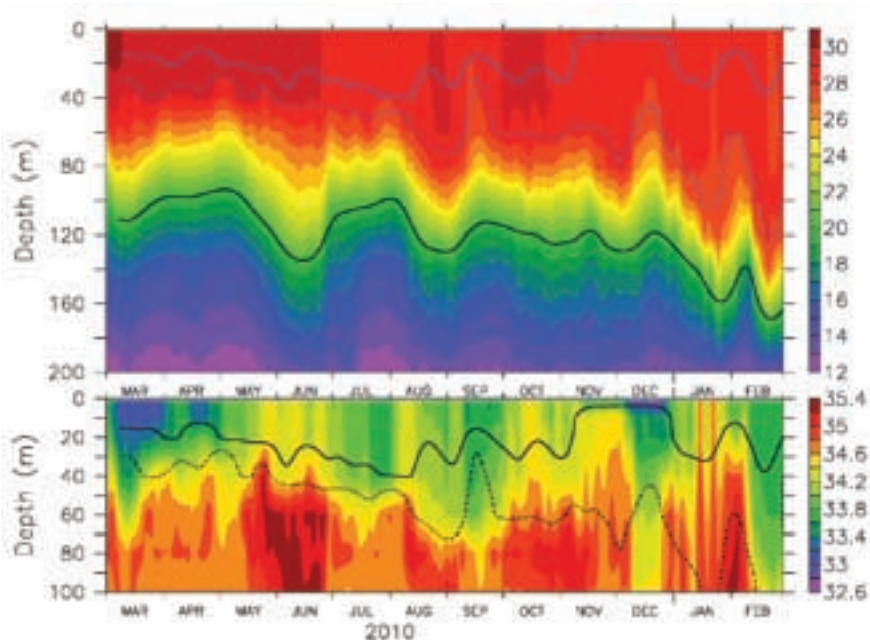
Fig.1 Upper ocean temperature (upper) and salinity (lower) data from Bailong buoy's first operation cycle (Mar 2010 to Feb 2011). The blue solid and dashed lines in the upper panel indicate the depth of the isothermal layer and the mixed layer, between which resides the barrier layer, while the solid black line in the upper panel represents the 20 °C isotherm. The black solid and dashed lines in the lower panel indicate the depth of the isothermal layer and the mixed layer.
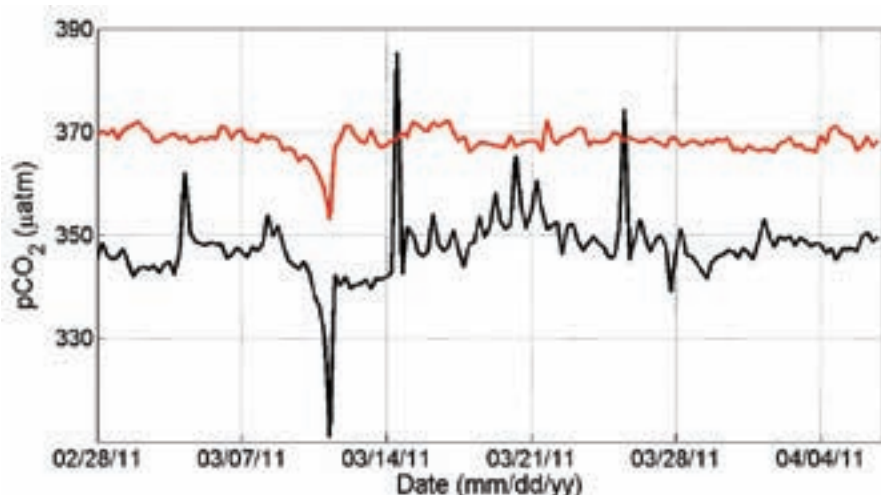

Fig.2 The pCO2 measurements of the air (red) and surfae water (black)
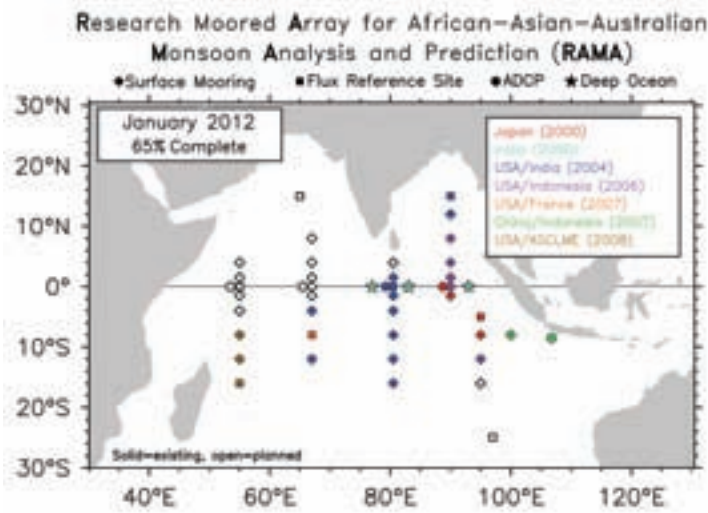
Fig.3 Schematic of RAMA as of Jan 2012. Filled symbols indicate occupied sites. Color coding indicates national support, with year of first involvement shown in the upper-right box. Open symbols indicate sites not yet instrumented. ASCLME is a consortium of nine African nations including Kenya, Tanzania, Mozambique, South Africa, Madagascar, Mauritius, Seychelles, Somalia, and Comoros.

Naming a western boundary current from Australia to the Solomon Sea

SPICE Community

* Corresponding author: alexandre.ganachaud@ird.fr

Upon arrival into the Coral Sea, the tropical part (~12°S-18°S) of the South Equatorial Current (SEC), encounters the coast of Australia and forms an equatorward western boundary current. This current carries important climate signals, which led to measurement campaigns in the early '80s, and more recently the emergence of the CLIVAR Southwest PacIfic Ocean circulation and Climate Experiment (SPICE). Along the coast of Queensland, this boundary current begins as the subsurface Great Barrier Reef Under Current (GBRUC); as it expands to the surface north of about 15°S it is known as the North Queensland Current (NQC) (Figure 1). South of the Louisiade Archipelago, a strong eastward current was noticed and labeled with several different names over the years: NGCUC,

NQC, and "Hiri Current" (HC), referring to a traditional trade route of the Motu people of Papua New Guinea. The western boundary current is continuous with the New Guinea Coastal Undercurrent (NGCU) in the Solomon Sea. However, the NGCU in the Solomon Sea has a different character because it is fed by both the Coral Sea boundary current and by a direct inflow from SEC waters of lower latitudes.

The pathways inside the Gulf of Papua, from the coast of Queensland to the Louisiade Archipelago, are nevertheless little documented, and both numerical models and Argo float data are showing a continuous western boundary current along the coast. Because of its continuity in both dynamics and water properties, it is proposed here that this current be given a unique name which would encompass the GBRUC, NQC and Hiri Current. For clarity, and referring to historical practice in physical oceanography, we propose to use the geographical denomination "Gulf of Papua Current" (GPC), referring mainly to subsurface waters (σ =26.5). This would not preclude the use of the aforementioned regional names, but clearly identify this continuum. We encourage referring to this unique name, which would be an achievement of the regional coordination that was initiated with SPICE, and would avoid perpetuation of confusing references.

Recent SPICE references are listed on http://www.ird.nc/UR65/SPICE/spice.html
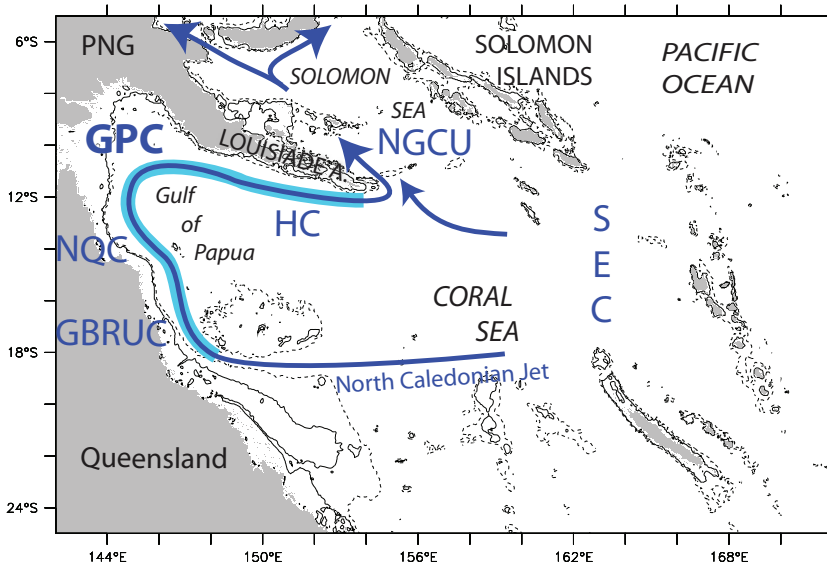

Fig 1: Topography and equatorward currents of the northwest Coral Sea. The westward flowing South Equatorial Current (SEC) feeds the Coral Sea western boundary current system: the Great Barrier Reef Under Current (GBRUC); the North Queensland Current (NQC); Hiri Current (HC) which constitute the continuous current around the Gulf of Papua, which we propose to name the "Gulf of Papua Current" (GPC). The 50 m and 1000 m isobaths are given respectively by the solid and continuous contour lines.

A first look at ENSO in CMIP5

Eric Guilyardi[1,2], Hugo Bellenger[1], Mat Collins[3], Samantha Ferrett[3], Wenju Cai[4], Andrew Wittenberg[5]

1   LOCEAN/IPSL, Paris, France
2   NCAS-Climate, University of Reading, UK
3   University of Exeter, UK
4   CSIRO, Melbourne, Australia
5   GFDL, Princeton, USA

Introduction

The El Niño–Southern Oscillation (ENSO) is a naturally occurring fluctuation that originates in the tropical Pacific region with severe weather and societal impacts worldwide (McPhaden et al. 2006). Despite considerable progress in our understanding of the impact of climate change on many of the processes that contribute to ENSO variability, it is not yet possible to say whether ENSO activity will be enhanced or damped, or if the frequency of events will change in the coming decades (Vecchi & Wittenberg 2010, Collins et al. 2010). As changes in ENSO have the potential to be one of the largest manifestations of anthropogenic climate change, this status has profound impacts on the reliability of regional attribution of climate variability and change.

One major reason for our lack of understanding is that, as ENSO involves a complex interplay of numerous oceanic and atmospheric processes, accurately modelling this climate phenomenon with Coupled Global Climate Models (CGCMs), and understanding, anticipating, and predicting its behaviour on seasonal to decadal and longer time scales still pose formidable challenges (Guilyardi et al. 2009a, Wittenberg 2009).

We here presents the first assessment of basic ENSO properties in control simulations of CMIP5 and a comparison with CMIP3. We use the metrics as developed within the CLIVAR Pacific Panel, which assess both the tropical Pacific mean state and interannual properties. The 4 ENSO metrics encompass ENSO amplitude (Niño3 SST std dev), structure (Niño3 vs. Niño4 amplitude), frequency (RMSE of Niño3 SSTA spectra) and heating source (Niño4 precipitation std dev). The other metrics deal with SST, zonal wind stress, precipitation and surface heat flux mean state and annual cycle (Guilyardi and Wittenberg 2010). We also take a preliminary look at simulations with increasing greenhouse gases (1%/year CO_2 increase and abrupt $4xCO_2$ idealised scenario) to examine if there are any robust signals of changes in ENSO in the new CMIP5 models.

We use multi-century pre-industrial simulations for both CMIP3 and CMIP5 as required to ensure statistical robustness (Wittenberg 2009, Stevenson et al. 2010). Simulation lengths are 300 years (but for MIROC-ESM-CHEM, 255 years and

HadGEM2CC, 240 years). The analysis in Figs 1 and 2 is presented per modelling centre to also assess progress (see Table 1 for official CMIP model names). Precise CMIP5-variables used in the analysis are detailed in the figure captions. Observations or reanalysis used for reference include HadISST1.1 (Rayner et al. 2003, years 1900-1999), ERA40 (Uppala et al. 2005), CMAP (Xie and Arkin 1997) and OAFlux (Yu and Weller 2007).

Modelling centre	CMIP3 model(s)	CMIP5 model(s)
BCC	n/a	BCC-CSM-1
CCCma	CGCM3.1	CanESM2
CNRM	CNRM-CM3	CNRM-CM5
CSIRO	CSIRO-Mk3.0	CSIRO-Mk3.6
GFDL	GFDL2.0 GFDL2.1	GFDL-ESM2M
GISS	GISS-AOM GISS-EH GISS-ER	GISS-E2-H GISS-E2-R
IAP	FGOALSg1.0	n/a
INM	INM-CM3.0	INM-CM4
IPSL	IPSL-CM4	IPSL-CM5A-LR IPSL-CM5A-MR
MIROC	MIROC3.2-MR MIROC3.2-HR	MIROC5 MIROC-ESM MIROC-ESM-CHEM
MOHC	HadCM3 HadGEM1	HadGEM2-CC HadGEM2-ES
MPI	ECHAM5/MPI-OM	MPI-ESM-LR
MRI	MRI-CGCM2.3.2	MRI-CGCM3
NCC	-	NorESM1-M

Table 1: CMIP3 and CMIP5 official model names per modelling centre.

Has ENSO performance in CGCMs improved since CMIP3 ?

A preliminary analysis of the metrics in Fig. 1 first shows that the range of modelled ENSO amplitude in CMIP5 (red dots in Fig. 1a) is reduced by about half compared to CMIP3 (blue dots). This is a clear improvement over the CMIP3 ensemble where this diversity was larger than could be explained by observational variability/uncertainty. Although we note that this is a preliminary result as not all modelling groups have submitted output at this stage and the spread of the CMIP5 models could still go up.

The ENSO amplitude, as measured by SST standard deviation, was too large in the central/west Pacific in CMIP3 CGCMs (Niño4 region, 0.8 °C compared to 0.65 °C in observations) and this has also improved in CMIP5 (0.6 °C). Nevertheless there is still the occasional model with spuriously more variability in the west than in the east Pacific (CSIRO-Mk3.6 in CMIP5, CCCma-CGCM3.1 in CMIP3). About half of the centres for which data is available for both CMIP3 and CMIP5 (11 centres) show an improvement in ENSO amplitude while the rest show no change or degradation.

The ENSO spectra metric (Fig. 1g) also shows an improved picture in CMIP5 when compared to CMIP3 even at the individual model level. As this metric is sensitive to slight shifts in modelled ENSO spectra and the real-world spectra may not be well constrained by the short observational record this result much be taken with caution. The heating source associated with ENSO, as measured by the Niño4 precipitation standard deviation (Fig. 1d), still exhibits large errors in most CMIP5 models with mixed improvements for individual centres.

The multi-model mean state metrics (Figs. 1c,e,f,h,i) do not exhibit significant changes from CMIP3 to CMIP5. At the individual level, half of the centres show some improvements, mostly marked for the mean zonal wind stress at the Equator in the Pacific (Fig 1h) while the net surface heat flux in the east Pacific is almost always degraded (Fig. 1i)

Atmosphere response during ENSO
Several studies point out the central role of the atmosphere general circulation model (GCM) response during ENSO in shaping the modelled ENSO (Capotondi et al. 2006, Kim et al.

2008, Guilyardi al. 2009b, Neale et al. 2008, Watanabe et al. 2010, Lloyd et al. 2011). The Bjerknes and heat flux response are computed in Fig. 2. There is no qualitative change in the multi-model mean Bjerknes feedback (Fig. 2a) although most centres exhibit an improvement in their models. The total heat flux response in Niño3 (Fig. 2b) is improved for a few models (CNRM, MIROC5) although most see a degradation (also seen in the mean heat flux - Fig. 1i) leading to more inter-model diversity than in CMIP3. Paradoxically, a number of centres have improved shortwave and latent heat flux response (Figs. 2c-d) even though the multi-model mean value does not evolve much. Conversely a number of models have degraded shortwave heat flux response with more models having a positive feedback instead of the observed negative value of -7 Wm^{-2}/C.

While it would have been tempting to conclude from simply looking at the Niño3 anomaly standard deviations (Fig 1a) that the CMIP5 ensemble is converging on reality, examination of these physical feedbacks highlights that there is the potential for the cancellation of errors leading to such convergence. This shows the power of examining these process-based metrics.
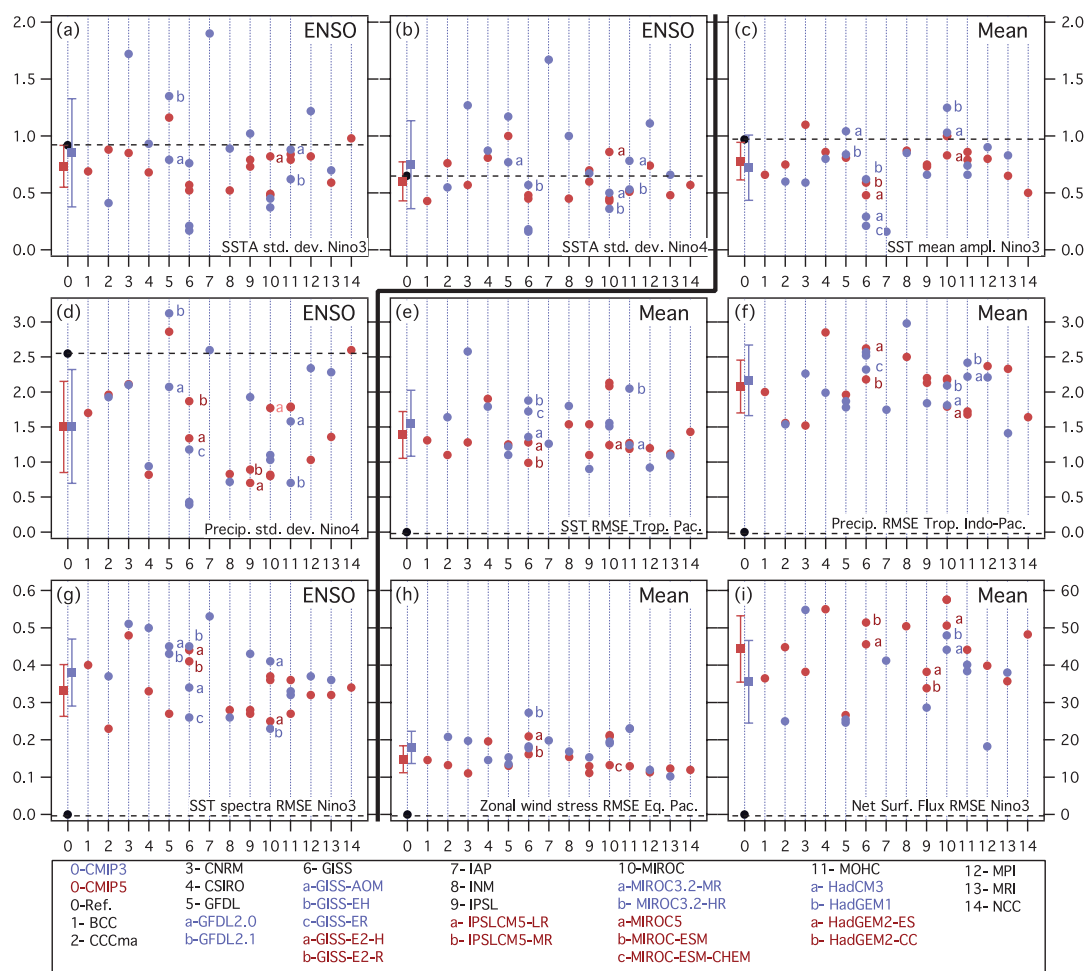

Fig. 1. ENSO and mean tropical Pacific metrics for pre-industrial control simulations - CMIP3 (blue) and CMIP5 (red). (a) and (b) SSTA std. dev. in Niño 3 and Niño 4 (°C), (c) SST annual cycle amplitude in Niño3, (°C), (d) precipitation response (std dev) in Niño4 (mm/day), (e) SST RMS error in tropical Pacific, (°C), (f) precipitation spatial RMS error over tropical Indo-Pacific, 30°N-30°S (mm/day), (g) ENSO power spectrum (Niño3) RMS error, (°C2), (h) zonal wind stress spatial RMS error over equatorial Pacific 5°N-5°S (10−3Nm−2), (i) net surface heat flux RMS error in Niño 3 (Wm−2). Reference datasets, shown as black solid circles and dashed lines: HadISST1.1 for (a), (b), (c), (e) and (g); ERA40 for (h); CMAP for (d)(f); OAFlux for (i). The CMIP3 and CMIP5 multi-model mean are shown as squares on the left of each panel with the whiskers representing the model standard deviation. Monthly atmosphere grid CMIP5-variable used: ts for (a), (b), (c), (e) and (g); tauu for ERA40 for (h); pr for (d)(f); hfls (latent), hfss (sensible), rlds (LW down), rlus, (LW up), rsds (SW down), rsus (SW up) to obtain qnet=-hfls-hfss+rlds+rsds-rlus-rsus (i). All fields were interpolated onto a common 1degree grid and then time averaged for mean fields. See metrics http://www.locean-ipsl.upmc.fr/~ENSO_metrics/index.html for details of computation.
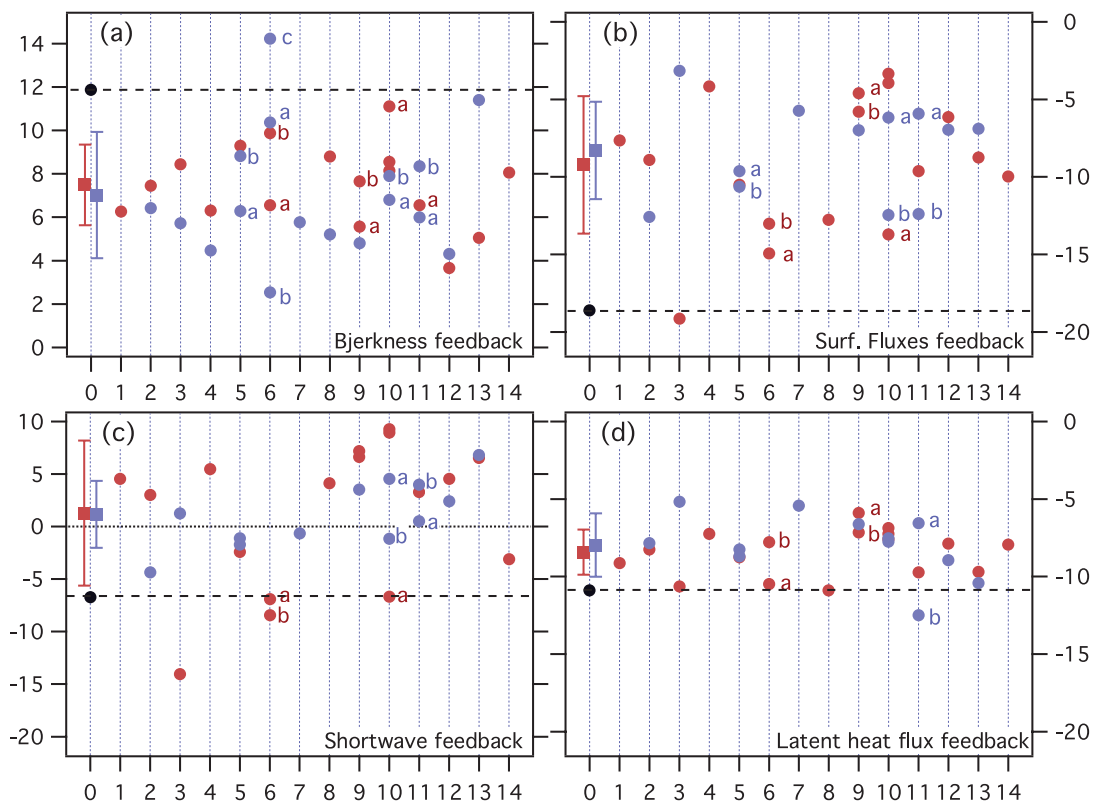
Fig. 2. Atmosphere feedbacks during ENSO for pre-industrial control simulations - CMIP3 (blue) and CMIP5 (red). (a) Bjerknes feedback, computed as the regression of Niño 4 wind stress over Niño3 SST (10−3Nm−2/C); (b) heat flux feedback, computed as the regression of total heat flux over SST in Niño3 (Wm-2/C); (c) Shortwave component of (b); (d) Latent heat flux component of (b). References: ERA40 for (a) and OAFlux for (b), (c) and (d). Monthly atmosphere grid CMIP5-variable used as described in Fig. 1. See models and centres legend in Fig. 1.

ENSO in a warmer world

Under increasing greenhouse gases, a fairly robust signal of changes in mean climate was seen in the CMIP3 models (Vecchi et al., 2006; Collins et al., 2010) and preliminary analysis of changes in mean circulation and SST in the CMIP5 models (figures not shown) indicates similar patterns.

Changes in mean climate can disrupt the balance of feedbacks in the ENSO cycle and lead to changes in the average amplitude of events. Because the balance of feedbacks is different in different models (Fig. 2), any changes in feedbacks, even if they are robust across models, can lead to different changes in basic ENSO characteristics (e.g. Philip and van Oldenborgh, 2006). Some CMIP3 CGCMs exhibited increasing ENSO variability in the future simulations, some showed a decrease and some

showed no change. While the reasons for the spread in models results have been better understood in recent years, attaching likelihood to the different models and projecting future changes have not been possible.

It appears, from the preliminary analysis presented in Fig. 3, that the situation is not changed in the CMIP5 models. Six CGCMs show no significant change in Niño3 standard deviation, five show a significant increase and two show a significant decrease. Further analysis for the reasons for these changes is required. A preliminary analysis of the power spectra of Niño3 SST anomalies of events also reveals that there is no consistent picture of changes in the time scale of ENSO as greenhouse gases rise.
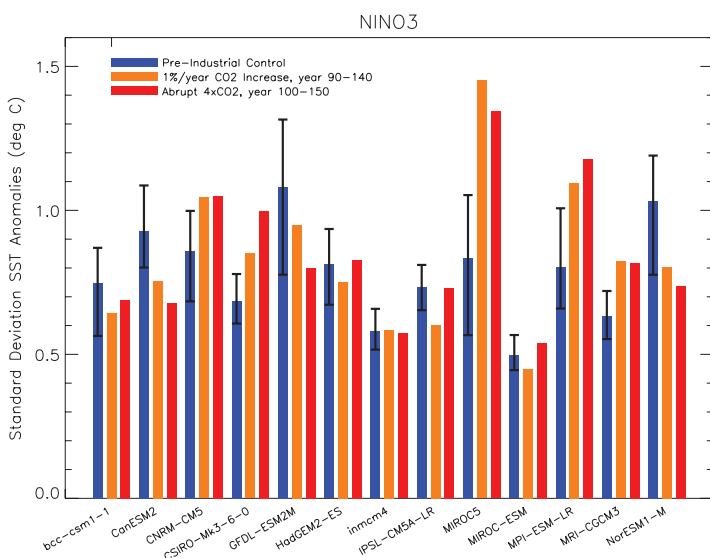

Fig. 3: Standard deviation of Niño3 SST anomalies for CMIP5 model experiments. Blue bars, pre-industrial control experiments, orange bars, years 90-140 from the 1%/year CO_2 increase experiments, red bars years 50-150 from the abrupt 4xCO_2. Calculations are performed for the models indicated on the x-axis. The black 'error bar' indicates the minimum and maximum of 50-year windowed standard deviation of Niño3 anomalies computed from the multi-century control experiments. Thus, when the Niño3 standard deviation in one of the CO2 runs falls below or above the error bar, the changes are deemed to be significant. If significant changes are seen in both experiments that indicates a more robust response in that model.

Conclusion and next steps

With only part of the data available, CMIP5 as a multi-model ensemble does not exhibit a quantum leap in ENSO performance or sensitivity, compared to CMIP3 as a multi-model ensemble. Looking at individual modeling centres, about half show an improvement in ENSO amplitude. The multi-model mean state does not exhibit significant changes from CMIP3 to CMIP5, although a number of individual centres saw an improvement. Very few models score better for all metrics and most have pluses and minuses. Examination of a selection of physical feedbacks highlights that there is still the potential for the cancellation of errors and that a process-based analysis is fundamental to properly assess ENSO in CGCMs. As in CMIP3, CMIP5 CGCMs exhibit a range of behaviour for ENSO variability in the future simulations, some showing an increase, others a decrease and some no change.

We also note that many of the new CGCMs are simulating much more processes than they were in CMIP3 – aerosol indirect effect, stratosphere/troposphere interactions, land ice, flowing rivers, carbon cycle, ecosystems, and forcing by emissions rather than concentrations. This makes things more challenging: there are new feedbacks to amplify biases, more uncertain model parameters to constrain and more constraints when finalizing the model set up. But this also holds promise: new avenues for improvement, better contact with observational & theoretical constraints, and new realms of ENSO impacts to be explored.

To help make further progress, a CLIVAR-sponsored workshop held in 2010 (Guilyardi et al. 2012) reviewed "new strategies for evaluating ENSO processes in climate models". Main recommendations included:
- Reduce mean state biases in CGCMs and develop pathways to understand and reduce modeled ENSO biases, including process-based analysis;
- Understand causes for El Niño and La Niña inter-event diversity, low-frequency modulation of ENSO and its impacts and how weather and climate of the mid-latitudes and other tropical regions may influence ENSO;
- Understand how ENSO may change under global warming, including quantifying and reducing uncertainty in projections;
- Continue to "bring together the different communities of experts to collectively make significant progress in the representation of ENSO in CGCMs and in the use of CGCMs in addressing open questions in ENSO science."

References

Capotondi, A., A. Wittenberg, and S. Masina, 2006: Spatial and temporal structure of tropical Pacific interannual variability in 20th century coupled simulations. Ocean Modelling, 15, 274-298.

Collins, M., et al., 2010: The impact of global warming on the tropical Pacific Ocean and El Niño. Nature Geosci., 3 (6), 391–397, URL http://dx.doi.org/10.1038/ngeo868.

Guilyardi, E., A. Wittenberg, A. Fedorov, M. Collins, C.Z. Wang, A. Capotondi, G.J. van Oldenborgh, and T. Stockdale (2009a): Understanding El Niño in ocean-atmosphere General Circulation Models: Progress and challenges. Bull. Amer. Met. Soc., 90, 325–340

Guilyardi E., P. Braconnot, F.-F. Jin, S. T. Kim, M. Kolasinski, T. Li and I. Musat (2009b). Atmosphere feedbacks during ENSO in a coupled GCM with a modified atmospheric convection scheme. J. Clim., 22, 5698-5718

Guilyardi E. and A. Wittenberg (2010). ENSO and tropical Pacific metrics for CMIP5. IPCC Expert meeting on Assessing and Combining Multi Model Climate Projections, Boulder, USA, January 2010

Guilyardi, E., W. Cai, M. Collins, A. Fedorov, F.-F. Jin, A. Kumar, D.-Z. Sun, A. Wittenberg (2012). CLIVAR workshop summary: New strategies for evaluating ENSO processes in climate models. Bull. Amer. Met. Soc., in press now published doi:10.1175/BamS-d-11-00106.1 BAMS vol 92(check), 335-338

Kim, D., J.-S. Kug, I.-S. Kang, F.-F. Jin, and A. T. Wittenberg, 2008: Tropical Pacific impacts of convective momentum transport in the SNU coupled GCM. Climate Dyn., 31, 213-226. doi:10.1007/s00382-007-0348-4.

Lloyd, J., E. Guilyardi and H. Weller (2011), The role of atmosphere feedbacks during ENSO in the CMIP3 models, Part II: using AMIP runs to understand the heat flux feedback mechanisms, Clim. Dyn. 37, 1271-1292, DOI: 10.1007/s00382-010-0895

McPhaden, M. J.; Zebiak, S. E. & Glantz, M. H. (2006). ENSO as an Integrating Concept in Earth Science science, 314, 1739-1745

Neale, R. B., Richter, J. H., & Jochum, M. (2008). The Impact of Convection on ENSO: From a Delayed Oscillator to a Series of Events. Journal of Climate, 21(22), 5904–5924. doi:10.1175/2008JCLI2244.1

Philip, S. Y. & van Oldenborgh, G. J. (2006). Shifts in ENSO coupling processes under global warming. Geophys. Res. Letts. 33, L11704

Rayner NA, Parker DE, Horton EB, Folland CK, Alexander LV, Rowell DP, Kent EC, Kaplan A (2003) Global analyses of sea surface temperature, sea ice, and night marine air temperature since the late nineteenth century. J Geophys Res (Atmos) 108:4407

Stevenson, S., Fox-Kemper, B., Jochum, M., Rajagopalan, B., & Yeager, S. G. (2010). ENSO Model Validation Using Wavelet Probability Analysis. Journal of Climate, 23(20), 5540–5547. doi:10.1175/2010JCLI3609.1

Uppala et al. (2005) The ERA-40 Re-analysis. Quart J R Met Soc 131:2961–3012

Vecchi, G. A., and A. T. Wittenberg, 2010: El Niño and our future climate: Where do we stand? Wiley Interdisciplinary Reviews: Climate Change, 1, 260-270. doi:10.1002/wcc.33

Vecchi, G. A. et al. Weakening of tropical Pacific atmospheric circulation due to anthropogenic forcing. Nature 441, 73–76 (2006).

Watanabe, M., Suzuki, T., O'ishi, R., Komuro, Y., Watanabe, S., Emori, S., Takemura, T., et al. (2010). Improved Climate Simulation by MIROC5: Mean States, Variability, and Climate Sensitivity. Journal of Climate, 23(23), 6312–6335. doi:10.1175/2010JCLI3679.1

Wittenberg, A. T. (2009), Are historical records sufficient to constrain ENSO simulations?, Geophys. Res. Lett., 36, L12702, doi:10.1029/2009GL038710.

Xie, P., and P.A. Arkin, 1997: Global precipitation: A 17-year monthly analysis based on gauge observations, satellite estimates, and numerical model outputs. Bull. Amer. Meteor. Soc., 78, 2539 - 2558.

Yu, L., and R. A. Weller, 2007: Objectively Analyzed air-sea heat Fluxes for the global oce-free oceans (1981–2005). Bull. Ameri. Meteor. Soc., 88, 527–539

Seasonal and Interannual Variability of the North Equatorial Current Bifurcation off the Philippines

Dunxin Hu[1,2*], Fangguo Zhai[1,2,3], Fujun Wang[1,2]

1   Key Laboratory of Ocean Circulation and Waves (KLOCAW), Chinese Academy of Sciences, Qingdao, 266071, China
2   Institute of Oceanology, Chinese Academy of Sciences (IOCAS), Qingdao, 266071, China
3   Graduate University of Chinese Academy of Sciences, Beijing, China

* Corresponding Author: Prof. Dunxin Hu, Key Laboratory of Ocean Circulation and Waves (KLOCAW), Institute of Oceanology, Chinese Academy of Sciences, 7 Nanhai Road, Qingdao, 266071, China, Tel/Fax: 86-532-82898678, Email: dxhu@qdio.ac.cn.

1. Introduction

The North Equatorial Current (NEC) bifurcates into the northward flowing Kuroshio Current (KC) and southward flowing Mindanao Current (MC), comprising the so-called NEC-MC-KC (NMK) current system (Figure 1a; also see Nitani, 1972; Hu and Cui, 1989, 1991; Toole et al., 1990; Qiu and Lukas, 1996; Qu and Lukas, 2003; Yaremchuk and Qu, 2004). Among others, the NEC bifurcation latitude (NBL) is an important indicator of the partition of water mass, heat, salt, and biological properties between the KC and MC (e.g., Toole et al., 1990; Qu and Lukas, 2003; Yaremchuk and Qu, 2004). Therefore NBL and its variability on different time scales have been extensively studied through theoretical derivation, data analysis and numerical modeling (e.g., Qiu and Lukas, 1996; Qu and Lukas, 2003; Kim et al., 2004; Yaremchuk and Qu, 2004; Wang and Hu, 2006; Qiu and Chen, 2010; Wang and Hu, 2012; Zhai and Hu, 2012). Using a climatology constructed from historical hydrographic observations, Qu and Lukas (2003) pointed out that NBL shifts northward with depth, from about 13.3°N near the sea surface to about 20°N near 1000 m depth. On the seasonal time scale, NBL reaches its northernmost position during winter and southernmost during summer (Figure 1b; Qu and Lukas, 2003; Yaremchuk and Qu, 2004; Wang and Hu, 2006; Wang and Hu, 2012). On the interannual time scale, NBL is closely associated with El Niño-Southern Oscillation (ENSO) (Figure 2a; see also Qiu and Lukas, 1996; Wang and Hu, 2006; Qiu and Chen, 2010; Zhai and Hu, 2012), shifting northward during El Niño years while southward during La Niña years.

However, the detailed underlying dynamics of these variabilities is poorly understood. Aiming to observe, simulate and understand the variability and dynamics of the Northwestern Pacific ocean circulation and its effect on climate, the Northwestern Pacific Ocean Circulation and Climate Experiment (NPOCE) program pays close attention to the above topic. The present paper concludes the newest progress on understanding the dynamics of seasonal and interannual variabilities of NBL made by oceanographers from NPOCE program in Institute of Oceanology, Chinese Academy of Sciences.

2. Seasonal Variability of NBL

The NMK current system is well depicted by Munk's theory in 1950 in terms of steady state. In this section, a time-dependent analytic model is proposed to examine the seasonal variability of NBL. In the model, the x-axis is set directing eastward along the equator and the y-axis northward, supposing no friction near the ocean bottom. With baroclinicity, the equation for stream function can be expressed as in Eq.(1). As it is known, NBL occurs at the zero line of the stream function, so the solution will show the seasonal variability of NBL.

$$(L_d^2)^{-1}\psi_t - \Delta\psi_t + A_H\Delta^2\psi - \beta\psi_x = -curl_z\tau \tag{1}$$

where ψ is the stream function, $L_d = \sqrt{g'H}/f$ is the baroclinic Rossby radius of deformation, $A_H' = 3\times10^7\,cm^2/s$ is the eddy viscosity pertaining to horizontal shear, $A_H = A_H'/\rho$ is the effective kinematic eddy viscosity. The boundary condition is given as $\psi = 0, \partial\psi/\partial x = 0$ at $x = 0$, and $x = r$, where r is the zonal scale of the study area.

As the focus area is from 0°N to 30°N, the boundary condition in y direction will not affect the solution. For convenience, we set the baroclinic Rossby radius of deformation as a constant about 110 km.

The form of the wind stress curl (WSC) as a function of time and space needs to be given for the solution to Eq.(1). The seasonal fluctuation of the WSC can be well represented by the following formula given by Qiu and Lukas (1996)

$$curl_z\tau = -\left\{A\cos[\omega(t-\phi)] + B\right\}\sin[\frac{2\pi}{L}(y-15+\alpha\sin\omega t)] \tag{2}$$

where $A = 0.2[1+0.025(y-7°)]\times10^{-7}\,Nm^{-3}$, $B=3.5A$, $t = 0$ corresponds to January 1, $\phi = 60$ days denotes the time when the WSC reaches its maximum after January 1, $L = 40°/[1-0.05(y-15)]$ is the meridional wavelength of the tropical/subtropical wind belts, $\omega = 2\pi/1\,year$, and $\alpha = 4°$ is the amplitude of the WSC zero-line north-south migration. The stream function can be written as follows

$$\psi(x,y,t) = \zeta(x,y,t) + \Phi(y,t). \tag{3}$$

Substituting Eq.(3) into Eq.(1), the equation associated with $\Phi(y,t)$ will be

$$\frac{\partial\Phi(y,t)}{L_d^2\partial t} - \frac{\partial}{\partial t}\frac{\partial^2\Phi(y,t)}{\partial y^2} + A_H\frac{\partial^4\Phi(y,t)}{\partial y^4} = -curl_z\tau(y,t) \tag{4}$$

We assume that $\Phi(y,t)$ can be expanded in two-dimensional Fourier series. The Fourier expansion in time is the basic one, while the Fourier expansion in space is taken into account as the coefficient of the Fourier expansion in time. Then $\Phi(y,t)$ can be written as

$$\Phi(y,t) = -\left\{ \sum_{k=1}^{\infty}\sum_{n=1}^{4}\left(a_0 + a_n\cos\frac{n\pi y}{S} + b_n\sin\frac{n\pi y}{S}\right)\cos(k\omega t) \right.$$
$$+ \sum_{k=1}^{\infty}\sum_{n=1}^{4}\left(c_0 + c_n\cos\frac{n\pi y}{S} + d_n\sin\frac{n\pi y}{S}\right)\sin(k\omega t) \qquad (5)$$
$$\left. + \sum_{n=1}^{4}\left(e_n\cos\frac{n\pi y}{S} + f_n\sin\frac{n\pi y}{S}\right)\right\},$$

where $n \le 4$ (the reason will be shown later), and $S = 30°$. With some mathematic manipulation, the right hand side of Eq.(4) can also be written in the form of two-dimensional Fourier expansion. The terms associated with k and n in the left hand side of Eq. (4) correspond to those in the right hand side. The terms for $k, n \ge 2$ are much smaller than those for $k, n = 1$, and therefore only those for $k = n = 1$ are considered. In this case, $\Phi(y,t)$ can be approximately written as

$$\Phi(y,t) \approx -\left\{ (S/\pi)^4[rA\sin(\omega\phi)\cos 2\pi(y-15)/L \right.$$
$$+ (1-r^2)B\sin 2\pi(y-15)/L]/A_H$$
$$+ [a_0 + a_1\cos(\pi y/S) + b_1\sin(\pi y/S)]\cos(\omega t) \qquad (6)$$
$$\left. + [c_0 + c_1\cos(\pi y/S) + d_1\sin(\pi y/S)]\sin(\omega t)\right\},$$

where $r = \alpha\pi/L$. The coefficients can be determined as $a_0 = 10.43\times10^8\,Nsm^{-1}$, $c_0 = -1.07\times10^8\,Nsm^{-1}$, $a_1 = -27.39\times10^8\,Nsm^{-1}$, $b_1 = 21.87\times10^8\,Nsm^{-1}$, $c_1 = 5.09\times10^8\,Nsm^{-1}$ and $d_1 = -0.39\times10^8\,Nsm^{-1}$. From Eq.(6), NBL is about 14.5°N on average and reaches its northernmost position at 15°N in December, while southernmost at 14°N in June (Figure 1b); the result is quite consistent with those of Qu and Lukas (2003) and Wang and Hu (2006) derived from observations.

The equation for $\zeta(x,y,t)$ is

$$(L_d^2)^{-1}\zeta_t - \Delta\zeta_t + A_H\Delta^2\zeta - \beta\zeta_x = 0 \qquad (7)$$

As Munk (1950) did, we assume that

$$\psi(x,y,t) = \zeta(x,y,t) + \Phi(y,t) = RA_H n^4\beta^{-1}X_n\Phi(y,t) \qquad (8)$$

where X is a function of x. With the boundary condition in x direction, the solution for X is derived as

$$X(x) = -(2/\sqrt{3} - \sqrt{3}/KR)\exp(-\frac{1}{2}Kx)\cos(\frac{\sqrt{3}}{2}Kx + \frac{\sqrt{3}}{2KR} - \frac{\pi}{6})$$
$$+ 1 - \frac{1}{KR}[Kx - \exp(-K(R-x)) - 1],$$

where $K = \sqrt[3]{\beta/A_H}$ designates the Coriolis-friction wave number, assumed constant. According to Munk's manipulation (1950) about approximate conditions for X, a minimum zonal wave length of $\frac{2\pi}{n\pi/S}$ is about 1500 km. And then the maximum of n in our model is 4, which means the function $\Phi(y,t)$ is convergent.

Through all the manipulations above, the final analytical solution to Eq.(1) is the following in terms of stream function

$$\psi(x,y,t) = RA_H(\pi/S)^4\beta^{-1}X(x)\Phi(y,t)$$
$$\approx -RA_H(\pi/S)^4\beta^{-1}X(x)\left\{-(S/\pi)^4[rA\sin(\omega\phi)\right.$$
$$\cos 2\pi(y-15)/L + (1-r^2)B\sin 2\pi(y-15)/L]/A_H \qquad (9)$$
$$+ [a_0 + a_1\cos(\pi y/S) + b_1\sin(\pi y/S)]\cos(\omega t)$$
$$\left. + [c_0 + c_1\cos(\pi y/S) + d_1\sin(\pi y/S)]\sin(\omega t)\right\}.$$

The time-dependent stream function expresses the seasonal variability of NBL, which can be reduced to the Munk theory under steady and barotropic state.

Qiu and Lukas (1996) concluded that NBL reaches its southernmost position in February and northernmost position in October, almost simultaneously responding to the wind forcing. The present result shows that NBL reaches its minimum in June and maximum in December about three months lagging the wind forcing (Wang and Hu, 2012) due to the baroclinicity taken into account.

3. Interannual Variability of NBL

Figure 2a shows the interannual variations of NBL at sea surface derived from altimetry, which indicate a close relationship of NBL with the Niño-3.4 sea surface temperature (SST) anomalies (e.g., Wang and Hu, 2006; Qiu and Chen, 2010; Zhai and Hu, 2012). Associated circulation variations are investigated through composite analysis of anomalies of monthly sea surface height (SSH) and correspondingly derived sea surface geostrophic currents (SSGC). The anomalies are obtained through first subtracting the monthly climatology from the monthly mean variables and then applying a 5-month running mean filter. During October 1992-July 2009 when altimetry data are available, there are five El Niño warm events (1994–1995, 1997–1998, 2002–2003, 2004–2005, and 2006–2007) and four La Niña cold events (1995–1996, 1998–2000, 2005–2006, and 2007–2008) recognized (Figure 2a). With reference to previous studies, six phases of the El Niño/La Niña cycle are defined: antecedent (August-October of year −1), germination (from November of year −1 to January of year 0), development (March-May of year 0), onset (July-September of year 0), mature (from November of year 0 to January of year +1), and decay (February-April of year +1), where year 0 is the El Niño/La Niña year, in which anomalous high/low SST first appears and subsequently amplifies in the eastern tropical Pacific Ocean, and year −1 and +1 are the previous and subsequent year, respectively. All La Niña cold events follow El Niño warm events during this period. During El Niño (La Niña) events, in the western tropical North Pacific Ocean (NPO) there are significant changes in SSH decreasing (increasing) with evolution of a cyclonic (anticyclonic) gyre anomaly (Figures 2b and 2c). During El Niño events, negative SSH anomalies in the western tropical NPO first appear in the Mindanao Eddy (ME) region in the antecedent phase, gradually spread meridionally and zonally in the following three phases, peak around the mature phase, and weaken in the decay phase. The maximum negative SSH anomalies occur mainly in the area of 0–15°N, 130°E–160°E. As the SSH falls, the thermocline rises. Geotropically, a cyclonic gyre anomaly forms west of the dateline and results in a northward NBL shift. The first

three phases of La Niña events during the 17-year period show features of El Niño events. From the onset phase, however, the negative SSH anomalies in this region are replaced with positive ones, which peak around the mature phase and then weaken. The maximum positive SSH anomalies take place in the same region as the maximum negative ones during El Niño events. These positive SSH anomalies induce an anticyclonic gyre anomaly, resulting in a southward NBL shift.

The variations of SSH and SSGC are mainly forced by sea surface winds along the same latitude bands (e.g., Meyers, 1979; Kessler, 1990; Capotondi and Alexander, 2001; Capotondi et al., 2003; Qiu and Chen, 2010; Zhai and Hu, 2012). Then the evolution of the wind forcing during El Niño/La Niña cycle is described through composite analysis of anomalies of monthly wind stress vector, and corresponding Ekman pumping velocity calculated using the same method as those of SSH and SSGC. During El Niño events, the composite patterns of the two kinds of anomalies in pre-mature phases are similar to those described by Wang (1995), which include the development of the Philippine Sea cyclone in the antecedent and germination phases, development of westerly wind anomalies in the equatorial western Pacific Ocean in the development phase, and eastward movement of equatorial westerly wind anomalies in the onset phase (Figure 2d). The westerly wind anomalies north of the equator bring about cyclonic WSC anomalies in the north, reaching their easternmost position near the dateline before the mature phase. These wind anomalies induce westward propagating upwelling Rossby waves, lowering the SSH and lifting the thermocline in the western tropical NPO. Around the mature phase, an anticyclone forms in that region, which exerts downward Ekman pumping on the ocean, depresses the thermocline and weakens the negative SSH anomalies. In the east-central NPO, the northeast trade wind is strengthened because of warming in the east-central equatorial Pacific Ocean, causing anticyclonic WSC anomalies in the north. These wind anomalies generate oceanic downwelling Rossby waves, propagating westward and weakening the negative SSH anomalies. In the onset phase of La Niña events, the west-central tropical NPO is dominated by easterly wind anomalies and downward Ekman pumping, while the eastern tropical NPO is dominated by upward Ekman pumping (Figure 2e). The wind anomalies in the west-central tropical NPO, which begin to decay slowly in subsequent phases, induce downwelling Rossby waves, which propagate westward and cause thermocline deepening and SSH rising. These processes can be quantified with a 1 ½ layer reduced gravity model with long wave approximation and assumptions of low frequency and quasi-geostrophy (e.g., Meyers, 1979; Capotondi and Alexander, 2001; Capotondi et al., 2003; Qiu and Chen, 2010; Zhai and Hu, 2012). The SSH anomaly (η') can be simply estimated by integrating the effects of wind-induced Ekman pumping along the Rossby wave characteristics from the eastern basin boundary:

$$\eta'(x,y,t) = -\frac{g'}{g}\int_x^{x_e}\frac{1}{C_R}\vec{k}\bullet\nabla\times\left[\frac{\vec{\tau}(x',y,t+\Delta t)}{\rho_0 f}\right]e^{\varepsilon\Delta t}dx' \qquad (10)$$

where $x = x_e$ denotes the eastern basin boundary, $\vec{\tau}'$ is the wind stress vector anomaly, g' is the reduced gravity, ε is

the Newtonian dissipation rate, $\Delta t = \int_{x'}^x d\xi/C_R$ is the negative transit time needed for the first-mode baroclinic Rossby waves generated in the east to propagate westward to the target point, and $C_R = \beta\lambda^2$ is the phase speed of first-mode baroclinic Rossby waves. Eq.(10) is applied to integer latitudes from 6°N to 17°N with parameters g' and ε being determined through comparing observed and modeled SSH anomalies. Overall, Eq.(10) captures well the low frequency variations of SSH. In the region of interest, the modeled and observed SSH anomalies have correlation coefficients as high as 0.8 above 95% confidence level. Then Eq.(10) is used to quantify the relative contributions of the wind forcing in different Pacific basin. The results show that most of the interannual variance of SSH in the western tropical NPO is induced by the wind forcing in the western-central tropical NPO. Within the latitude band of 7°N-15°N, more than 80% of the interannual variance of SSH west of 160°E is induced by the wind forcing west of the dateline.

4. Concluding Remarks

A time-dependent, baroclinic, analytical model is proposed, which can degenerate to Munk's theory under steady and barotropic state, to investigate the seasonal variability of the NEC bifurcation. With this model, the zero-line of stream function fluctuates with season: NBL reaches its minimum in June and maximum in December in response to the wind forcing with about a three-month lag. The fundamental reason for the difference between the seasonal variability of the wind forcing and NEC bifurcation is the baroclinicity involved in the present model, which can delay the response of the bifurcation latitude to the wind field. The result is quite consistent with results of Qu and Lukas (2003) and Wang and Hu (2006) derived from observations.

Meanwhile, a composite analysis method is applied to anomalies of monthly SSH and SSGC to examine the physical processes underlying the relationship between the interannual variability of NBL and ENSO events. The results indicate that during the warm/cold phase of ENSO, the SSH (thermocline) in the western tropical NPO falls/rises (shoals/deepens), with maximum changes in the region 0–15°N, 130°E–160°E; this generates a cyclonic/anticyclonic gyre anomaly west of the dateline. Since the climatological ocean circulation in this area (Figure 1a) is essentially cyclonic, the cyclonic/anticyclonic gyre anomaly induces a northward/southward NBL shift. Variations of SSH and upper layer currents are mainly caused by the evolution of wind forcing anomalies in the west-central tropical NPO, which is a westerly wind anomaly before the mature phase of El Niño events, and an easterly wind anomaly after the development phase of La Niña events. These wind anomalies and associated WSC anomalies generate upwelling/downwelling Rossby waves, which propagate westward, causing falling/rising (shoaling/deepening) of SSH (thermocline) and thus formation of the cyclonic/anticyclonic gyre anomaly.

References

Capotondi A., and M. Alexander, 2001: Rossby waves in the tropical North Pacific and their role in decadal thermocline variability. J. Phys. Oceanogr., 31, 3496-3515.

Capotondi A., M. Alexander, and C. Deser, 2003: Why are there Rossby wave maxima in the Pacific at 10°S and 13°N? J. Phys. Oceanogr., 33, 1549-1563.

Hu D., and M. Cui, 1989: The western boundary current in the far western Pacific Ocean. In: Picaut J, Lukas R, Delcroix T eds. Proceedings of Western International Meeting and Workshop on TOGA COARE, May 24-30, 1989, Noumea, New Caledonia, pp. 123-134.

Hu D., and M. Cui, 1991: The western boundary current of the Pacific and its role in the climate. Chin. J. Oceanol. Limnol., 9, 1-14.

Kessler W., 1990: Observation of long Rossby waves in the northern tropical Pacific. J. Geophys. Res., 95, 5183-5217.

Kim Y., T. Qu, T. Jensen, T. Miyama, H. Mitsudera, H.W. Kang, and A. Ishida, 2004: Seasonal and interannual variations of the North Equatorial Current bifurcation in a high-resolution OGCM. J. Geophys. Res., 109, C03040, doi:10.1029/2003JC002013.

Meyers G., 1979: On the annual Rossby wave in the tropical North Pacific Ocean. J. Phys. Oceanogr., 9, 663-674.

Munk W., 1950: On the wind-driven ocean circulation. J. Meteor.. 7, 81-93.

Nitani H., 1972: Beginning of the Kuroshio. In: Stommel H, Yoshida K eds. Kuroshio: Its Physical Aspects. University of Washington Press, p. 129-163.

Qiu B., and R. Lukas, 1996: Seasonal and interannual variability of the North Equatorial Current, the Mindanao Current, and the Kuroshio along the Pacific western boundary. J. Geophys. Res., 101(C5), 12 315-12 330.

Qiu B., and S. Chen, 2010: Interannual-to-decadal variability in the bifurcation of the North Equatorial Current off the Philippines. J. Phys. Oceanogr., 40, 2525-2538.

Qu T., and R. Lukas, 2003: The bifurcation of the North Equatorial Current in the Pacific. J Phys Oceanogr., 33, 5-18.

Toole J., R. Millard, Z. Wang, and S. Pu, 1990: Observations of the Pacific North Equatorial Current bifurcation at the Philippine coast. J. Phys. Oceanogr., 20, 307-318.

Wang B., 1995: Interdecadal changes in El Niño Onset in the last Four decades. J. Climate, 8, 267-285.

Wang F., and D. Hu, 2012: A time-dependent baroclinic model on NEC bifurcation. Chin. J. Oceanol. Limnol., 30, 186-191.

Wang Q., and D. Hu, 2006: Bifurcation of the north equatorial current derived from altimetry in the Pacific Ocean. J. Hydrodyn., 18, 620-626.

Yaremchuk M., and T. Qu, 2004: Seasonal variability of the large-scale currents near the coast of the Philippines. J. Phys. Oceanogr., 34, 844-855.

Zhai F., and D. Hu, 2012: Interannual variability of transport and bifurcation of the North Equatorial Current in the tropical North Pacific Ocean. Chin. J. Oceanol. Limnol., 30, 177-185.
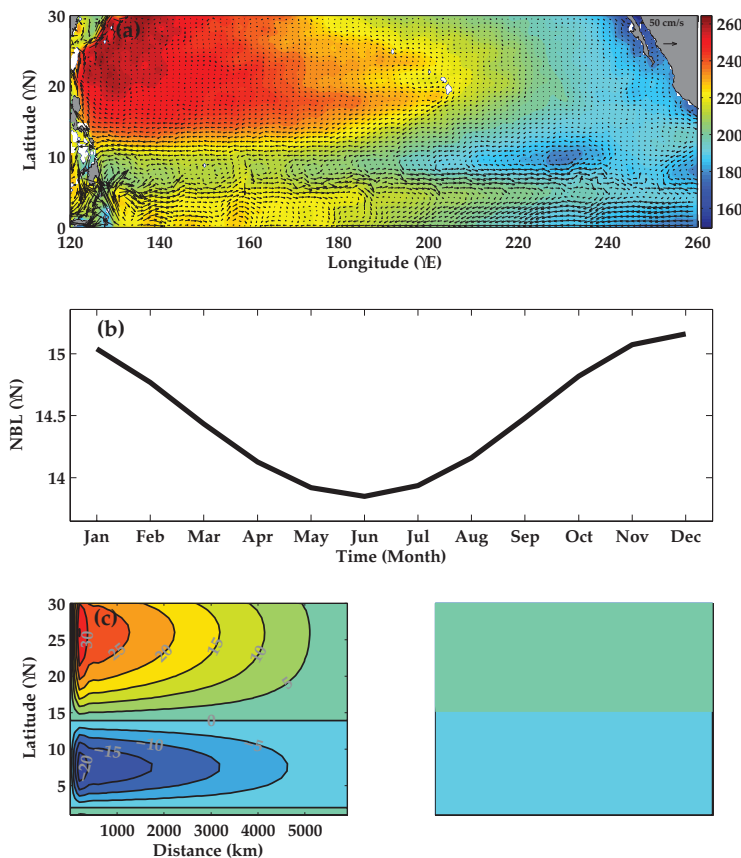
Fig 1. (a) Mean sea surface height (cm) and sea surface geostrophic currents (cm s⁻¹) derived from altimetry observations in North Pacific Ocean between 0°N and 30°N. (b) Seasonal NBL derived from Eq.(6). (c) Stream function in June from Eq.(9). (d) Same as (c) but in December.
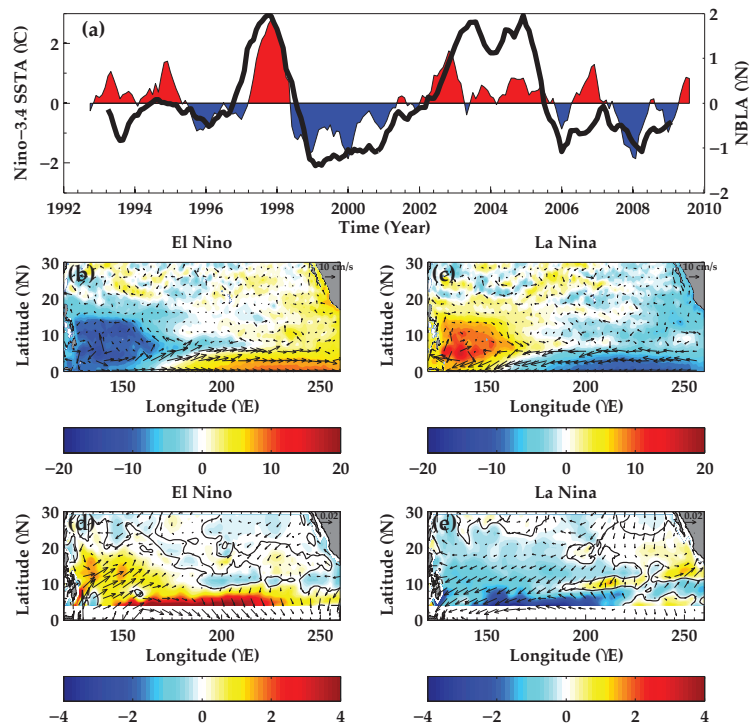

Fig 2. (a) Anomalies of Niño-3.4 SST (color) and NBL (black line) at sea surface. (b) Anomalies of SSH (cm) and SGCC (cm s⁻¹) during the mature phase of El Niño events. (c) Same as (b) but of La Niña events. (d) Anomalies of sea surface wind stress vector (N m⁻²) and wind induced Ekman pumping velocity (10⁻⁶ m s⁻¹) during the onset phase of El Niño events. (e) Same as (d) but of La Niña events.

Climate Change in the Pacific: Scientific Assessment and New Research

by S. Power (s.power@bom.gov.au), K. Hennessy, G. Cambers, J. Rischbieth, S. Baldwin, Jo Brown, D. Collins, R. Colman, D. Irving, J. Katzfey, P. Kokic, B. Murphy, D. Abbs, Jaclyn Brown, J. Church, F. Delage, A. Sen Gupta, D. Jones, S. McGree, M. Hopkins, A. Moise, S. Perkins, A. Schiller, B. Tilbrook, X. Zhang (Pacific Climate Change Science Program), M. Vaiimene, D. Maihia, N. Bates (Cook Islands) , T. Terencio, F. Moniz, S. da Silva (East Timor), D. Aranug, J. Berdon, E. Skilling (Federated States of Micronesia), A. Waqaicelua, A. Daphne, B. Prakash, V. Vuniyayawa, R. Kumar (Fiji), U. Toorua, T. Tetabo, R. Abeta, N. Teuatabo (Kiribati), R. White, L. Jacklick, N. Lobwij (Marshall Islands), A. Kaierua, F. Teimitsi, D. Audoa (Nauru), R. Misiepo, A. Misikea, F. Pihigia Talagi (Niue), M. Ngemaes, D. Ngirengkoi, G. Sisior (Palau), K, Inape, M. Virobo (Papua New Guinea), F. Lagomauitumua, S. K. Seuseu , T. Faasaoina (Samoa), D. Hiriasia, L. Tahani (Solomon Islands), O. Fa'anunu, M. Lakai (Tonga), H. Vavae, K. Epu (Tuvalu), S. Kaniaha, P. Malsale (Vanuatu), on behalf of all PCCSP staff and others who contributed to the report or its production.

A 530 page, two volume scientific report called "Climate Change in the Pacific: Scientific Assessment and New Research" (Figure 1) was recently released as part of the AUD$20m Pacific Climate Change Science Program (PCCSP). The full report is available at the PCCSP website:

http://www.pacificclimatechangescience.org.

A limited number of hard copies are still available (jill.rischbieth@csiro.au). This report builds on the IPCC Fourth Assessment report, drawing on more recent research conducted around the world, including PCCSP research. "Climate Change in the Pacific" complements the excellent and recently released reports by Lough et al. (2011) and Ganachaud et al. (2011).

The PCCSP (Power et al. 2011) was a major research program aimed at helping 14 developing island countries in the Pacific (Cook Islands, Federated States of Micronesia, Fiji, Kiribati, Marshall Islands, Nauru, Niue, Palau, Papua New Guinea, Samoa, Solomon Islands, Tonga, Tuvalu and Vanuatu) and East Timor (see Figure 2) gain a better understanding of how climate has changed in the past and how it may change in the future. Over 100 people contributed to the production of this report, some of whom are shown in Figure 3. The PCCSP began in 2009 and ran to the end of December 2011. The PCCSP has been extended and expanded through the AUD$30m Pacific Australia Climate Change Science and Adaptation Program (PACCSAP), which will run to at least June 2013. The PCCSP was and PACCSAP is part of the Australian Government's International Climate Change Adaptation Initiative.

Volume One: Regional Overview describes past and future climate variability and trends in the Pacific (25°S-20°N and 120°E-150°W), the main factors influencing climate in the region, observed trends, the ability of climate models to simulate Pacific climate, and projections of future Pacific climate based on new analyses of WCRP/CMIP3 models and dynamical downscaling. Twenty-first Century projections are provided for temperature, rainfall, humidity, evaporation, solar radiation, extreme events, (including tropical cyclones, extreme hot days and heavy rainfall days), sea-surface temperature and salinity, ocean acidification, and sea-level rise. Projections are given for three 20-year periods centred on 2030, 2055 and 2090, for three different scenarios of future greenhouse gas and aerosol emissions (B1, A1B, and A2). The report also describes uncertainties associated with the projections, and concludes with recommendations to further advance the science of climate change in the Pacific.

Individual reports tailored for the 15 participating countries are presented in the second volume. Each of the country reports has four main sections: (1) seasonal cycles, (2) climate variability, (3) observed annual trends, and (4) projections for atmospheric and oceanic variables.

The technical information contained in the report was used to produce 15 less technical country-specific brochures which can also be downloaded from the PCCSP web-site. Web-based tools for use in the islands were also developed, and training was undertaken in each country and at several regional workshops.

The major conclusions are outlined in the Executive Summary, so here we will only cover a subset of the key issues.

Climatology

The impact of the West Pacific Monsoon, the Inter-tropical Convergence Zone, the South Pacific Convergence Zone (SPCZ) and El Niño-Southern Oscillation (ENSO) on the islands - and the ability of climate models to simulate these phenomena - was closely examined. This information was used to help assess the confidence we have in the projections based on climate models.

Observed changes in temperature, rainfall, wind and salinity

All of the island stations analysed have exhibited warming trends since 1960 (Figure 4). Over the past 50 years rainfall has increased north-east of the SPCZ, and declined to the south. Sea-surface temperatures of the Pacific Ocean have generally increased since 1950. In addition, the western tropical Pacific Ocean has become significantly less salty, while regions to the east have generally become saltier.

A distinctive pattern of intensified warming of surface waters and cooling of sub-surface equatorial waters centred near a depth of 200 m is also apparent over the past 50 years in the Pacific Ocean. These patterns of observed change in the ocean are reproduced in climate model simulations that include increased atmospheric greenhouse gases. In combination, these changes have driven an increase in the stratification of the upper ocean.

Equatorial easterlies in the Pacific weakened during the 20th Century, which is attributed to a combination of human-forced climate change and natural climate variability. The weakening of the equatorial trade winds was accompanied by a strengthening of off-equatorial trade winds in the SE Pacific.

Projected warming

The projections centred on the three 20-year periods (relative to 1990 baseline temperatures) show that by 2030, the projected regional warming is around 0.5 to 1.0°C, regardless of the emissions scenario. By 2090, the warming is around 1.5 to 2.0°C for B1, 2.0 to 2.5°C for A1B, and 2.5 to 3.0°C for A2. Large increases in the incidence of extremely hot days and warm nights are also projected.

Ocean acidification

As a consequence of higher CO_2 concentrations in the atmosphere, the oceans are absorbing more CO_2 and the pH across the region is decreasing as part of broader ocean acidification. Acidification is accompanied by a decrease in the seawater saturation state of carbonate minerals that are secreted as shells and skeletal material by many key species in reef ecosystems. Aragonite is the form of calcium carbonate precipitated by reef building corals and studies have shown that coral growth declines as the aragonite saturation state of seawater decreases. Aragonite saturation states above a value of 4 are considered optimal for coral growth and for the development of healthy reef ecosystems. Throughout

most of the sub-tropical and tropical Pacific Island region, the saturation state in pre-industrial times exceeded 4. By the mid 1990s, the uptake of anthropogenic CO_2 resulted in a widespread decline in the aragonite saturation state. As CO_2 concentrations continue to increase aragonite saturation values below 3.5 are projected to become more widespread and have the potential to disrupt the health and sustainability of reef ecosystems.

Sea-level

Sea-level estimates exhibit rising trends across the region, with substantial interannual variability linked to ENSO, and longer-term variability linked to Interdecadal Pacific Oscillation/Pacific Decadal Oscillation variability.

Global climate models reproduce the observed pattern of the regional distribution of sea-level reasonably well. Models indicate that the rise will not be geographically uniform. However, spatial contrasts between model projections make regional estimates uncertain. The magnitude of sea-level rise in the PCCSP region is similar to the global average. Projections of sea-level rise require consideration of ocean thermal expansion, the melting of glaciers and ice caps, the surface mass balance and dynamic response of the ice sheets of Antarctica and Greenland, and changes in terrestrial water storage. Current projections indicate sea-levels will continue to rise, on average, during this century. As detailed in the Fourth Assessment Report of the IPCC (IPCC, 2007), global average sea-level is projected to rise by 0.18 to 0.59 m by 2080–2099, relative to 1980–1999, with an additional potential contribution from the dynamic response of the ice sheets. By scaling to global temperature changes this additional rise was estimated to be 10 to 20 cm, but larger increases could not be ruled out. Observations indicate sea-level is currently rising at near the upper end of the projected range. Sea-level increases larger than the IPCC projections have been argued by some researchers but one recent study suggests that global-mean sea-level rise greater than 2 m by 2100 is physically untenable and that a more plausible estimate is about 80 cm, consistent with the upper end of the IPCC estimates and the present rate of increase. However, improved understanding of the processes responsible for ice sheet changes is urgently required to improve estimates of the rate and timing of 21st Century and longer-term sea-level rise.

Tropical cyclones

There are no significant trends in the overall number or intensity of tropical cyclones in the South Pacific in the satellite record since the early 1980s. However, this is a short period of time for the analysis of infrequent extreme events such as tropical cyclones. Equally, determining trends over longer periods is difficult due to the lack of adequate data prior to the satellite era. Other records reveal that the number of severe tropical cyclones making landfall in a 1600 km strip in NE Australia (SW of the SPCZ) decreased during the period 1872/73 - 2009/10.

It is difficult to make projections of tropical cyclone activity because features of a tropical cyclone occur at a smaller spatial scale than can be represented by current climate models, and

because climate models vary in their ability to simulate large-scale environmental conditions that are known to influence tropical cyclones (e.g. ENSO, the SPCZ).

To help assess uncertainty, three different methods were used by the PCCSP to diagnose tropical cyclones from global climate models. Whilst significant uncertainty remains, the results from this study indicate that the frequency of tropical cyclones in the PCCSP region is projected to decrease by the late 21st Century. While the sign of the change is consistent, there is little consistency in the magnitude of changes between either the models or the analysis methods.

References

Australian Bureau of Meteorology and CSIRO, 2011: Climate Change in the Pacific: Scientific Assessment and New Research. Volume 1: Regional Overview. Volume 2: Country Reports.

Ganachaud, A.S., A. Sen Gupta, J.C. Orr, S.E. Wijffels, K.R. Ridgway, M.A. Hemer, C. Maes, C.R. Steinberg, A.D. Tribollet, B. Qiu and J.C. Kruger, 2011: Chapter 3: Observed and expected changes to the tropical Pacific Ocean. In: Bell JD, Johnson JE and Hobday AJ (Editors), 2011: Vulnerability of Tropical Pacific Fisheries and Aquaculture to Climate Change. Secretariat of the Pacific Community, Noumea, New Caledonia.

Lough, JM, GA Meehl and MJ Salinger, 2011: Chapter 2: Observed and projected changes in surface climate of the tropical Pacific. In: Bell JD, Johnson JE and Hobday AJ (eds), 2011: Vulnerability of Tropical Pacific Fisheries and Aquaculture to Climate Change. Secretariat of the Pacific Community, Noumea, New Caledonia.

Power, S.B., G. Cambers, A. Schiller, D. Jones and K. Hennessy, 2011: The Pacific Climate Change Science Program. Bull. American Meteorolog. Soc., 92, 1409–1411.
doi: http://dx.doi.org/10.1175/BAMS-D-10-05001.1

Fig 1. Front covers of the two volumes.

Fig 2. Developing countries (in blue) participating in the PCCSP and PACCSAP, and in the production of the report.

Fig 3. Participants at one of the many training and research workshops held in the region as part of the PCCSP (Darwin, June 2010).
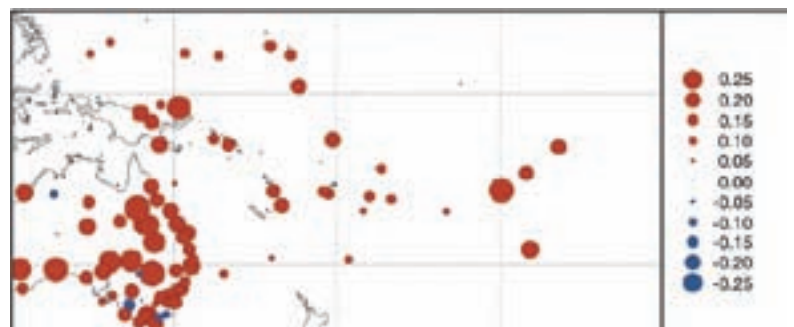

Fig 4. Sign and magnitude of trends (˚C/decade) in annual mean temperature at Pacific island meteorological stations across for 1960-2009. Australian stations are included for comparison.

Antarctic Bottom Water changes during the last fifty years

Marina Azaneu[1], Rodrigo Kerr[1]*,
Mauricio M. Mata[1], and Carlos A. E.
Garcia[1]

1   Laboratório de Estudos dos Oceanos e Clima, Instituto de
     Oceanografia, Universidade Federal do Rio Grande (FURG),
     Rio Grande, RS, 96201-900, Brazil.

*Corresponding author: Email: rodrigokerr@furg.br
Phone number: +55 53 3233-6854 / 6861
Fax number: +55 53 3233-6611

1. Introduction

The formation of deep and bottom water masses in the Southern Ocean plays a significant role in both global ocean circulation and climate. Antarctic Bottom Water (AABW) formation occurs in some specific areas around the Antarctic margins with contribution of different source waters (Carmack and Foster, 1975). The surface forcing for the formation of this dense water can be cooling by heat loss and increase in salinity (e.g., sea ice formation and brine rejection, among other processes; Killworth, 1983). However, recent studies have documented changes in regional climate around the Antarctic continent, such as the evident atmospheric warming (Turner et al., 2005a) and glaciers retreat in the Antarctic Peninsula region during the last 50 years (Cook and Vaughan, 2010). Gille (2002) pointed to a significant increase in temperature (~0.2°C) of intermediate waters of the Antarctic Circumpolar Current during the 1990s. A similar warming trend for Warm Deep Water (WDW; ~0.012 °C.year^{-1}) was also noted by Robertson et al. (2002) in the Weddell Gyre, while Jacobs and Giulivi (2010) have found a decrease in salinity (freshening) in the Ross Sea. In addition, Rintoul (2007) documented a rapid freshening of the Antarctic Bottom Water (AABW) in the Indian and Pacific sectors of the Southern Ocean during the 1995-2005 period.

The trends found by those previous studies reveal a complex and variable change in the ocean-atmosphere-cryosphere climate system, which are still barely understood. The purpose of this work is to investigate the space-temporal variability of the deep and bottom water masses properties in the Southern Ocean to infer any temporal trend in the AABW properties.

2. Southern Ocean database and Methodology

The dataset used for this study is derived from three distinct sources: (1) World Ocean Database 2009 (WOD09, Boyer et al., 2009) which consists of bottle, profiling floats, and CTD data spanning from 1958 to 2010; (2) German Alfred-Wegener-Institute (AWI) database gathered in the Antarctic waters from 2003 to 2010; (3) Brazilian High Latitude Oceanography Group (GOAL) dataset from 2003-2005 and 2008-2010 periods. The three sets of data together cover a total period of 52 years. In addition to the quality control included in WOD09, we also avoided the use of duplicated stations and restricted our analysis to the austral summer (November to March) due to the seasonal variability and lack of observation during other seasons. The parameters analyzed in this work were potential temperature (θ), salinity (S) and neutral density (γ^n). The last was determined according to Jackett and McDougall (1997). Since AABW density values vary around the Southern Ocean, we used the neutral density of 28.27 kg m^{-3}, as considered by Orsi et al. (1999).

In order to avoid problems associated with irregular spatial and temporal coverage, two approaches were considered in this work. The first consisted of a space-temporal selection, in which only data within a 220 km radius around a recent measurement (i.e., collected during the last decade) were considered. The second approach was a geographic bin criterion, in which annual means of properties were calculated for a two-degree grid and then averaged for the entire region. Due to differences between coastal and oceanic hydrographic regimes (regions), the dataset was selected following the isobaths of 1300 m. Linear fitting and p-value were calculated for each time series. The latter indicates if the linear fit is statistically significant, whose value must be lower than 0.05 for the time series can be considered significant at 95% level. The selection excluded all data in the oceanic region collected during 1962, which had the largest standard deviation of the time series. In the shelf region, no data were collected in 1999. Figure 1 shows the distribution of all the data used in this study. Among the most frequently sampled regions were: the oceanic regions of Weddell, Indian and Western Pacific sectors and the continental shelves of the Ross Sea, Weddell Sea, Bransfield Strait, and Prydz Bay.

3. Results and Discussion

The time series of the oceanic regime (Fig. 2) shows warming (0.0037 °C.year^{-1}), freshening (-0.0003 year^{-1}) and lightening (-0.0012 kg m^{-3}.year^{-1}) trends. In the shelf region (Fig. 2) temperature and salinity annual mean values also presented positive (0.0084 °C.year^{-1}) and negative (-0.0012 year^{-1}) trends, respectively. The consequences of temperature increase and salinity decrease over time lead to a density decrease (-0.0026 kg m^{-3}.year^{-1}) over the entire period.

Figure 3 shows the time series of gridded data that are statistically significant according to the linear fitting applied. In the Weddell, Indian and Western Pacific sectors, where data coverage is more consistent, an increase in deep ocean temperature (Fig. 3A) can be noticed for the oceanic region, mainly in the Weddell sector. This temperature trend (0.0167 °C.year^{-1}) is one order of magnitude higher than the one calculated using all oceanic data. This trend is probably related to the WDW warming reported by Fahrbach et al. (2004) and Robertson et al. (2002), considering the importance of this water mass to the formation of deep dense water in those regions. The warming of oceanic dense waters can also be related to the rising

SAM index, since it can lead to a more intense WDW upwelling into the shelf break, therefore rising the contribution of WDW to high density water formation (Jacobs, 2006).

Despite the positive (and statistically significant) temperature trend obtained in the shelf region, when all data were used, high dispersion of temperature annual means is found for the gridded data time series (not shown). This is not the case for oceanic data, which presented a homogeneous distribution (and trend) over time. In fact, in the shelf region the temporal trends of water properties were statistically significant mostly in well sampled regions, such as the Ross Sea, Bransfield Strait, and Prydz Bay, where negative temperature trends (Fig. 3A) were observed. The highest rate value (-0.0137 °C.year^{-1}) was found in the West Antarctic Peninsula (WAP) region, which is considered one of the most susceptible areas to climate change (Meredith and King, 2005).

In the oceanic region (depth >1300 m), no trend was observed with the salinity values while freshening is clearly identified in the shelf waters (Fig. 3B). This freshening is observed in the same regions where the cooling of shelf waters was identified, i.e. Ross Sea, Bransfield Strait and Prydz Bay. In that case, the Ross Sea region presented the highest freshening trend (-0.0033 year^{-1}) compared to the Bransfield Strait region (-0.0012 year^{-1}). The freshening and cooling noticed for the Ross Sea in this study have already been reported by Jacobs and Giulivi (2010). The authors calculated a salinity decrease trend of -0.003 year^{-1} for the High Salinity Shelf Water (HSSW) and -0.004 year^{-1} for Modified Circumpolar Deep Water (MCDW) and a cooling rate of -0.0125 °C.year^{-1} for MCDW. Jacobs (2002) stated that this long-term variability is possibly related to ice sheet melting in WAP.

The neutral density time series (Fig. 3C) reflected the changes in both temperature and salinity over the 50-year period. For instance, a decrease in density by -0.0013 kg m^{-3}.year^{-1} has been calculated for the oceanic sectors, which is probably caused by an increase in temperature in those regions. In the shelf region (Fig. 3C), a decrease in neutral density values over time can be found in the Ross Sea, Prydz Bay and next to the tip of the Antarctic Peninsula. Considering the decrease in temperature found for those regions found in this study, the freshening process is probably leading to lighter deep and bottom water masses varieties. Despite the differences of the hydrographic properties of those studied regions, the derived density trends presented similar values in the Antarctic Peninsula and Prydz Bay region (-0.0022 kg m^{-3}.year^{-1}) and in the Ross Sea (-0.0026 kg m^{-3}.year^{-1}).

4. Summary
In this study we investigated the variability of high dense waters of the Southern Ocean using hydrographic data from 1958 to 2010. The dataset was divided into oceanic (depth >1300 m) and shelf (depth <1300 m) regimes. A decreasing trend was found for both salinity and neutral density shelf and oceanic time series. The salinity trends vary regionally in oceanic waters, being more evident in the shelf, with important contributions from dense water mass formation areas (i.e. Ross Sea, Bransfield Strait, and Prydz Bay), as indicated by

the spatial trend of the salinity field. In the Ross Sea, several authors have reported a freshening of shelf and dense waters (e.g., Jacobs, 2002, 2006). Jacobs and Giulivi (2010) stated that changes in precipitation, sea ice production, ocean circulation strength and mostly continental ice melting are possible causes of the freshening process reported and are anti-correlated with the rising annual Southern Annular Mode (SAM) index.

In general, the spatial trends show a warming in the Weddell, Indian and Western Pacific oceanic sectors. Besides the warming of WDW reported by Robertson et al. (2002) and Fahrbach et al. (2004), the warming of oceanic dense waters can also be related to the rising SAM index.

The combination of freshening in shelf waters and warming of oceanic water masses leads to the AABW density decrease over the 50-year period analyzed here, with a trend of 0.0026 and 0.0012 kg m^{-3}.year^{-1} for shelf and oceanic waters, respectively. Kerr et al. (2011) also indicated that recent shelf waters freshening trends around the Antarctic continent, based on model outputs, are likely to be related to changes in the AABW outflow rates.

The results reported here not only emphasize that shelf waters are becoming fresher (e.g. Jacobs and Giulivi, 2010; Hellmer et al., 2011), as earlier reported for several regional areas (Weddell, Ross and Adelie Land shelves) around the Southern Ocean, but also that the AABW, produced and consequently exported to the global ocean, are becoming lighter.

Acknowledgements

References
Boyer, T.P., J. I. Antonov, O. K. Baranova, H. E. Garcia, D. R. Johnson, R. A. Locarnini, A. V. Mishonov, D. Seidov, I. V. Smolyar, and M. M. Zweng, 2009: World Ocean Database 2009, Chapter 1: Introduction, NOAA Atlas NESDIS 66, Ed. S. Levitus, U.S. Gov. Printing Office, Wash., D.C. , 216 pp.

Carmack, E.C. and Foster, T.D., 1975: On the flow of water out of the Weddell Sea, Deep-Sea Res., 22, pp. 711-724.

Cavalieri, D.J. and Parkinson, C.L., 2008: Antarctic sea ice variability and trends, 1979–2006. Journal of Geophysical Research, 113(C7), pp.1-19.

Cook, A., Fox, A., Vaughan, D. and Ferrigno, J., 2005: Retreating glacier fronts on the Antarctic Peninsula over the past half-century, Science, 308, pp. 541-544.

Fahrbach, E., Hoppema, M., Rohardt, G., Schröder, M. and Wisotzki, A., 2004: Decadal-scale variations of water mass properties in the deep Weddell Sea. Ocean Dynamics, 54, pp. 77-91.

Gille, S. T., 2002: Warming of the Southern Ocean since the 1950s. Science, 295, pp. 1275– 1277.

Hellmer, H. H., Huhn, O., Gomis, D., and Timmermann, R., 2011: On the freshening of the northwestern Weddell Sea continental shelf, Ocean

Sci., 7, 305-316, doi:10.5194/os-7-305-2011.

Jackett, D.R., McDougall, T.J., 1997: A neutral density variable for the world's ocean. Journal of Physical Oceanography 27 (2), pp. 237-263.

Jacobs, S. S. and Giulivi C. F., 2010:Large Multidecadal Salinity Trends near the Pacific−AntarcticContinental Margin. Journal of Climate, vol. 23. (doi:10.1175/2010JCLI3284.1)

Kerr, R., Heywood, K. J., Mata, M. M., and Garcia, C. A. E., 2011: On the export of dense water from the Weddell and Ross Seas, Ocean Sci. Discuss., 8, 1657-1694, doi:10.5194/osd-8-1657-2011.

Killworth, P.D., 1983: Deep Convection in the World Ocean. Reviews of Geophysics and Space Physics, 21(1), pp.1-26.

Lumpkin, R., Speer, K., 2007: Global ocean meridional overturning. Journal of Physical Oceanography 37, 2550–2562.

Meredith, M.P. and King, J.C., 2005: Rapid climate change in the ocean west of the Antarctic Peninsula during the second half of the 20th century, Geophysical Research Letters, 32, L19604. (doi:

10.1029/2005GL024042).

Orsi, A.H., Johnson, G.C., Bullister, J.L., 1999: Circulation, mixing and production of Antarctic Bottom Water. Progress in Oceanography 43, pp. 55–109.

Rintoul, S.R., 2007: Rapid freshening of Antarctic Bottom Water formed in the Indian and Pacific oceans. Geophysical Research Letters, 34(6), pp.1-5.

Robertson, R. et al., 2002: Long-term temperature trends in the deep waters of the Weddell Sea. Deep Sea Research Part II: Topical Studies in Oceanography, 49(21), pp.4791-4806.

Turner, J., Colwell, S.R., Marshall, G.J., Lachilan-Cope, T.A., Carleton, A.M., Jones, P.D., Lagun, V., Reid, P.A. and Iagovkina, S., 2005a: Antarctic climate change during the last 50 years. International Journal of Climatology, 25, pp. 279-294
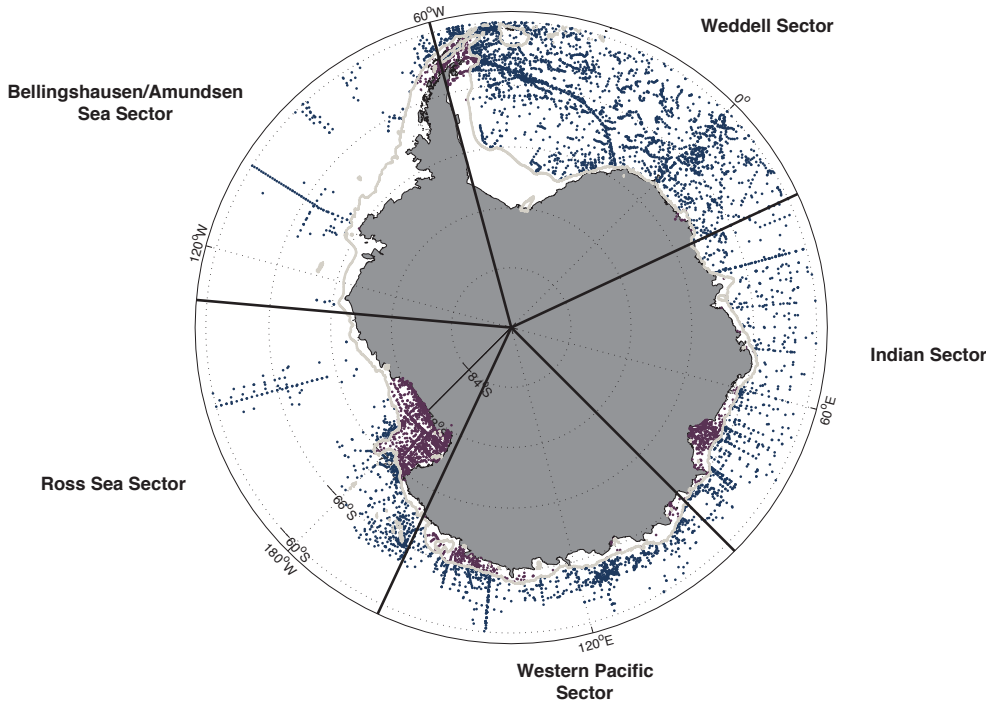
Fig 1: The distribution of observational data in the Southern Ocean. Dots in magenta represent data in the shelf regime (depth <1300 m) while blue dots are in the oceanic region (depth >1300 m). Gray lines indicate the 1300 m isobath and black lines delimit the hydrographic sectors of Weddell Sea, Indian Sector, Western Pacific, Ross Sea, and Bellingshausen/Amundsen Sea (as defined by Cavalieri and Parkinson, 2008).
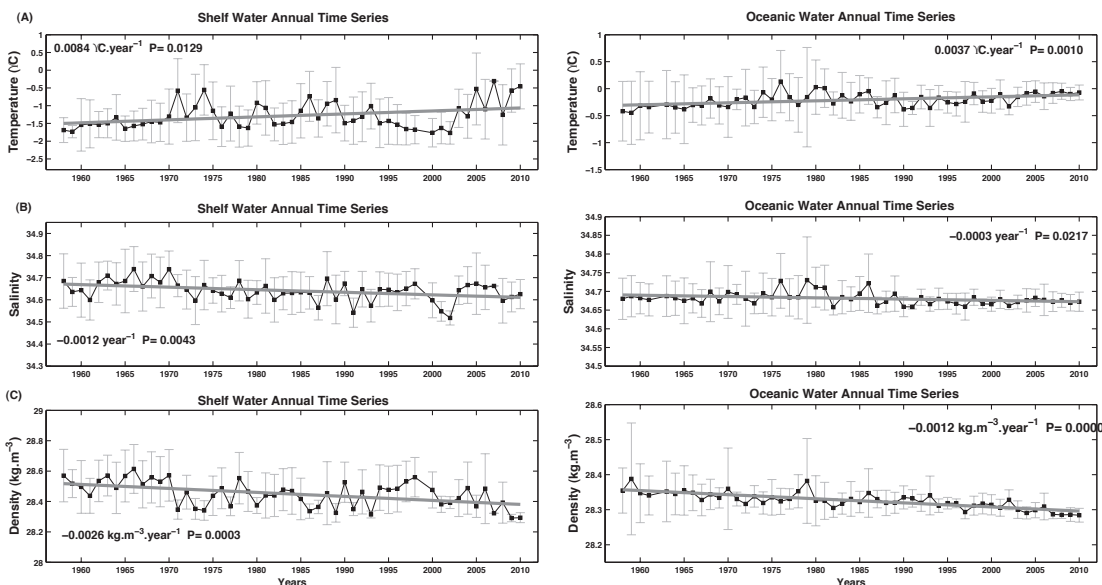

Fig 2: The annual average of potential temperature (upper), salinity (middle) and neutral density (lower) for shelf (left) and oceanic (right) regions, respectively, during the 50-year period. Error bars represent one standard deviation of the values. The gray solid lines represent the linear fit to the average values for each regime (or region). The temporal rate of change and P values are also added to the figures.
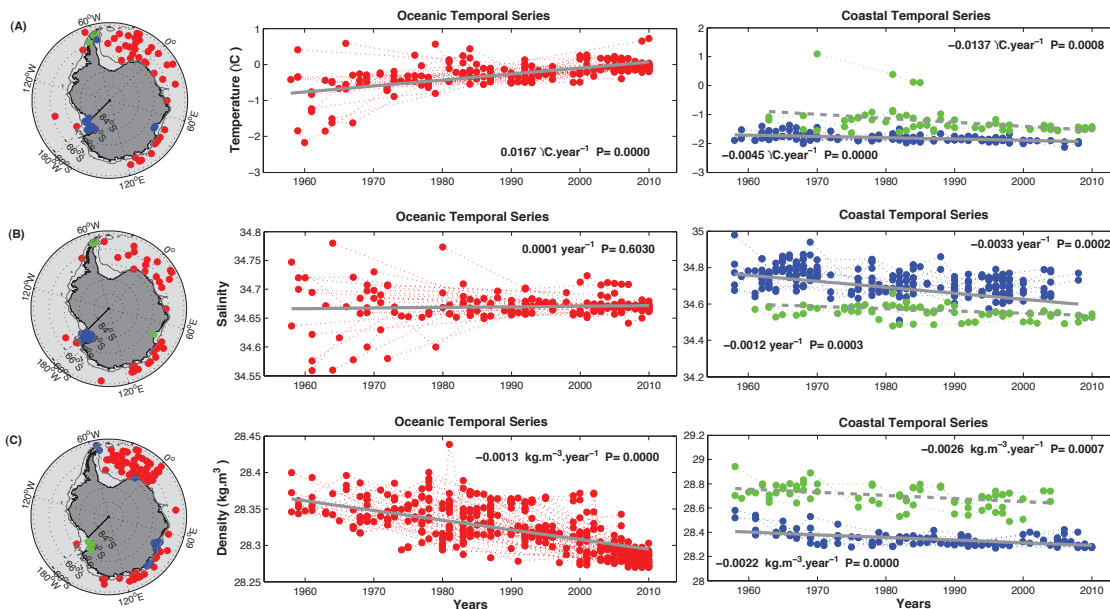
Fig 3: Potential temperature (A), salinity (B) and neutral density (C) time series of the gridded data for oceanic (middle) and shelf (right) waters. The position of each gridded data can be seen on map (left), where the red color denotes oceanic regions and the blue and green denotes shelf regions.

Developing a Vision for Climate Variability Research in the Southern Ocean-Ice-Atmosphere System

Kevin Speer[1], Nicole Lovenduski[2], Matthew England[3], David Thompson[4], Catherine Beswick[5]

1   Florida State University, USA
2   University of Colorado, Boulder, USA
3   University of New South Wales, Sydney, Australia
4   Colorado State University, Fort Collins, USA
5   International CLIVAR Project Office, UK

The Southern Ocean region is currently accumulating more heat and anthropogenic carbon than anywhere else in the ocean, which could have global ramifications. Climate models poorly resolve this key region, and produce a wide variety of projected climate states in the future. Ongoing greenhouse gas increases and ozone recovery are both expected to modify Southern Hemisphere wind patterns, with likely implications for ocean heat and carbon uptake (Figure 1). This will exert a strong influence on the global climate system. Much effort has recently gone into improving ocean model representation of the role of eddies, yet these processes are not yet adequately represented in coarse IPCC-class climate models. Improvements to models and our understanding of the role of eddies and air-sea-ice interactions in the Southern Ocean system have been made, but large gaps still exist. To compound this situation, there is a

paucity of observations in the Southern Ocean climate system, including ocean circulation/hydrography, air-sea fluxes, and atmospheric properties. The CLIVAR/CliC/SCAR Southern Ocean Panel (SOP) has had a sustained interest in driving forward the observational programmes required in this region, with some notable achievements (e.g. the Southern Ocean Observing System; SOOS).

During 19 - 21 October 2011, the SOP held its seventh meeting (SOP-7) in Boulder, Colorado, USA. The meeting convened experts from three key areas of Southern Ocean research – Southern Ocean carbon, atmospheric processes over the Southern Ocean, and Southern Ocean physics – with the overarching objective to generate an overview of current understanding in these three main areas. Under each of the three themes, invited speakers highlighted to the panel key open questions and discussed gaps in our current understanding. This will ultimately feed into the vision document being developed by the panel: A Vision for Climate Variability Research in the Southern Ocean-Ice-Atmosphere System. The following three sections summarize in turn the main issues highlighted during the meeting across the above three thematic areas.

Southern Ocean Carbon

The Southern Ocean is an important regulator of atmospheric carbon dioxide (CO_2). In this region, old, CO_2-rich water is ventilated to the atmosphere, and nearly half of the ocean's anthropogenic CO_2 is absorbed and stored. It is therefore important to quantify and understand the processes controlling air-sea CO_2 exchange in the Southern Ocean, given the implications for the global climate system.

Results based on coarse-resolution ocean models suggest that the physical circulation of the Southern Ocean governs the exchange of CO_2 across the air-sea interface, and that changes in the physical circulation have altered the uptake and release of CO_2 from the region (Figure 1). However, the community remains concerned about certain aspects of these modeling studies. Central to their concerns are two questions: (1) Can

coarse-resolution ocean models accurately represent Southern Ocean circulation and CO2 uptake?; and (2) Do we have enough observational evidence to support these model-based findings?

Learning more about Southern Ocean carbon uptake will require a sustained international effort to observe Southern Ocean biogeochemistry. Such an effort has been proposed by Sarmiento and collaborators (SOBOM; The Southern Ocean Biogeochemical Observations and Modeling Program); they aim to deploy autonomous ARGO floats with biogeochemical sensors in the Southern Ocean region, and to use these observations to better constrain eddy-resolving models of the Southern Ocean.

Analysis of Drake Passage pCO2 and d14C observations suggests that there has been an increase in the vertical transport of CO2-rich and d14C-depleted waters over the past few decades in the region south of the Polar Front. This finding is remarkably consistent with results from coarse-resolution ocean models (Sweeney et al., personal comm.).

Through sustained observations, the Palmer Long-Term Ecological Research (PAL LTER) program has successfully demonstrated the impact of physical climate variability on the Southern Ocean ecosystem. In particular the Western Antarctic Peninsula (WAP) has warmed rapidly over the past few decades, sea ice has dramatically decreased in this region, and phytoplankton productivity has declined in the north WAP and increased in the south WAP (Stammerjohn et al., personal comm.). Such changes have had consequences for all trophic levels.

HIAPER Pole-to-Pole Observations, or HIPPO, an airborne, observational campaign that aims to sample atmospheric O2 and CO2, has completed five missions over the last two years. These data are currently being processed an analyzed. Preliminary results suggest large interannual air-sea O2 flux variability over the Southern Ocean (Bent et al., personal comm.).

The Community Earth System Model (CESM) is being used to assess variability in Southern Ocean carbon uptake. As a full coupled climate model with a state-of-the art ocean biogeochemical submodel, CESM has been fairly successful at representing observed CO2 variability in the region. Results from this model suggest that advection of dissolved inorganic carbon is the dominant control on air-sea CO2 flux variability in the Southern Ocean, with biological processes playing a smaller role (Long et al., personal comm.).

Wang and Moore (2012) coupled an older version of the Community Climate System Model to a modified ocean biogeochemical model, in order to assess the role of the biological pump in controlling air-sea CO2 flux variability over the Southern Ocean. The model included an improved parameterization of the iron cycle, an additional phytoplankton group, Phaeocystis Antarctica, and an improved representation of Southern Ocean mixed layer depths. This study suggests that biological production and circulation play equally important roles in controlling Southern Ocean CO2 flux variability.

Southern Ocean Atmosphere

The Southern Annular Mode (SAM) is the prominent pattern of large-scale climate variability in Southern Hemisphere mid-high latitude circulation. Variations in the SAM influence weather across broad regions of the Southern Hemisphere ocean and land areas (see Thompson et al., 2011, for a recent review). Thus understanding how the SAM will respond to anthropogenic forcing is of key societal importance.

The SAM is believed to be sensitive to both increases in greenhouse gases and decreases in stratospheric ozone. Ozone depletion appears to have played a dominant role in driving low frequency variability in the SAM during the 20th Century; increases in greenhouse gases are expected to play a similarly important role during the 21st Century. But there is considerable uncertainty regarding the underlying dynamical mechanisms. It is unclear for example why the SAM responds to ozone-induced cooling in the polar stratosphere. It is also unclear why the SAM responds to increases in greenhouse gases. In fact, it is arguably unclear why the SAM exists in the first place.

The SOP-7 talks on atmospheric dynamics over the Southern Ocean emphasized the key role of feedbacks between the mean flow and the wave fluxes of heat and momentum in the Southern Hemisphere atmosphere. They explored the role of the SAM in driving changes in the strength and position of the Antarctic Circumpolar Current. They examined the processes that drive variability in the SAM and they explored the mechanisms whereby both the SAM and tropical climate variability influence Antarctic climate.

Southern Ocean Physics

The Southern Ocean is thus far responding to climate change very differently to the Northern Hemisphere; for example the rapid warming observed over subpolar northern latitudes has not yet materialized over the Southern Ocean. The primary reason appears to be the large uptake of heat by the Southern Ocean, although the precise mechanisms at play remain uncertain. Furthermore, there is inconsistency in model estimates of the magnitude of this anthropogenic heat uptake. Recent progress has been made in formulating eddy parameterizations more appropriately in coarse resolution models, so that to first order the response of the Southern Ocean to wind changes is correctly captured (Gent and Danabasoglu, 2011). Ongoing eddy-permitting and eddy-resolving model development is also targeting this issue, to bridge the gap between IPCC-class climate models and the eddy-rich flow patterns seen in observations and high-resolution models.

Other recent work was also highlighted during the meeting. Drake Passage transport was monitored as part of the cDrake study using pressure sensors and echo sounders and bottom velocity sensors. Results show sustained high velocities 50 m off the ocean floor. A significant challenge for climate models is to match these velocities at the bottom, in the presence of bottom topography that controls flow configuration.

Eddying models as well as direct observations have shown that as the Southern Hemisphere subpolar westerly winds increase, so too does eddy activity, producing a greater eddy-

driven component to the MOC. This poleward eddy-driven flow mostly balances the wind-driven Ekman increase in the MOC. In contrast, there is unlikely to be such compensation in the net meridional heat flux in response to wind changes, as eddies and Ekman fluxes both modulate heat transfer with different depth profiles. Correct resolution of the poleward eddy heat transport is thus an important consideration in getting the correct temperature and sea ice response to anthropogenic climate change. The eddy response appears to be too weak in current models; consequently the response to Southern Hemisphere wind shifts might not be correct.

Sea ice extent in the Arctic has broadly decreased over the last 30 years, whereas Antarctic sea-ice has shown opposing trends over the western and eastern regions. Kirkman and Bitz (2011) have investigated why no net trend has been observed in the Antarctic. Antarctic warming over the last 50 years has been more prevalent in the west, as compared with the east. Warming is also occurring at depth in the Southern Ocean. Loss of sea ice in the Bellingshausen Sea appears to be via tropical teleconnections and/or changes in the SAM. But there are multiple theories for the expansion elsewhere, including 1) SAM trends (driven primarily by ozone) and 2) freshwater flux trends (either via precipitation changes or ice melt). Warming could be shrinking the overall thickness of Antarctic sea ice but observations are thus far insufficient to detect this.

It is unclear why models do not capture observed Antarctic sea-ice trends. A serious problem for future prediction is that the models show quite large disagreement. This is a key issue as it hampers predictions of future change, even to the extent that the sign of the change is unknown in some cases. One major uncertainty is the contribution from sea ice to salinity budgets in the Southern Ocean. Evidence suggests that sea ice is thinning in some areas; where this occurs, the ice will persist less, resulting in longer periods of open water. This trend could be inferred from water isotopes. However, direct sea-ice measurement systems are one of the most difficult observational programs to sustain on a large-scale. Remote sensing offers some hope of regular measurement.

Progress in other areas includes the incorporation of observations into a statistical estimate of ocean circulation; e.g. the SOSE (Southern Ocean State Estimate) program (Mazloff et al., 2010). As sensors for biogeochemistry become available they are being integrated into Argo profiles, and these might in turn be incorporated into ocean biogeochemistry state estimates. For SOSE going forward, there is a need for better geoid products and mean dynamic topography products in order to improve the mass balance of ocean volume. State estimates based on a dynamical model such as SOSE provide a basis for evaluating and calibrating climate models. Without adequate observations, no such state estimate is feasible. A concerted community effort is required to bring together the vast array of measurements needed to improve global climate prediction.
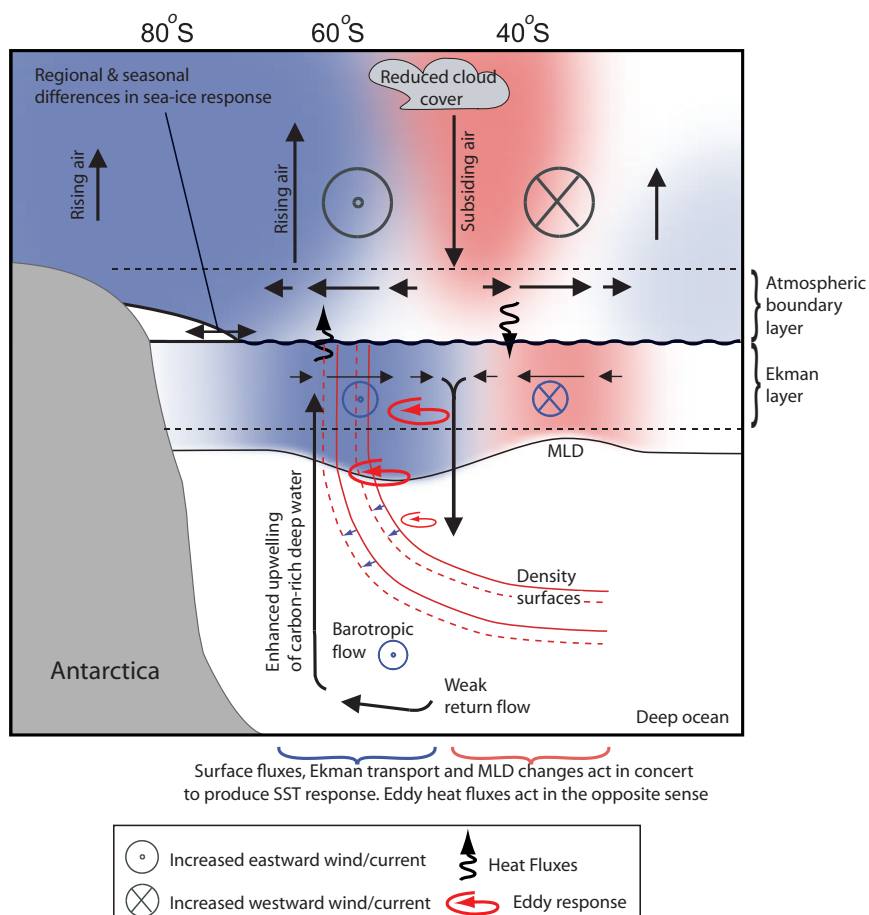
References

Gent, P. R. and G. Danabasoglu, 2011: Response to increasing Southern Hemisphere winds in CCSM4. J. Clim. 24, 4992–4998.

Kirkman, C. and C.M. Bitz, (2011), The Effect of the Sea Ice Freshwater Flux on Southern Ocean Temperatures in CCSM3: Deep Ocean Warming and Delayed Surface Warming, J. Climate, 24, pp. 2224-2237 doi: 10.1175/2010JCLI3625.

Mazloff, M.R., P. Heimbach and C. Wunsch, 2010: An Eddy-Permitting Southern Ocean State Estimate. J. Phys. Oceanogr., 40(5), 880-899.

Thompson, D.W.J., S. Solomon, P.J. Kushner, M.H. England, K.M. Grise and D.J. Karoly, 2011: Signatures of the Antarctic ozone hole in Southern Hemisphere surface climate change, Nature Geoscience, 4, 741-749 (doi:10.1038/ngeo1296).

Wang, S. and J. K. Moore (2012), Variability of primary production and air-sea CO2 flux in the Southern Ocean, Global Biogeochem. Cycles, 26, GB1008, doi:10.1029/2010GB003981.

Fig 1. Schematic response of the ocean to the high-index polarity of the Southern Annular Mode (from Thompson et al., 2011). Solid arrows indicate meridional and vertical motion in the atmosphere and ocean. Warm colors correspond to increases in temperature or heat content, and cooler colors to decreases. MLD refers to the ocean mixed-layer depth. All other responses are labeled on the figure or in the legend. All results indicate the climate response to the SAM on timescales less than a season with the exception of the oceanic eddy field, which indicates the response on timescales of 2–3 years. The ocean carbon response indicated remains uncertain; such a response would be considerably weaker if oceanic eddies compensate Ekman fluxes at the near-surface. (taken from Thompson et al. 2011)

The Diapycnal and Isopycnal Mixing Experiment: A First Assessment

Sarah T. Gille[1], James Ledwell[2], Alberto Naveira-Garabato[3], Kevin Speer[4], Dhruv Balwada[4], Alex Brearley[3], James B. Girton[5], Alexa Griesel[6], Raffaele Ferrari[7], Andreas Klocker[7], Joseph LaCasce[8], Peter Lazarevich[4], Neill Mackay[9], Michael P. Meredith[10], Marie-José Messias[9], Breck Owens[2], Jean-Baptiste Sallée[10], Katy Sheen[3], Emily Shuckburgh[10], David A. Smeed[3] Louis C. St. Laurent[2], John M. Toole[2], Andrew J. Watson[9], Nicolas Wienders[4], and Uriel Zajaczkovski[1]

1   Scripps Institution of Oceanography, University of California San Diego, USA
2   Woods Hole Oceanographic Institution, Woods Hole, USA
3   National Oceanography Centre, Southampton, United Kingdom
4   Florida State University, Tallahassee, USA
5   Applied Physics Laboratory, University of Washington, Seattle, USA
6   University of Hamburg, Germany
7   Massachusetts Institute of Technology, Cambridge, USA
8   University of Oslo, Norway
9   University of East Anglia, Norwich, United Kingdom
10 British Antarctic Survey, Cambridge, United Kingdom

The Diapycnal and Isopycnal Mixing Experiment in the Southern Ocean (DIMES) was designed as a multi-pronged US and UK CLIVAR effort to measure and to better understand diapycnal mixing and along-isopycnal eddy transport in the Antarctic Circumpolar Current (ACC), because these processes together appear to play a key role in the Merdional Overturning Circulation (MOC) (Gille et al., 2007). The project represents an unusual effort to evaluate simultaneously the roles of diapycnal and isopycnal mixing, and the program has benefited from close collaboration between observationalists, theoreticians and modelers. Fieldwork for DIMES began in early 2009, and the initial phase of the field observations is now wrapping up. This article provides a brief preliminary summary of early DIMES findings.

The DIMES field program was centered around the 2009 release of 76 kg of trifluoromethyl sulfur pentafluoride, CF3SF5, in the ACC near 105°W (yellow star in Figure 1) between the Subantarctic Front (SAF) and the Polar Front (PF). Starting in 2010, the tracer concentration has been measured at regular intervals in order to evaluate the displacement and vertical diffusion of the tracer throughout the southeastern Pacific and the Scotia Sea. Microstructure measurements have been collected at the same time to provide a direct measurement of the small-scale turbulence that controls tracer diffusion. Over 200 RAFOS floats were also released, starting with 75 floats near 105°W in 2009 and 105 floats at about the same location in 2010 (blue dots). Sound sources (cyan dots) were deployed throughout the southeastern Pacific and the Scotia Sea to track the floats. In late 2009 a mooring array was deployed east of Drake Passage to study energy transfer from the mesoscale through the internal wave field to mixing (blue star).

The experiment was planned so that the tracer and floats would first pass through the region of relatively smooth topography and low eddy energy of the eastern Pacific, and then through the region of relatively rough topography and high eddy energy in Drake Passage. Results available now include tracer survey data and microstructure measurements from the initial 2010 and 2011 surveys and trajectories from 44 of the RAFOS floats, along with independent ancillary data, including numerical simulations, Argo floats, surface drifters, and altimetry.

The tracer was released approximately 1500m deep on the $\gamma_n = 27.9$ kg m^{-3} neutral density surface, near the transition between Lower Circumpolar Deep Water and Upper Circumpolar Deep Water. These waters rise to the south to feed Antarctic Bottom Water that descends and spreads over the abyss in the "Lower Limb" of the MOC as well as Antarctic Intermediate Water and Subantarctic Mode Water that are driven north near the surface by the winds in the "Upper Limb". Eddy fluxes play a dominant role in cross-ACC transport of mass and properties in the waters above topography, i.e. above ~1500m. Diapycnal mixing is needed to transform abyssal water to deep water, closing the "Lower Limb". The degree to which diapycnal mixing modifies density in the upper waters, and thereby short-circuits the "Upper Limb" is an outstanding question. Observing diapycnal mixing throughout the water column, over both rough and smooth topography underlying the ACC, is one of the main objectives of DIMES.

Ledwell et al. (2011) reported on the initial assessment of vertical diffusivity obtained from the first year's tracer survey and microstructure measurements. Their measurements indicated weak mixing in the ocean interior upstream of Drake Passage, with the tracer indicating averaged diffusivities of $(1.3 \pm 0.2) \times 10^{-5}$ m^2 s^2, and microstructure profiles implying a diffusivity about half that size at $(0.75 \pm 0.2) \times 10^{-5}$ m^2 s^2. Measurements with profiling velocity-shear Argo floats – the Electromagnetic-Autonomous Profiling Explorer (EM-APEX) floats – indicate a peak in shear variance in June which may explain the difference between the tracer diffusivity, which

integrates over a year of mixing, and diffusivities K_ρ estimated from energy dissipation rates, which were measured in February/March 2010. From these results Ledwell et al. (2011) inferred that despite strong wind conditions that are common in the Southern Ocean, wind does not generate elevated internal wave activity to drive extra turbulent mixing in the mid-depth ocean. Levels of diapycnal mixing in the Southern Ocean, in the absence of strong bathymetry, appear to be similar to background levels in other areas of the ocean.

More detailed tracer surveys of the topographically rough Drake Passage region in 2011 indicate that the diapycnal spreading of the tracer was much greater to the east of Drake Passage than to the west (St. Laurent et al., 2012). Figure 2 shows mean vertical profiles of the tracer along two different meridional lines. S3 is located to the west of Drake Passage around 78°W, and SR1 is to the east of Drake Passage between 55°W and 60°W. The difference in the width gives a diapycnal diffusivity for the tracer of ~6×10^{-4} m^2 s^{-1}, based on a preliminary estimate of the mean velocity of the tracer between the sections. With account taken of the weaker stratification in the east than in the west, the diffusivity is around 30 times larger in Drake Passage than in the eastern Pacific.

Microstructure measurements are consistent with the tracer findings and provide evidence of the vertical variations in diapycnal diffusivity. In Drake Passage, measurements were collected in early 2010 along the rough topography of Phoenix Ridge (approximately 65°W). At the tracer level, on the γ_n = 27.9 kg m^{-3} neutral density surface the mean diffusivity K_ρ was found to be more than an order of magnitude greater than that found from dissipation rates in the eastern Pacific. Microstructure measurements have typically shown diffusivities of order 10^{-3} m^2 s^{-1} within 1000 m of the bottom. To the west of Phoenix Ridge, microstructure stations occupied in December 2010 over smoother topography indicated an intermediate diffusivity, with a mean value of K_ρ at the surface γ_n = 27.9 kg m^{-3} about 3 times greater than in the eastern Pacific (St. Laurent et al., 2012).

The preliminary float data (Figure 3) indicate that the large scale Lagrangian flow on the γ_n = 27.9 kg m^{-3} surface closely mirrors geostrophic contours implied by satellite altimetry measurements (not shown). Similarly, Argo temperature and salinity profiles also indicate that subsurface anomalies correlate well with eddy variability at the surface from altimetry. Argo-based TS correlations are strongest at mid-depth, since the upper ocean temperature structure is strongly influenced by transient air-sea exchanges. These findings suggest that eddy variability measured by altimetry can serve as a proxy for subsurface eddy variability, thus providing a means to enhance the analysis of the float observations. Independent observations are also critical for identifying the background mean state, in order to evaluate the dispersion.

At the same time, assessments of artificial "floats" deployed in numerical models have indicated that traditional particle dispersion methods used to infer Lagrangian diffusivities agree with Eulerian diffusivities. Isopycnal diffusivities derived from numerical model output typically range between 200 and 1500

m^2 s^{-1}. However, statistics based on Lagrangian methods are slow to converge, requiring many hundreds or thousands of particles to reduce error bars (Griesel et al., 2009; Klocker et al., 2012a; Sallée et al., 2012), and they can be biased. This has introduced a new challenge to identify the most robust measures of diffusivities. Both Lyapunov-exponent based methods and Nakamura (1996) diffusivities are being explored using model output and the new observations.

Theory predicts low diffusivities near the surface and high diffusivities at a subsurface critical depth below the core of the ACC, where the eastward ACC velocity approximately balances the westward Rossby wave phase speed. This works well for an equivalent barotropic system, with sufficient information (Klocker et al., 2012b). However, results may prove more difficult to interpret in systems with realistic bathymetry and additional forcing mechanisms (Griesel et al., 2009; Sallée et al., 2012). The DIMES float program, in combination with a variety of ocean models, will provide data to help assess these processes.

In summary, the first DIMES data to emerge indicate low diapycnal diffusivities in the eastern Pacific and elevated diapycnal diffusivities in Drake Passage. Efforts to understand the mechanisms driving the diapycnal mixing, to extrapolate the results to the whole ACC, and to assess implications for the overturning circulation are underway. Float data are providing constraints on along-isopycnal diffusivities in the region; formal uncertainties are expected to be large, given the slow convergence of dispersion statistics. Thus, satellite remote sensing and model output, together with other ancillary data will be critical for evaluating the strength and impact of along-isopycnal diffusion.

The DIMES program continues. Additional DIMES floats are now arriving at the surface, and these will allow a more complete effort to analyze dispersion on isopycnal surfaces. The in situ measurement program for tracer and microstructure will continue into 2014 with additional ship time scheduled primarily aboard the British Antarctic Survey research vessel RRS James Clark Ross, in order to track the tracer all the way through the topographically-complex Scotia Sea and into the Atlantic Ocean. Further information about DIMES is available from http://dimes.ucsd.edu.

Acknowledgements

References

Gille, S. T., K. Speer, J. R. Ledwell, and A. C. Naveira Garabato, 2007. Mixing and Stirring in the Southern Ocean, EOS, 88(39), 25 September 2007, pp. 382-383.

Griesel, A., S. T. Gille, J. Sprintall, J. L. McClean, J. H. LaCasce, and M. E. Maltrud , 2009. Isopycnal diffusivities in the Antarctic Circumpolar Current inferred from Lagrangian floats in an eddying model, J. Geophys. Res., 115, C06006, doi:10.1029/2009JC005821.

Klocker A., R. Ferrari, J. LaCasce, and S. Merrifield, 2012a. Reconciling float-based and tracer-based estimates of eddy diffusivities, J. Mar. Res., submitted.

Klocker A., R. Ferrari, and J. LaCasce, 2012b: Estimating suppression of eddy mixing by mean flows, J. Phys. Oceanogr., submitted.

Ledwell, J. R., L. C. St. Laurent, J. B. Girton, and J. M. Toole, 2011. Diapycnal mixing in the Antarctic Circumpolar Current, J. Phys. Oceanogr., 41, 241-246.

Nakamura, N., 1996. Two-dimensional mixing, edge formation, and permeability diagnosed in area coordinates. J. Atmos. Sci., 53, 1524–1537.

Sallée, J.-B., K. Speer, and S. Rintoul, 2012. Mean-flow and topographic control on surface eddy-mixing in the Southern Ocean. J. Marine Res., accepted.

St. Laurent, L., A. C. Naveira Garabato, J. R. Ledwell, A. M. Thurnherr, and J. M. Toole, 2012. Turbulence and diapycnal mixing in Drake Passage, in preparation / submitted.

Fig 1: Schematic diagram showing location and timeline for the DIMES field program. Tracer and floats were initially released in early 2009 at 105°W. Subsequent float releases were also concentrated at 105°W, and tracer and microstructure surveys have progressively moved downstream as the tracer has been advected by the Antarctic Circumpolar Current.
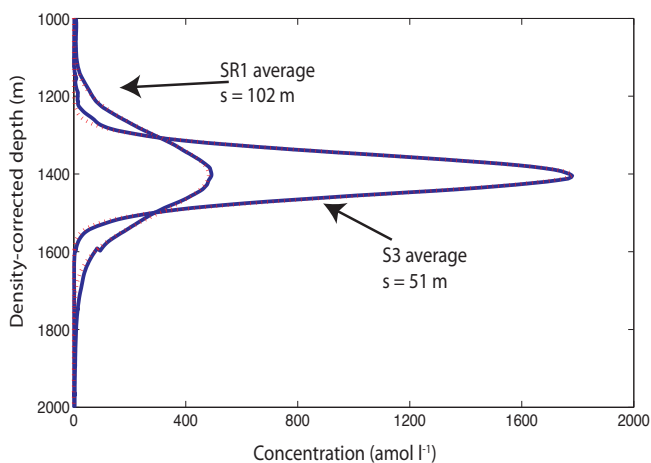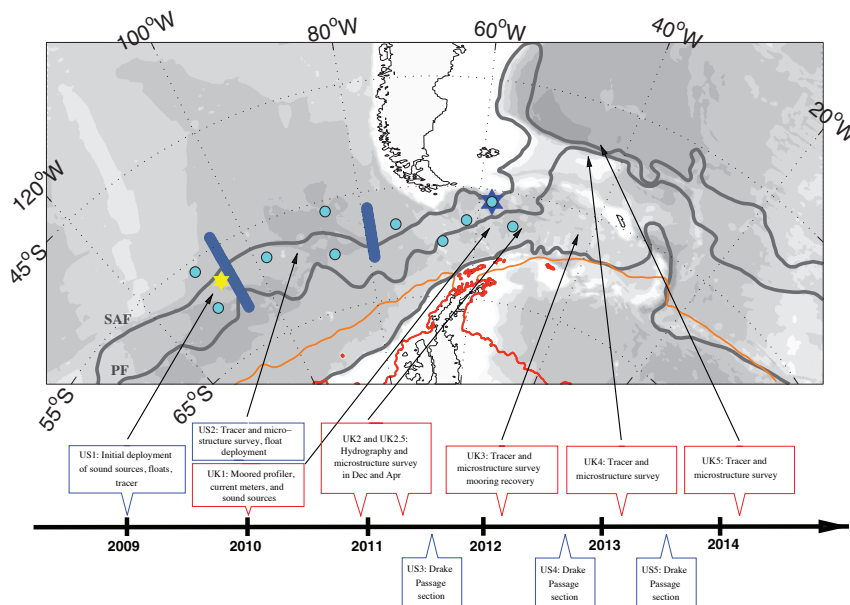
Fig 2. Mean vertical profiles of tracer (blues lines) from west of Drake Passage (S3) and east of Drake Passage (SR1), with Gaussian fits to the curves (red dotted lines). Both profiles were obtained in April 2011, 26 months after tracer release. The depth is from the mean depth/density relation for April 2011.

Fig 3. Preliminary two-year float trajectories from the first 44 DIMES RAFOS floats show that a few floats were advected rapidly downstream by the ACC, while many of the floats circulated around the basin upstream of Drake Passage.
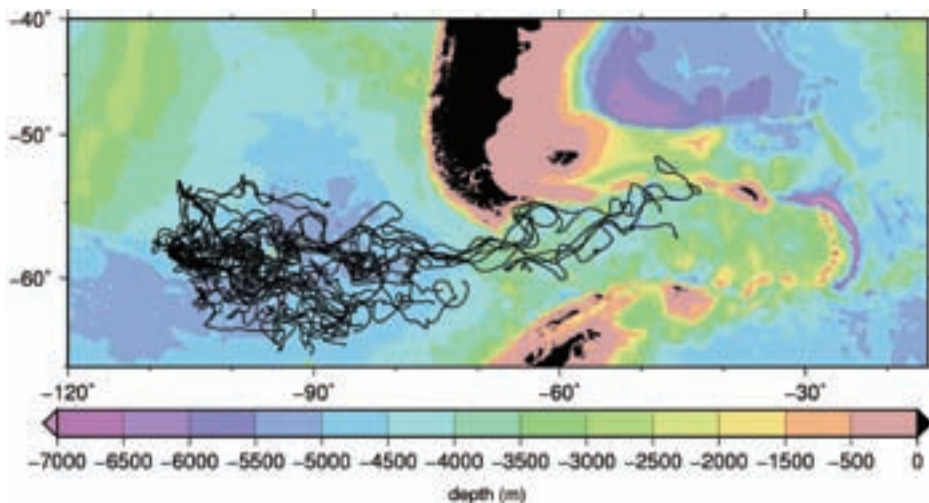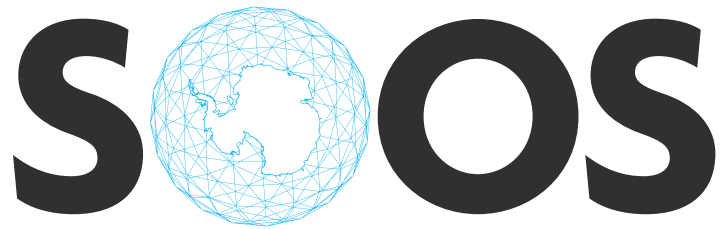
The Southern Ocean Observing System

Louise Newman[1], Steve Rintoul[2], Michael P. Meredith[3], Eberhard Fahrbach[4], John Gunn[5], Mike Sparrow[6], Victoria Wadley[7], Kevin Speer[8], Eileen Hofmann[9], Colin Summerhayes[10], Ed Urban[11], and Richard Bellerby[12] and the SOOS community

1   SOOS International Project Office, Institute for Marine and Antarctic Studies, University of Tasmania, Australia
2   CSIRO and Antarctic Climate and Ecosystems Cooperative Research Centre, Hobart, Australia
3   British Antarctic Survey, Cambridge, United Kingdom
4   Alfred Wegener Institute for Polar and Marine Research, Bremerhaven, Germany
5   Australian Institute of Marine Science, Townsville, Australia
6   Scientific Committee on Antarctic Research, Scott Polar Research Institute, United Kingdom
7   Department of Sustainability, Environment, Water, Population and Communities, Marine Division, Hobart, Australia
8   Florida State University, Tallahassee, USA
9   Old Dominion University, Norfolk, USA
10 Scott Polar Research Institute, Cambridge, United Kingdom
11 Scientific Committee on Oceanic Research, Newark, USA
12 Bjerknes Centre for Climate Research, Bergen, Norway

The Southern Ocean

Due to its position as the principal connector of the major ocean basins, the Southern Ocean strongly impacts climate, sea level, biogeochemical cycles and biological productivity on a global scale. The Southern Ocean influences the global distribution and movement of heat and carbon (e.g. Rintoul et al., 2001), and it features a vigorous overturning circulation that drives deep-water carbon and nutrients to the surface and draws down anthropogenic carbon from the atmosphere, with implications for global climate change and large-scale productivity (Sarmiento et al., 2004; le Quere et al., 2007; Meredith et al., 2012). The Southern Ocean exerts a strong influence on sea levels via melting of glacial ice (Rignot and Jacobs, 2002; Rignot et al., 2011), and it encompasses a sea-ice system that provides an important habitat for marine organisms, and which influences surface albedo and air-sea gas and heat exchange (Thomas and Dieckmann, 2002). The Southern Ocean also includes some of the most productive and vulnerable marine ecosystems on Earth, many of which support economically important species.

Given the significance of the Southern Ocean to the Earth system, any change in the region will have global ramifications.

SOUTHERN OCEAN OBSERVING SYSTEM

Recent scientific advances suggest that change is indeed already underway. The Southern Ocean is warming and freshening throughout most of the ocean depth (Böning et al., 2008; Gille, 2008), and major currents are postulated to be shifting south in some regions, causing regional changes in sea level (Sokolov and Rintoul, 2009a,b) and shifts in the distribution of organisms (Cubillos et al., 2007). These changes, and enhanced upwelling due to strengthening winds, have resulted in the supply of additional heat to the rim of Antarctica in some sectors, increasing melt rates of glacial ice (Jacobs, 2006; Jacobs et al., 2011) and impacting strongly on marine ecosystems (Schofield et al., 2010). Further, the future of the Southern Ocean carbon sink is a topic of vigorous debate (le Queré et al., 2007; Böning et al., 2008; Meredith et al., 2012), with the Southern Ocean taking up a large percentage of anthropogenic carbon, resulting in an increase in acidity of 30% (Rintoul et al., 2012). Complex feedbacks in the Southern Ocean will impact on the future trajectory of the climate system and ecosystems, but these are currently poorly understood, hindering our predictive skill.

Progress in understanding Southern Ocean processes has been slowed by a lack of observational data. The Southern Ocean is remote from population centres and shipping lanes, and the hostile environment has hampered data collection efforts. Over the last few decades, several international initiatives have focussed on monitoring aspects of the Southern Ocean (e.g., ISOS, POLEX-South, WOCE, JGOFS, BIOMASS, GLOBEC); however these initiatives had discrete foci, were generally based on observational programmes that were widely separated in space and time, and were often heavily biased to the summer months. More recently, growing recognition of the importance of the Southern Ocean has resulted in an increasing focus on the region, and new technologies have improved our ability to observe this region. Against this background, the International Polar Year (IPY; 2007-2008) was well timed to harness the human and logistic resources of the international community, and exploit technological developments to deliver an unprecedented view of the status of the Southern Ocean.

During IPY, most of the WOCE/CLIVAR repeat hydrographic sections were re-occupied, providing a near-synoptic snapshot of the physical and biogeochemical state of the Southern Ocean through the full water depth. Argo floats collected more than 60,000 temperature and salinity profiles during the 24-month IPY period, providing broad-scale, quasi-synoptic, year-round sampling of the upper 2 km of the Southern Ocean. Oceanographic sensors on marine mammals provided a similar number of profiles, including measurements from

regions where traditional oceanographic instruments have difficulty sampling, such as the sea-ice zone in winter. Moorings provided continuous time-series measurements of dense water overflows and boundary currents, major currents like the Antarctic Circumpolar Current and the Antarctic Slope Front, and coastal sea level. DNA barcoding and environmental genomics provided a completely new way of investigating evolution and biodiversity, ecosystem function and biological processes. New cryospheric satellites increased our ability to measure variables such as sea-ice volume.

Perhaps most importantly, IPY activities spanned all disciplines of Southern Ocean science and demonstrated that an integrated, multi-disciplinary, sustained observing system is feasible and urgently needed to address issues of high scientific and societal relevance. In recognition of this, the scientific community, under the guidance of the Scientific Committee on Antarctic Research (SCAR), the Scientific Committee on Oceanic Research (SCOR), the World Climate Research Programme (WCRP, specifically the CLIVAR/CliC/SCAR Southern Ocean Panel) and others, developed a strategy for sustained observations of the Southern Ocean, the Southern Ocean Observing System Initial Science and Implementation Strategy (available for download from www.soos.aq).

The Southern Ocean Observing System

SOOS will address six fundamental challenges of scientific and societal importance:

1) The role of the Southern Ocean in the planet's heat and freshwater balance,
2) The stability of the Southern Ocean overturning circulation,
3) The role of the ocean in the stability of the Antarctic ice sheet and its contribution to sea-level rise,
4) The future and consequences of Southern Ocean carbon uptake
5) The future of Antarctic sea ice, and
6) The impacts of global change on Southern Ocean ecosystems.

The following elements have been identified as being critical to the success of the SOOS in delivering the data required to address these challenges.

Repeat hydrography: Hydrographic sections from research vessels are the only means of sampling the full ocean depth for many variables. Repeat hydrography provides water samples for analysis of those properties for which in situ sensors do not exist, the highest precision measurements for analysis of change and for calibration of other sensors, accurate transport estimates, and a platform for a wide range of ancillary measurements.

Underway sampling from ships: The hydrographic sections need to be complemented by more frequent underway sampling transects, to reduce aliasing of signals with time-scales shorter than the 5-7 year repeat cycle of the repeat hydrography. Such underway sampling can be undertaken by supply vessels and tourist ships, as well as dedicated research vessels.

Enhanced Southern Ocean Argo: Year-round, broad-scale measurements of the ocean are needed to address many of the key science challenges in the Southern Ocean. These measurements can only be obtained using autonomous platforms like profiling floats. A sustained commitment to maintain and enhance a profiling float array in the Southern Ocean is critical, including a sub-sea ice component.

Time-series stations and monitoring of key passages: Several key passages and boundary currents in the Southern Ocean are high priorities for sustained observations because of their role in the global-scale ocean circulation and because they offer the best opportunities to measure water mass transport. High priority sites include Drake Passage and other chokepoint sections across the Antarctic Circumpolar Current and the dense water overflows and boundary currents carrying Antarctic Bottom Water to lower latitudes as part of the lower limb of the global overturning circulation.

Phytoplankton and primary production: Sustained observations of phytoplankton biomass, species distributions and primary production are needed to relate biological variability to environmental change. Ocean colour satellites are critical because they provide the only circumpolar view of biological activity in the Southern Ocean. In situ measurements are needed to refine algorithms used to interpret the satellite data, to relate surface chlorophyll to column-integrated production, for analysis of additional pigments and phytoplankton community composition, and to relate biological variables to simultaneous measurements of the physical and chemical environment.

Zooplankton and micro-nekton: Antarctic plankton may be particularly sensitive and vulnerable to climate change. Global warming will affect sea ice patterns and, therefore, plankton distributions (e.g., a decrease in the geographical extent of sea ice has been linked to a decline in krill numbers). Increased UV levels, ocean acidification, invasive plankton species, pollution and harvesting impacts are also potential threats. Underway sampling by continuous plankton recorders is required, as are targeted net tows and acoustic sampling.

Ecological monitoring: Observations of the distribution and abundance of top predators (fish, penguins, sea birds, seals and whales) can provide indications of changes in the ecosystem as a whole. The SOOS will provide the integrated multi-disciplinary observations needed to understand the interactions between physics, chemistry and biology in the Southern Ocean. Continued long-term and large-scale observations of functional and structural changes in ecosystems are essential to assess the sensitivity of ecologically key species, document biological responses and trends, and to ground-truth predictive models. In addition there is a need to develop new sensors to rapidly measure biological and chemical variables.

Animal-borne sensors: Oceanographic sensors deployed on birds and mammals can make a significant contribution to SOOS in two ways: by relating predator movements, behaviour and body condition to fine-scale ocean structure, and by providing profiles of temperature and salinity from regions of the Southern Ocean that are difficult to sample by other means (e.g., beneath the winter sea ice). The SOOS requires continuation and enhancement of the program of seal tag

deployments established during IPY, and development of a multi-species tagging approach along the lines of the Global Tagging of Pelagic Predators (GTOPP) and Tagging of Pacific Predators (TOPP) programmes.

Sea-ice observations: Measurements of both the extent and thickness of sea ice are needed to monitor changes in sea-ice production and related impacts on the climate and Southern Ocean ecosystem processes. A variety of satellite instruments provide continuous, circumpolar observations of sea-ice extent, with varying spatial resolution. Measuring sea-ice volume, however, remains a significant challenge and requires in situ sampling to provide ground-truth data for the satellite sensors. These measurements need to include a combination of sampling from ice stations, helicopters, autonomous vehicles, moorings and underway observations.

Observations of floating ice shelves and glacier tongues: Basal melting and freezing on the undersides of floating ice shelves exert significant influences on the ocean close to the Antarctic margin. These processes impact strongly on shelf water characteristics and the dense precursors of Antarctic Bottom Water. Ocean circulation and properties under shelf ice have been measured in only a few locations (Figure 1), and sustained measurements are needed to track the impacts of ocean climate changes on the ice shelves, and the subsequent feedbacks.

Enhanced meteorological and surface flux observations: The air-sea fluxes of heat, moisture, momentum and other climatically important properties are poorly known at high southern latitudes. Improvements are needed to accurately diagnose the interactions between atmosphere, ocean and sea ice that lie at the heart of climate variability and change, and the ecosystem responses to these. SOOS implementation requires improvements in surface flux measurements that parallel the improvements in the oceanic observational network.

Remote sensing: Access to high-quality remote sensing data is particularly critical in the Southern Ocean, where in situ data are difficult to obtain. High-priority satellite measurements include radar and laser satellite altimetry, ocean colour, scatterometer, infrared and microwave sea surface temperature, passive microwave, and synthetic aperture radar. Recommendations for satellite observations of the cryosphere, including sea ice, are given in the Cryosphere Theme document produced for the Integrated Global Observing Strategy (IGOS) Partnership (http://www.eohandbook.com/igosp/cryosphere.htm).

Towards Implementation

Commitments have already been made to complete many of the key elements of the SOOS. For example, most of the repeat hydrographic lines will be re-occupied within the next five years through the GO-SHIP programme (Figure 2; Hood et al., 2010). Several countries have long-standing commitments to monitor Drake Passage with annual full-depth hydrography, more frequent sampling of the upper ocean, and moored instruments including continuations of the long-term bottom pressure recorder deployments and tide gauge observations (Meredith et al., 2011). A well-established network of underway

observations has been in place for more than a decade and is expected to continue. Several moored arrays in the Weddell Sea have been maintained for a decade and are planned to continue. Similar programmes are being established in other locations around Antarctica (Figure 3), for example in the eastern South Pacific sector (www.oceanobservatories. org/infrastructure/ooi-station-map/southern-ocean/). Plans are being developed for a comprehensive system to monitor circulation in the South Atlantic Ocean through the South Atlantic Meridional Overturning Circulation (SAMOC) programme. With regard to biological sampling, the Palmer LTER on the western Antarctic Peninsula has been in operation for 30 years, and the long-term monitoring conducted by the CEMP and Rothera Time Series (RaTS) programmes also have long-standing commitments. Several nations have committed to ongoing CPR transects across the Southern Ocean. The number and breadth of biological measurements being made from ships of opportunity is slowly growing.

While the list of existing commitments provides some grounds for optimism and a firm foundation on which to build, there is substantial work to be done to secure the resources for a truly sustained and comprehensive observing system in the Southern Ocean. Programmes like the Argo profiling float array and the Marine Mammals Exploring the Oceans Pole to Pole (MEOP) network of tagged seals have helped to revolutionise our ability to observe the Southern Ocean. However, there is as yet no firm commitment to long-term sustained funding of these systems. Challenges facing the SOOS are common to the global ocean observing system as a whole (e.g., sustained funding; biological and biogeochemical sampling in winter and at large scales; lack of time-series data, particularly for biology and biogeochemistry; inadequate integration of physical, biological and biogeochemical observations; sparse sampling of the deep ocean; and adequate access to research vessels). Almost all elements of the observing system require enhancement to reach the sampling required to address the key scientific challenges.

A first step in the implementation of SOOS is to design optimal sampling plans for each element, and an overall integrated sampling scheme. This will provide the quantitative targets for the number and frequency of observations that are required, so that progress towards implementation of SOOS can be assessed. For some elements of the SOOS, these requirements have been defined (e.g., repeat hydrography, Argo, surface drifters, and ice drifters). For others, including many of the biological parameters, the further work that is required will be conducted in the early stages of SOOS implementation.

The provision of high-quality, easily accessible and, where possible, real-time data is a key objective of the SOOS. For the SOOS to succeed, it is critical that a data system be established that ensures that both past and future data sets are accessible and of known quality. A SOOS Data Management Sub-Committee is currently being developed to ensure the data strategy objectives are met. The sub-committee will establish a SOOS data policy (based on IPY, ICSU and IOC policies) and will help to drive the development of a SOOS Data Portal, which will provide a central locale for access to all SOOS-relevant data.

The sub-committee will also be integral in developing other data products as needed by the community.

A programme of the scale and complexity of the SOOS requires an International Programme Office (IPO). The SOOS IPO will serve as a central contact point for SOOS, monitor progress towards SOOS goals, facilitate coordination of field work, assist in the organisation of workshops and synthesis activities, and coordinate a Web site and other activities to advertise the aims and achievements of the SOOS. The SOOS International Project Office has recently been established in Hobart, Australia, hosted by the Institute for Marine and Antarctic Studies (University of Tasmania), with additional support from the Australian Antarctic Division. Dr. Louise Newman has been appointed as SOOS Executive Officer.

Using the recently published science strategy as a solid foundation, SOOS will now identify and take clear steps to achieve the SOOS mission. Towards this, the SOOS Scientific Steering Committee (SSC) has been selected from an international pool of nominees, and will be chaired by Dr. Mike Meredith (BAS, UK) and Dr. Oscar Schofield (Rutgers University, USA). This committee recently held its inaugural meeting in Salt Lake City (Utah, USA) alongside the Ocean Sciences Meeting, to progress the implementation of SOOS. SCAR and SCOR sponsor the SSC and oversee the SOOS as a whole. Committee and meeting details will be announced on the SOOS website (www.soos.aq), which is currently being developed and will be fully functional in early 2012.

The success of SOOS will depend on effective integration and coordination of national and international research efforts. The Southern Ocean is a vast and remote domain and the logistical resources available for its study are relatively limited. This places a further imperative on effective coordination of research among nations and across disciplines.

For more information on the SOOS, or to receive a copy of the SOOS Initial Science and Implementation Strategy, please contact Louise Newman (Louise.Newman@utas.edu.au).

References

Böning, C.W., A. Dispertt, M. Visbeck, S. Rintoul and F.U. Schwarzkopf, 2008: The response of the Antarctic Circumpolar Current to recent climate change, Nature Geoscience, 1: 864 – 869.

Cubillos, J.C., S.W. Wright, G. Nash, M.F.D. Salas, B. Griffiths, B. Tilbrook, A. Poisson and G.M. Hallegraeff, 2007: Calcification morphotypes of the coccolithophorid Emiliania huxleyi in the Southern Ocean: Changes in 2001 to 2006 compared to historical data, Marine Ecology Progress Series, 248: 47-54.

Gille, S.T., 2008: Decadal-scale temperature trends in the Southern Hemisphere Ocean, Journal of Climate, 16: 4749-4765.

Hood, M., M. Fukasawa, N. Gruber, G.C. Johnson, A. Kortzinger, C. Sabine, B. Sloyan, K. Stansfield, and T. Tanhua, 2009: Ship-Based Repeat Hydrography: A Strategy for a Sustained Global Program, In Proceedings of OceanObs'09: Sustained Ocean Observations and Information for Society (Vol. 2), Venice, Italy, 21-25 September 2009, Hall, J., Harrison, D.E. & Stammer, D., Eds., ESA Publication WPP-306, doi:10.5270/OceanObs09.cwp.44.

Jacobs, S.S., 2006: Observations of change in the Southern Ocean, Philosophical Transactions of the Royal Society A, 364: 1657-1681.

Jacobs, S.S., A. Jenkins, C.F. Guilivi, and P. Dutrieux, 2011: Stronger ocean circulation and increased melting under Pine Island Glacier ice shelf, Nature Geoscience, 4: 519-524.

Le Quéré, C.L., C. Rodenbeck, E.T. Buitenhuis, T.J. Conway, R. Langenfelds, A. Gomez, C. Labuschagne, M. Ramonet, T. Nakazawa, N. Metzl, N. Gillett, and M. Heimann, 2007: Saturation of the Southern Ocean CO2 sink due to recent climate change, Science, 316: 1735-1738.

Meredith, M.P., P.L. Woodworth, T.K. Chereskin, D.P. Marshall, L.C. Allison, G.R. Bigg, K. Donohue, K.J. Heywood, C.W. Hughes, A. Hibbert, A. McC. Hogg, H.L. Johnson, L. Jullion, B.A. King, H. Leach, Y.-D. Lenn, M.A. Morales Maqueda, D.R. Munday, A.C. Naveira Garabato, C. Provost, J.-B. Sallee, and J. Sprintall, 2011: Sustained monitoring of the Southern Ocean at Drake Passage: Past achievements and future priorities, Reviews of Geophysics, 49: doi:8755-1209/11/2010RG000348

Meredith, M.P., A.C. Naveira Garabato, A. McC. Hogg, and R. Farneti, 2012: Sensitivity of the overturning circulation in the Southern Ocean to decadal changes in wind forcing, Journal of Climate, doi: 10/1175/2011JCLI4204.1

Rignot, E. and S.S. Jacobs, 2002: Rapid bottom melting widespread near Antarctic ice sheet grounding lines, Science, 296: 2020-2023.

Rignot, E., I. Velicogna, M.R. van den Broeke, A. Monaghan, and J. Lenaerts, 2011: Acceleration of the contribution of the Greenland and Antarctic ice sheets to sea level rise, Geophysical Research Letters, 38, L05503-L05508. doi 10.1029/2011GL046583

Rintoul, S.R., C.W. Hughes and D. Olbers, 2001: The Antarctic Circumpolar Current system, In: Ocean circulation and climate; observing and modelling the global ocean, G. Siedler, J. Church and J. Gould (eds), International Geophysics Series, 77: 271-302, Academic Press.

Rintoul, S.R., M. Sparrow, M.P. Meredith, V. Wadley, K. Speer, E. Hofmann, C. Summerhayes, E. Urban, and R. Bellerby, 2012: The Southern Ocean Observing System: Initial Science and Implementation Strategy, Scientific Committee on Oceanic Research and Scientific Committee on Antarctic Research, ISBN: 978-0-948277-27-6

Sarmiento, J. L., N. Gruber, M.A. Brzezinski and J.P. Dunne, 2004: High latitude controls of the global nutricline and low latitude biological productivity, Nature, 427: 56-60.

Schofield, O., H.W. Ducklow, D.G. Martinson, M.P. Meredith, M.A. Moline, and W.R. Fraser, 2010: How do polar marine ecosystems respond to rapid climate change? Science, 328: 1520-1523.

Sokolov, S, and S.R. Rintoul, 2009a: Circumpolar structure and distribution of the Antarctic Circumpolar Current fronts: 1. Mean circumpolar paths, Journal of Geophysical Research, 114(c11): C11018.

Sokolov, S. and S.R. Rintoul, 2009b: Circumpolar structure and distribution of the Antarctic Circumpolar Current fronts: 2. Variability and relationship to sea surface height, Journal of Geophysical Research, 114(c11): C11019.

Thomas, D.N. and G.S. Dieckmann, (eds), 2003: Sea ice: an introduction to its physics, chemistry, biology and geology, Oxford: Blackwell Science.
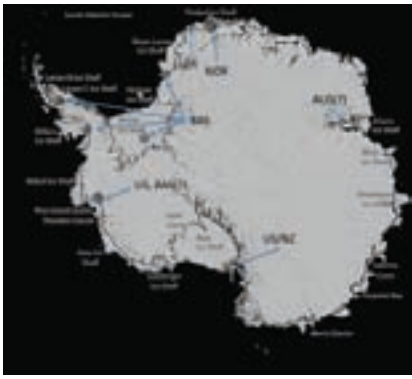
Fig 1: Location of existing or planned drill holes through ice shelves (circles), allowing sampling of underlying ocean waters.
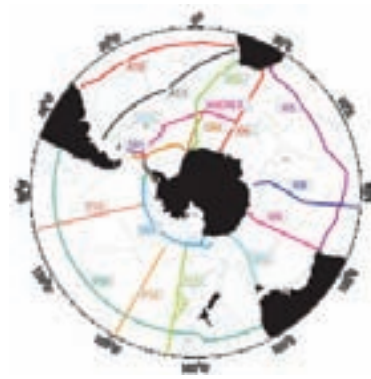

Fig 2: Repeat hydrographic sections that will contribute to the SOOS. Labels indicate the WOCE/CLIVAR designations for each line.
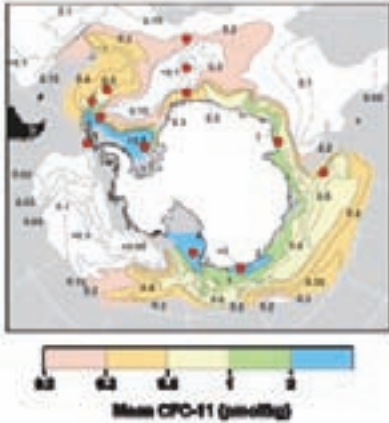

Fig 3: Map of proposed moored arrays (red circles) to sample the primary Antarctic Bottom Water (AABW) formation and export sites, as part of a coordinated global array to measure the deep limb of the global overturning circulation. Each of these sites has been occupied in recent years. The map shows the inventory of chlorofluorocarbon 11 (CFC-11) in the density layer corresponding to AABW. Modified by A. Orsi from figure in Orsi, A.H., G.C., Johnson, and J.L. Bullister. 1999: Circulation, mixing and production of Antarctic Bottom Water, Progress in Oceanography, 43: 55-109. Reprinted with permission from Elsevier.

Forthcoming International workshop on interdecadal variability of the global monsoons

Andy Turner[1], Bin Wang[2], Carlos Ereño[3]

1   NCAS-Climate, University of Reading, UK
2   International Pacific Research Center, School of Ocean and Earth Science and Technology, University of Hawaii, USA
3   International CLIVAR Project Office, University of Buenos Aires, Argentina

Understanding interdecadal variability of the climate system is a prerequisite for attribution of present and future changes under anthropogenic forcing. The Global Monsoon represents the dominant mode of annual variation of the tropical precipitation (1) and circulation (2) and is thus a defining feature of seasonality and a major mode of variability of the Earth's climate system. The components of the global monsoon (Asian-Australian; West African; American Monsoons) all feature seasonal reversals of surface winds and contrasting rainy summers and dry winters; domains as shown in Figure 1. While the regional monsoons show some cohesive variations on interannual timescales, there may also be important decadal variations with potential large socio-economic impacts. However there is little consensus on the character of this variability. Studies (e.g., 3-5) have highlighted interdecadal variability in:

• The various regional monsoons;
• Features embedded in the monsoon, such as tropical cyclones and monsoon depressions;
• The strength of monsoon teleconnections, impacting the prospect for seasonal prediction.

We therefore announce a major international workshop to: (a) review evidence of monsoon interdecadal variability collectively and regionally; (b) discuss how these variations are linked to each other and other major modes of interdecadal variability in the global oceans such as the PDO, IPO, or AMO, and to climate change as in Figure 1; (c) examine possible mechanisms underlying these interdecadal variations, including in simulations and numerical experiments that address driving physical processes with the goal of assessing the predictability of monsoon interdecadal variations.

Sessions will last around half a day each, consisting of invited speaker(s) and a period of discussion. The majority of scientific presentations will be made via interactive poster sessions:

• Session 1: Monsoon decadal variability in the modern observational era (19th/20th centuries).
• Session 2: What do palaeo-modelling and proxy data tell us about monsoon interdecadal variability?
• Session 3: Interconnections between the regional monsoons and other modes of climate variability.
• Session 4: Mechanisms for decadal modulation of the monsoon.
• Session 5: Using our knowledge of decadal variability to further monsoon prediction and projection.

The workshop will provide an overview of the state of knowledge and emerging issues in monsoon interdecadal variability and promote coordinated experimental designs to test possible causes and explore predictability. The workshop

will be of potential interest to climate scientists of the tropical monsoon regions, as well as those with expertise in ENSO and multi-decadal ocean variability, the seasonal forecasting, climate impacts and PAGES communities. We hope to promote current/palaeo-climate collaborations.

Venue: Nanjing University of Information Science and Technology (NUIST), China, 10-12 September 2012.

Organizers: Dr Andy Turner, Prof. Bin Wang and the WCRP CLIVAR Asian-Australian Monsoon Panel and local hosts Prof. Jinzhong Min & Dr Weiyu Pan of NUIST.

Financial support: We expect attendance of around 80 international scientists. Limited funding is currently available for some US graduate students and early career researchers courtesy of the NSF. Other funding may become available in due course. Please send a short (max 2 page) CV and statement explaining your interest and details of funding requested if you wish to be considered.

Deadline: The call for abstracts is now open until 1 May 2012 although applicants interested in support should apply more quickly. Please specify the main session of interest.
To be added to the list of interested participants or send an abstract please contact Dr Andy Turner a.g.turner@reading.ac.uk, cc Prof Bin Wang wangbin@hawaii.edu.

More information will also be made available via the following URL as the workshop approaches: http://www.clivar.org/organization/aamp/activities/international-workshop-interdecadal-variability-global-monsoons

References:

Trenberth KE, Stepaniak DP, Caron JM (2000) The Global monsoon as seen through the Divergent Atmospheric Circulation. Journal of Climate 13: 3969–3993.

Wang B, Ding QH (2008) Global monsoon: Dominant mode of annual variation in the tropics. Dyn Atmos Oceans 44:165-1833.

Wang B, Liu J, Kim HJ, Webster PJ, and Yim SY (2011) Recent change of global monsoon precipitation (1979-2008). Clim Dyn, doi:10.1007/s00382-011-1266-z.

Giannini, A, Saravanan, R, Chang, P (2003) Oceanic forcing of Sahel rainfall on interannual to interdecadal time scales. Science 302: 1027-1030, doi:10.1126/science.1089357.

Krishnamurthy, V, Goswami, BN (2000) Indian monsoon-ENSO relationship on interdecadal timescale Journal of Climate 13: 579-595, doi:10.1175/1520-0442(2000)013%3C0579:IMEROI%3E2.0.CO;2.
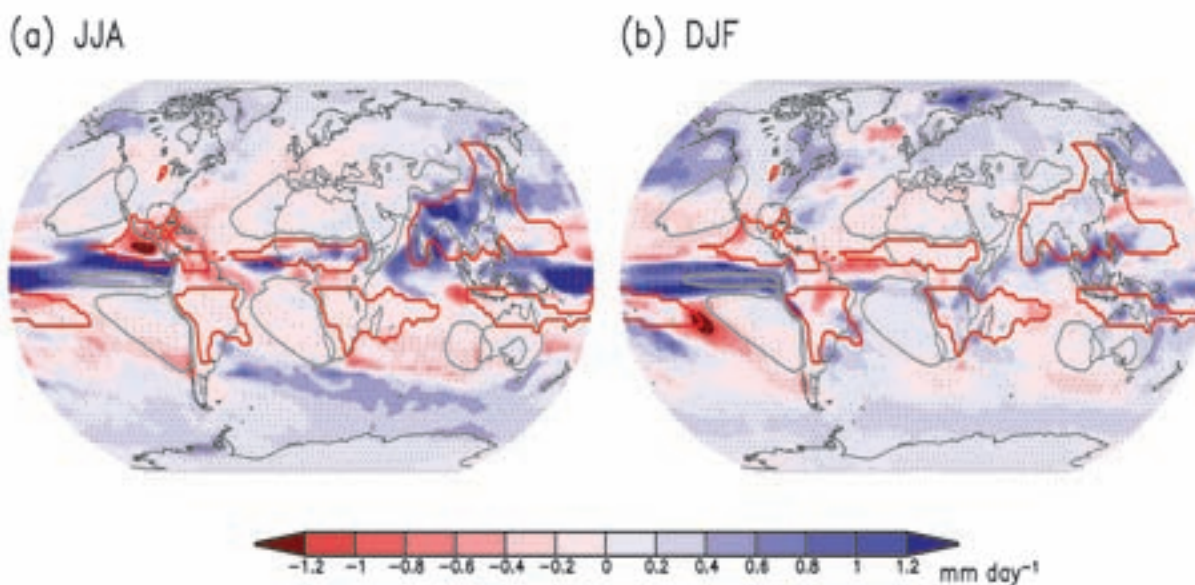
Fig. 1: CMIP5 multi-model mean changes in precipitation for (a) boreal summer (JJA) and (b) boreal winter (DJF) for the period 2070-2099 in RCP4.5 relative to 1980-2005 in the historical run. Stippling denotes areas where the magnitude of the multi-model ensemble mean exceeds the inter-model standard deviation. Using Global Precipitation Climatology Project and Climate Prediction Center Merged Analysis of Precipitation data the global monsoon domain is defined where the summer-minus-winter precipitation exceeds 2.5 mm/day and the summer precipitation exceeds 55% of the annual total (in red). The dry regions with summer precipitation <1 mm/day are outlined in grey. Understanding how multi-decadal variations in the global monsoon will support or oppose signals related to anthropogenic climate change will help reduce uncertainties in future projections of monsoon rainfall.

Call for CLIVAR Scientific Steering Group (SSG) Nominations

If you are interested in becoming a member of the CLIVAR SSG (or wish to nominate someone) then we would like to hear from you. Please send your nomination to icpo@noc.ac.uk, together with a short paragraph of background. Membership is usually on a 3-year rotational basis. For further information on the SSG see http://www.clivar.org/organization/ssg.

CLIVAR VAMOS Workshop on Modeling and Predicting Climate in the Americas, Petropolis, Brazil, June 4-6 2012

The overarching goal of VAMOS modeling is to improve the prediction of warm season precipitation over the Americas, for societal benefit, and to assess the implications of climate change. Success in meeting this overarching goal is critical to the new World Climate Research Program (WCRP) strategic framework. In meeting this goal, the VAMOS program works:

1) To describe, understand, and simulate the mean and seasonal aspects of the American monsoon systems,
2) To simulate American Monsoon System lifecycles, including diurnal cycles and the intraseasonal, interannual and interdecadal interactions with, and influences on, them,
3) To investigate American Monsoon System predictability and to make predictions to the extent possible,
4) To improve the predictive capability through model development and analysis techniques, and
5) To prepare products with a view to meeting societal needs, including studies of the impacts on the American Monsoon Systems of scenarios of climate change.

VAMOS focuses on rainfall and the probability of occurrence of significant weather events such as tropical storms, mesoscale convective systems, and persistent and heavy rains associated with synoptic systems and temperature extremes. The term "monsoon system" encompasses not only the summer monsoon rainfall in the tropical Americas, but also the perturbations in the planetary, synoptic and mesoscale flow patterns that occur in association with it, including those in the winter hemisphere. In addition, the region of interest covers both the tropical and the extratropical Americas and surrounding oceans. This complexity in terms of spatial and temporal scales and climate system interactions (i.e., land-atmosphere or ocean-atmosphere) necessitates an integrated multi-tiered modeling and data analysis and assimilation strategy.

To achieve its objectives, VAMOS has adopted a multi-scale approach, which includes monitoring, diagnostic and modeling activities on local, regional, and continental scales. In this multi-scale approach, local processes are embedded in, and are fully coupled with, larger-scale dynamics.

The modeling strategy which was approved in 2009 is organized into four science themes: (A) simulating, understanding and predicting the diurnal cycle, (B) predicting and describing the Pan-American monsoon onset, maturation and demise stages, (C) modeling and predicting SST variability in the Pan-American Seas, and (D) improving the prediction of droughts and floods. It is clear that all four of these science themes are interdependent; indeed, some of the scientific questions such as issues related to scale interactions transcend all four themes. Nevertheless, this organizational structure provides the focus required to tackle the most important modeling issues.

When the modeling plan was first developed it was recognized that over time the above themes would need to be revisited and modified according to improvements in modeling and understanding. Now is the time to assess VAMOS modeling progress and revisit and revise the modeling strategy. As such, the VAMOS panel is pleased to announce the CLIVAR VAMOS Workshop on Modeling and Predicting Climate in the Americas to be held at the Laboratorio Nacional de Computação Cientifica (LNCC) in Petropolis, Brazil, on June 4-6 2012.

The main goals of this workshop are to review the state of modeling research in the VAMOS domain related to: (i) sub-seasonal to multi-decadal climate prediction and (ii) understanding of dynamical and physical processes underpinning potential sources of predictability, variability and climate change. In order to advance prediction at all of these time-scales it is essential to develop, use and understand models that integrate all relevant physical and dynamical processes. This integrative approach is a core element of the Modeling Plan for VAMOS as it seeks to improve the prediction of warm season precipitation over the Americas, for societal benefit, and to assess the implications of climate change.

The workshop will be organized following the Modeling Plan for VAMOS. That is the workshop will have core themes:

a) Simulating, Understanding and Predicting the Diurnal Cycle
b) Predicting the Pan-American Monsoon Onset, Mature and Demise Stages
c) Modeling and Predicting SST Variability in the Pan-American Seas
d) Improving the Prediction of Droughts and Floods

While these core themes are focused on the VAMOS region, special emphasis will be placed on assessing how these aspects of the Pan-American monsoon are represented in global models. The workshop will also emphasize understanding and predicting extreme events in the VAMOS region, and how the VAMOS research contributes to climate change assessments.

In addition to reviewing the current state of modeling research, the workshop will have talks and discussion sessions specifically designed to develop the future of VAMOS modeling research as a fundamental contribution to the WCRP.

Abstracts should be submitted to Carlos Ereño (carlos_ereno@yahoo.com) by 15 April 2012.

CONTENTS

National Oceanography Centre
NATURAL ENVIRONMENT RESEARCH COUNCIL

Please recycle this newsletter by passing on to a colleague or library or disposing in a recognised recycle point